The effects of methylglyoxal, a metabolite derived from glycolysis, on metabolic responses of adipocytes

NG SU PING

2023

Abstract

Adipocytes play a crucial role in the regulation of systemic energy homeostasis by responding to hormones which activate metabolic signalling pathways regulating adipocyte glucose and lipid metabolism. While hormones play a large role in dictating adipocyte metabolic processes, it is becoming apparent that certain metabolites, such as adenosine monophosphate, also trigger signalling cascades that influence various aspects of metabolism. Methylglyoxal (MG), a natural metabolite derived from glycolysis, has been implicated in metabolic disorders such as obesity and diabetes, which may be attributed to its impairment of systemic glucose and lipid homeostasis. MG has also been implicated in adipose tissue dysfunction and insulin resistance. However, the full effects of MG on adipocyte metabolic functions remain unclear. Since MG has been found to contribute to the activation of signalling transduction pathways, this study investigated if the potential mechanism by which MG acts on adipocyte glucose and lipid metabolism is through its effects on signalling transduction. In the first part of the study, the effect of MG on adipocyte glucose metabolism was elucidated by its effects on insulin-stimulated glucose uptake. It was found that MG inhibited insulin-induced activation of one of the primary mediators of the insulin signalling pathway, insulin receptor substrate (IRS)-1, by activating mammalian target of rapamycin complex (mTORC)-1 via the inflammatory transforming growth factor-β-activated kinase (TAK)-1–p38 signalling pathway. In the second part of the study, the effect of MG on adipocyte lipid metabolism was elucidated by its effects on adrenergic-stimulated lipolysis and thermogenic gene expression. MG was found to have no effect on isoproterenol-induced free fatty acid release, but was instead found to attenuate the isoproterenol-induced gene expression of uncoupling protein 1 (UCP1), a thermogenic protein in adipocytes, via c-Jun N-terminal kinase (JNK). Altogether, these findings elucidate MG as a metabolite capable of modulating metabolic processes through its effect on signalling pathways in adipocytes.

Abbreviations

2-DG	2-Deoxyglucose
3-PG	3-Phosphoglycerate
3DG-H	3-Deoxyglucosone-derived hydroimidazolone isomers
AGEs	Advanced glycation end products
AMP	Adenosine monophosphate
AMPK	AMP-activated protein kinase
AP1	Activator protein 1
ASK1	Apoptosis signal-regulating kinase 1
ATF2	Activating transcription factor 2
ATGL	Adipose triglyceride lipase
ATP	Adenosine triphosphate
β-AR	β-Adrenergic receptor
BBGC	S-p-Bromo-benzylglutathione cyclopentyl diester
BMI	Body mass index
BPB	Bromophenol blue
cAMP	Cyclic AMP
Ccl2	Chemokine ligand 2 (gene encoding MCP1 protein)
CIDEA	Cell death inducing DNA fragmentation factor alpha-like effector A
CEdG	N^2-(1-carboxyethyl)-2'-dG
CEL	*N*ε-carboxyethyl-lysine
CMdG	N^2-carboxymethyl-dG
CML	*N*ε-carboxymethyl-lysine
CREB	cAMP response element-binding protein
COX2	Cyclooxygenase 2
DAG	Diacylglycerol
DALYs	Disability-adjusted life-years
DCFDA	Dichlorofluorescein diacetate
dG	Deoxyguanosine
DHA	Dihydroxyacetone
DHAP	DHA phosphate
DIO2	Iodothyronine deiodinase 2
DMEM	Dulbecco's modified Eagle's medium
DNA	Deoxyribonucleic acid
ERK	Extracellular receptor kinase
FBS	Foetal bovine serum
FGF21	Fibroblast growth factor 21
FFA	Free fatty acid
G-3-P	Glyceraldehyde-3-phosphate
GAP	GTPase-activating protein
G-H1	*N*δ-(5-Hydro-4-imidazolon-2-yl)ornithine
GLO	Glyoxalase

GLUT4	Glucose transporter 4
HAT	Histone acetyltransferase
HIF1α	Hypoxia inducible factor 1α
HRP	Horseradish peroxidase
HSL	Hormone sensitive lipase
IBMX	3-Isobutyl-1-methylxanthine
IGF1	Insulin-like growth factor 1
IκB	Inhibitor of nuclear factor kappa-B
IKK	IκB kinase subunit
IL	Interleukin
Ins	Insulin
IR	Insulin receptor
IRS	IR substrate
Iso	Isoproterenol
iWAT	Inguinal white adipose tissue
JNK	c-Jun N-terminal kinase
KEAP1	Kelch-like ECH-associated protein 1
KG	Ketoglutarate
KRPH	Krebs Ringer Phosphate HEPES
Luc	Luciferase
MAG	Monoacylglycerol
MAPK	Mitogen-activated protein kinase
MAPKAPK	MAPK-activated protein kinase
MAPKKK	MAPK kinase kinase
MCP1	Monocyte chemoattractant protein 1
MG	Methylglyoxal
MG-H1	*N*δ-(5-Hydro-5-methyl-4-imidazolon-2-yl)-ornithine
MHO	Metabolically healthy obese
MICA	Methylimidazole crosslink between proximal cysteine and arginine residues
mTORC	Mammalian target of rapamycin complex
MTS	3-(4,5-Dimethylthiazol-2-yl)-5-(3-carboxymethoxyphenyl)-2-(4-sulfophenyl)-2H-tetrazolium
MSK1	Mitogen- and stress-activated protein kinase 1
NAC	*N*-acetyl-L-cysteine
NAD	Nicotinamide adenine
NADH	Reduced NAD
NRF2	Nuclear factor erythroid 2-related factor 2
Oxo	(5*Z*)-7-oxozeaenol
PAI1	Plasminogen activator inhibitor-1
PBS	Phosphate buffered saline
PDEM	Phosphorylation dependent electrophoretic mobility shift
PDK1	PI3-dependent kinase 1
PGC1α	PPARγ coativator 1α

PHD2	Prolyl hydroxylase domain-containing 2
PI3K	Phosphatidyl-inositol-3-kinase
PKA	Protein kinase A
PKC	Protein kinase C
PLIN	Perilipin
PPARγ	Peroxisome proliferator-activated receptor γ
Ppargc1α	PPARγ coativator 1α (gene encoding PGC1α protein)
Ptgs2	Prostaglandin-endoperoxide synthase 2 (gene encoding COX2 protein)
RAGE	Receptor for advanced glycation end products
Rap	Rapamycin
RING	Really interesting new gene
ROS	Reactive oxygen species
S6K	Ribosomal protein S6 kinase
SAPKs	Stress-activated protein kinases
SB	SB203580 (p38 inhibitor)
SDS	Sodium dodecyl sulphate
SDS-PAGE	SDS-polyacrylamide gel electrophoresis
SEM	Standard error of the mean
Ser	Serine
SP	SP600125 (JNK inhibitor)
T1D	Type one diabetes
T2D	Type two diabetes
T_3	3,3',5'-Triiodo-L-thyronine
TAG	Triacylglycerol
TAK	Transforming growth factor-β-activated kinase
TBC1D1	TBC1 domain family member 1
TCA	Tricarboxylic acid
Thr	Threonine
TET	Ten-eleven translocation
TNF	Tumour necrosis factor
TRAF	TNF receptor-associated factor
TRPA1	Transient receptor potential A1
TSC	Tuberous Sclerosis Complex
Tyr	Tyrosine
UCP1	Uncoupling protein 1
UPLC-MS/MS	Ultra-performance liquid chromatography tandem mass spectrometry
WAT	White adipose tissue

Contents

Chapter 1 1

General Introduction

Chapter 2 15

The first study: The effect of methylglyoxal on insulin-stimulated glucose uptake in adipocytes

Chapter 3 59

The second study: The effect of methylglyoxal on isoproterenol-induced free fatty acid release and uncoupling protein 1 expression in adipocytes

Chapter 4 89

Summary

References 92

Acknowledgements 110

List of Publications 114

Chapter 1

General Introduction

The rise of worldwide diabesity

There are currently more people who are obese than underweight globally [1]. Yet, the total number of obese and severely obese people are projected to still increase across all continents, especially in Europe, Latin America and Asia [1]. According to the latest statistics provided by the World Obesity Atlas 2022 [2] which was published by the World Obesity Federation, it is estimated that one in five women and one in seven men will be obese, amounting to one billion obese people by 2030. Obesity is a significant risk factor for a number of other non-communicable diseases such as type two diabetes (T2D), heart disease and cancer [2]. Seeing that obesity has been thought to account for about 80–85% of the risk of developing T2D, and that more than 90% of patients with T2D have a body mass index (BMI) ≥25.0 kg/m^2 [3], it is undeniable that obesity is strongly associated with T2D, so much so that the term, Diabesity, has been used to describe diabetes in the context of obesity [4].

Diabetes, a disease characterized by hyperglycaemia, is one of the top ten leading causes of death in adults aged between 20 and 79 years old worldwide, corresponding to 12.2% of global deaths from all causes in 2021, which amounts to up to 6.7 million deaths [5]. As of 2021, the International Diabetes Federation estimated that globally, there were 537 million people, aged 20-79 years old with diabetes, and this number is projected to increase to 783 million by 2045 [5]. While global age-standardized rate of mortality and disability-adjusted life-years (DALYs) for type one diabetes (T1D) has declined, total diabetes (including both T1D and T2D) continues to increase, reflecting the fact that most of the global burden of diabetes falls on T2D, which affects 90% of diabetic patients [6]. Globally, high BMI and

behavioural factors such as inappropriate diet, smoking, and low physical activity contributed the most attributable death and DALYs of diabetes; but as of 2017, the leading three risk factors have been narrowed down to high BMI, dietary risks (diet low in whole grains, diet low in nuts and seeds, diet low in fruits, diet high in sugar-sweetened beverages, diet high in processed meat, diet high in red meat) and ambient particulate matter pollution [6]. In more detail, high BMI, dietary risk, and ambient particulate matter pollution was responsible for 30.8%, 24.7%, and 13.4% deaths respectively, and 45.8%, 34.9%, 15.4% of DALYs respectively [6]. These data solidify the strong correlation between obesity, diet, and diabetes.

The adipose tissue and its contribution towards insulin resistance and T2D

Obesity is characterised by ectopic accumulation of white adipose tissues (WATs). The strong correlation between obesity and T2D [6] is observed through the aforementioned fact that 90% of patients with T2D have a high BMI≥25.0 kg/m^2 [3]. This correlation between ectopic WAT accumulation and T2D is further strengthened through findings that the hallmark T2D symptoms, insulin resistance and high blood glucose levels, can be improved through increasing physical activity [7] and weight reduction via calorie restriction [8] or bariatric surgery [9], all of which promote the reduction of WAT. These findings make WAT a significant organ to study the pathology of T2D.

WATs comprise 20–25% of body mass in healthy adult humans, and may go above 50% of body mass in cases of obesity [10,11]. WATs play a crucial role in the maintenance of systemic energy homeostasis, functioning mainly as an energy depot by storing excess glucose and fatty acids from the periphery as triacylglycerols (TAGs) during times of energy abundance, and releasing the stored energy by breaking down the stored TAGs to glycerol and fatty acids for release during times of energy deprivation [12]. The adipose tissues comprise of a variety of cells, but it is the adipocytes, which consist of the majority of its cellular makeup, making

up more than 50% of the adipose tissue [12], that confer these metabolic functions. To perform these functions, adipocytes respond to hormones such as insulin and catecholamines which activate the corresponding metabolic signalling pathways to ultimately induce metabolic processes such as glucose uptake or free fatty acid (FFA) release, respectively [13]. Apart from the passive release of energy, adipocytes are also capable of actively converting chemical energy as heat via uncoupling protein 1 (UCP1), a mitochondrial transporter protein located at the inner mitochondrial membrane which generates heat by catalysing the dissipation of the mitochondrial proton motive force. *Ucp1* gene expression is activated upon catecholamine stimulation, and adipocytes with high expression of UCP1 within the WATs are termed "beige" adipocytes due to their possession of a high number of mitochondria [14]. Dysregulation of these metabolic signalling pathways often lead to adipocyte dysfunction which ultimately impact systemic metabolism negatively.

Insulin activates the insulin signalling pathway in adipocytes which gears cellular processes towards increasing cellular glucose uptake for *de novo* lipogenesis [15,16]. The insulin signalling pathway (**Fig. 1-1**; [15,16]) involves the binding of insulin to the insulin receptor (IR), which activates its tyrosine kinase to phosphorylate multiple tyrosine residues in IR substrate (IRS)-1. This activates IRS-1, which transduces the signal downstream which sequentially induce the activation of phosphatidyl-inositol-3-kinase (PI3K), PI3-dependent kinase (PDK)-1, Akt and so on, ultimately promoting the translocation of glucose transporter (GLUT)-4 to the cellular membrane for glucose uptake into cells [15]. The insulin signalling pathway also has a negative feedback control mechanism via Akt involving mammalian target of rapamycin complex (mTORC)-1, among others, that terminates its activation to avoid excessive signalling by increasing the phosphorylation of serine residues in IRS-1, which impairs the ability of IRS-1 to activate downstream PI3K-dependent pathways by blocking IRS-1 tyrosine phosphorylation [16].

On the other hand, the protein kinase A (PKA) signalling pathway (**Fig. 1-1**; [17]) is triggered by β-adrenergic receptor stimulation through catecholamines. This leads to the activation of PKA, which in addition to phosphorylating perilipin (PLIN), also phosphorylate downstream lipolytic proteins, such as adipose triglyceride lipase (ATGL), hormone sensitive lipase (HSL), to initiate lipolysis [17]. Apart from lipolysis, PKA signalling also activates thermogenesis, which is mainly conferred by UCP1. PKA-induced activation of UCP1 involves p38 mitogen-activated protein kinase (MAPK) as well as cAMP response element-binding protein (CREB), which work together to promote *Ucp1* gene expression as well as subsequent beiging and thermogenesis [18,19]. Altogether, the above illustrates the core role PKA plays in the regulation of the energy expending lipolysis and thermogenesis in adipocytes.

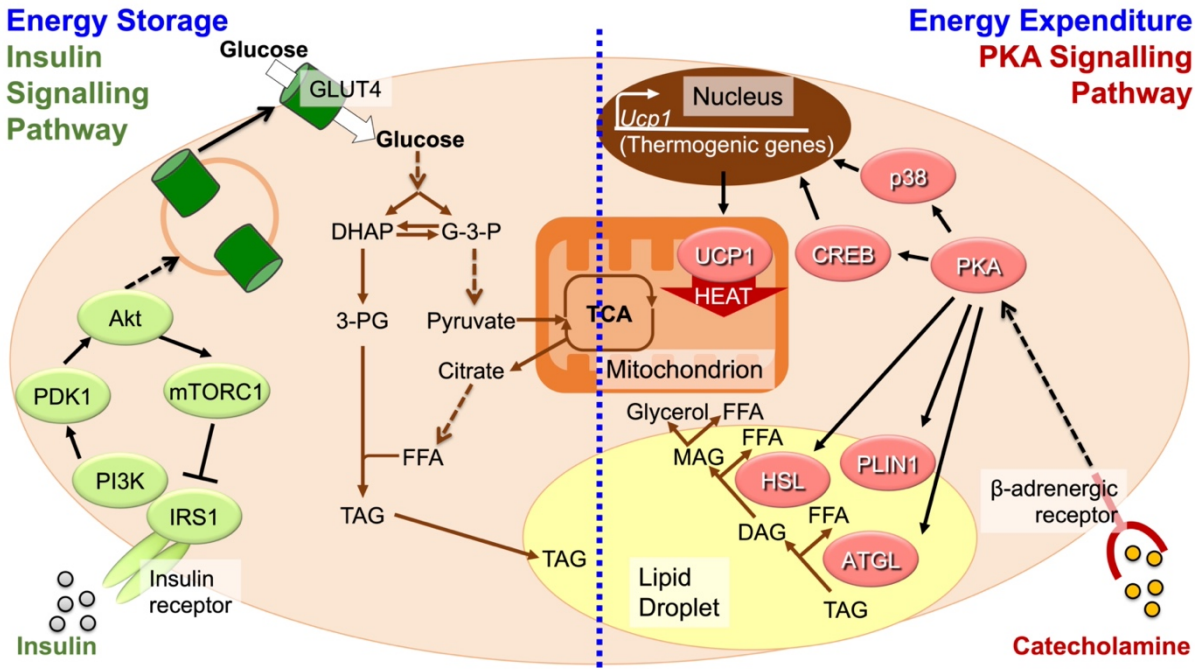

Figure 1-1. The insulin (left) and PKA (right) signalling pathway in coordinating the respective energy storage and expenditure processes in adipocytes

3-PG, 3-phosphoglycerate; ATGL, adipose triglyceride lipase; CREB, cAMP response element-binding protein; DAG, diacylglycerol; DHAP, dihydroxyacetone phosphate; FFA, free fatty acid; G-3-P, glyceraldehyde-3-phosphate; GLUT4, glucose transporter 4; HSL, hormone sensitive lipase; IRS1, insulin receptor substrate 1; MAG, monoacylglycerol; mTORC1, mammalian target of rapamycin complex 1; PDK1, PI3-dependent kinase 1; PI3K: phosphatidyl-inositol-3- kinase; PKA, protein kinase A; PLIN1, perilipin 1; TAG, triacylglycerol; TCA, tricarboxylic acid cycle; UCP1, uncoupling protein 1

While hormones play a large role in dictating these adipocyte metabolic processes, it is becoming apparent that certain metabolites like adenosine monophosphate (AMP), nicotinamide-adenine dinucleotide (NAD), acetyl-CoA, and α-ketoglutarate (2-oxopentanedioic acid; α-KG), which are produced by glycolysis and the tricarboxylic acid cycle also play a profound role in the metabolic state of adipocytes [20,21] which subsequently contribute to systemic energy homeostasis (**Fig. 1-2**). Metabolites such as NAD^+, AMP and lactate influence the metabolic state of adipocytes by means such as the initiation of signalling cascades [22], or the regulation of the expression of certain genes including those which may also dictate immune responses [23,24,25]. For example, NAD^+ acts as a cofactor for sirtuins which regulates AMP-activated protein kinase (AMPK); while AMP also allosterically activates AMPK [21,22]. Increased AMPK activity subsequently triggers a phosphorylation cascade which culminates in a synergistic response that inhibits anabolic pathways while stimulating catabolic pathways to replenish cellular ATP levels and restore energy homeostasis

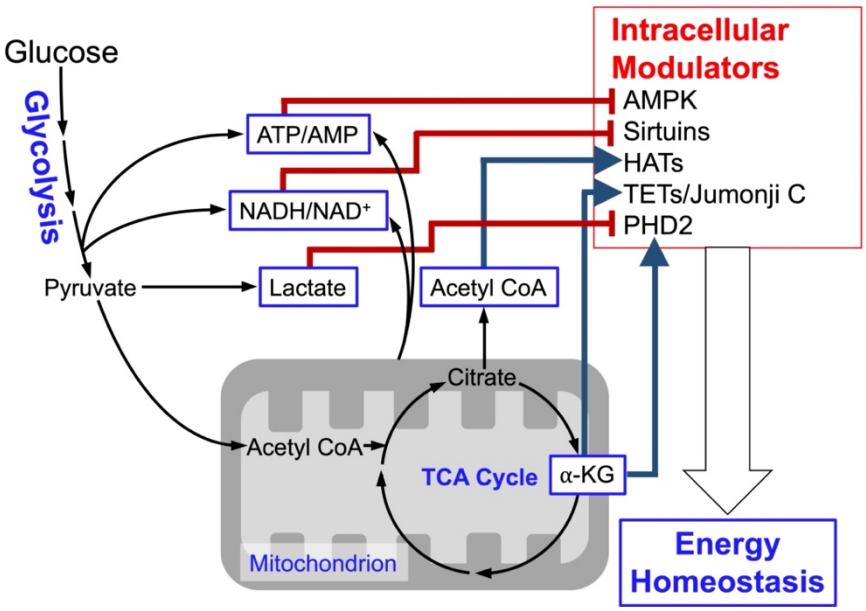

Figure 1-2. Metabolites that interact with intracellular modulators to influence energy homeostasis

AMP, adenosine monophosphate; AMPK, AMP-activated protein kinase; ATP, adenosine triphosphate; HAT, histone acetyltransferase; KG, ketoglutarate; NAD, nicotinamide adenine dinucleotide; NADH, reduced NAD; PHD2, prolyl hydroxylase domain-containing 2; TCA, tricarboxylic acid; TET, ten-eleven translocation

[22]. On the other hand, lactate directly targets and inhibits prolyl hydroxylase domain-containing (PHD)-2 activity by binding to its catalytic domain, blocking the access of PHD2 to its natural substrate, α-KG [23]. The inhibition of PHD2 prevents the destabilization of hypoxia inducible factor (HIF)-1α via hydroxylation by PHD2, consequently increasing HIF1α protein levels which drives the mRNA expression of HIF1α downstream genes which include inflammatory cytokines [23]. These examples highlight that metabolites also possess regulatory functions in influencing adipocyte metabolism in addition to their innate nutritional function. Contrarily, this also shows that metabolic imbalance may also be a factor which contributes to the pathophysiology of diseases such as inflammation, obesity as well as T2D. These suggest that diet components, upon being broken down into their simplest metabolites, may also significantly affect systemic metabolism, possibly explaining why certain types of food are considered worse than others. While it is still not fully clear how metabolic disturbances that accompany the onset of obesity or T2D contribute to the pathophysiology of the disease, analyses of these metabolic changes have led to the recognition that certain metabolite biomarkers may have the potential to be used as diagnostic criteria for pre-diabetes [26,27].

It is still not fully understood how obesity and diet is linked to the development of T2D. Although obese individuals have higher chances in progressing to T2D compared to healthy ones, in reality, not all obese and morbidly obese patients progress to T2D. These individuals are referred to as metabolically healthy obese (MHO), and among the traits that they possess which differ them from their unhealthy counterparts are: higher insulin sensitivity, lower levels of inflammatory markers and normal adipose tissue function [28,29]. These traits point out the possibility of inflammation and adipocyte dysfunction as the link connecting the pathophysiology of obesity and insulin resistance, which have been substantiated by many studies about T2D that confirm so [16,17,30,31].

Inflammation has been found to be a major determinant for adipocyte dysfunction, negatively affecting both anabolic and catabolic metabolic processes in adipocytes, consequentially affecting whole body metabolism. Inflammation negatively regulates insulin signalling in adipocytes, impairing glucose metabolism and causing consequent systemic insulin resistance [16,17]. This impairment of insulin signalling by proinflammatory cytokines such as tumour necrosis factor (TNF)-α, interleukin (IL)-1β and IL6 is mainly attributed to the inhibitory phosphorylation of IRS by serine kinases such as inhibitor of nuclear factor kappa-B kinase subunit (IKK)-β, c-Jun N-terminal kinase (JNK), ribosomal protein S6 kinase (S6K) and mTOR [16,32,33], which reduce adipocyte sensitivity towards insulin stimulation. Aside from their negative effect on insulin signalling, inflammation has also been correlated with catecholamine resistance [34,35]. Among the mechanisms involved in catecholamine resistance include increased lipolysis upon inflammatory cytokine stimulation [30], which increases intracellular fatty acids to reduce adenylyl cyclase activity [36]. Fasting fatty acid concentrations in the circulation are estimated at 0.4–0.8 mM in the lean state, and the abnormally increased circulatory FFA levels during chronic inflammation has also been reported to mediate insulin resistance in other organs such as the muscle and pancreas [30, 37]. Also, seeing that many studies on the association of UCP1 with obesity and T2D till the present have negatively correlated UCP1 activity to those diseases [38,39,40], the reduction in *Ucp1* expression caused by inflammation-induced catecholamine resistance [36] may also exacerbate T2D under conditions of obesity as the adipose tissues are unable to rid excess circulating glucose and fatty acids via energy expending thermogenesis. Altogether, increased inflammation under metabolically unhealthy obese conditions contributes towards adipocyte dysfunction by resulting in both insulin and catecholamine resistance. This consequent derangement of metabolism due to the dulled response of adipocytes towards hormonal stimulation may eventually lead towards the progression towards T2D; still, it is not known

what is the trigger for adipocyte inflammation in metabolically unhealthy obesity, which subsequently manifests as T2D after full blown systemic metabolic dysregulation.

The metabolite, methylglyoxal, in the pathophysiology of T2D

The levels of the dicarbonyl compound, methylglyoxal (MG), are found to be significantly higher in the blood and tissues of obese and diabetic patients compared to healthy individuals [41,42,43]. MG levels determined from the plasma and tissues of healthy individuals range from 60 nM to 400 μM, the large variation in MG concentration being most likely due to pre-analytical sample processing [43]. By utilising ultra-performance liquid chromatography tandem mass spectrometry (UPLC-MS/MS), the current state-of-the art technique for measuring MG, it has been estimated that typical plasma levels of MG in healthy individuals are at ~60–250 nM, whilst cellular MG levels are at ~1–5 μM [43], which is higher than extracellular MG. Plasma levels of MG in obese and newly diagnosed T2D patients have been reported to be 1.5-fold that of control individuals [41], while higher stage T2D patients with diabetic complications such as diabetic nephropathy have been reported to have up to six-fold higher plasma levels of MG than control individuals [43,44], showing that plasma MG levels increase with the stage of disease. Since cellular MG levels are higher than extracellular MG levels, it can therefore be expected that cellular levels of MG during obesity and diabetes also increase beyond the typical concentrations of ~1–5 μM. This correlation between MG and the pathophysiology of diabetes also extends to the development of other diabetic complications such as diabetic retinopathy and neuropathy [43]. Upon studying if MG contributed to the pathogenesis of T2D, MG accumulation through a diet enriched with the MG precursor, fructose; or MG supplementation in high fat diet have been found to contribute to adipose tissue dysfunction and insulin resistance in rats [45,46]. More recently, functional genome analyses in various animal models including fruit flies and zebrafish elucidate that dysfunctional MG

metabolism is correlated with impaired glucose and lipid homeostasis as well as the development of diabetic complications [47,48,49]. Altogether, these findings demonstrate the potential pathogenic role of MG in diabetes, making MG a metabolite of interest in the study of the pathophysiology of T2D. However, the mechanisms underlying the role of MG in altering adipose tissue and adipocyte function in the pathogenesis of metabolic syndrome is still not fully elucidated.

MG is a highly reactive α-oxoaldehyde metabolite derived mostly from glucose that is produced both exogenously as well as endogenously. MG is up to 20,000-fold more reactive than glucose with regard to glycation, despite low levels of MG in plasma when compared to glucose (~25,000-fold lower) [50]. Exogenously, sources of MG include food products as well as beverages, and within these, MG originates from sugars, the products of the Maillard reaction, lipids, and metabolic products of microorganisms formed during industrial processing, cooking, and prolonged storage [51]. Endogenously, one of the most important ways of MG production is from glycolysis, the central metabolic pathway used by all cells for the oxidation of glucose to generate energy. Glucose, the most significant source of endogenous MG, contributes to systemic MG levels both from its nonenzymatic breakdown (autoxidation) and from the triose phosphate isomerase reaction in glycolysis, the latter playing a more significant role in endogenous MG production from glucose. Approximately 0.1% of the glycolytic flux gives rise to MG, translating to approximately 125 μmol/kg cell mass per day [43,52]. This means that for an adult human of 70 kg body mass with 25 kg body cell mass, the predicted whole-body rate of MG formation would be 3.125 mmol per day. Since endogenous MG is generated from the triose phosphate isomerase reaction in glycolysis, other nutrients such as fructose that directly feed into this reaction would incur a further increase in cellular MG levels. Other than glycolysis, MG is also produced during glyceroneogenesis and lipid peroxidation. The contribution of exogenous sources of MG towards systemic MG levels are reported to be

much lower (< 1%) compared to the contribution of MG that has been generated endogenously (> 90%) [43,53]. This higher contribution of endogenous MG to systemic MG levels may be one explanation as to why cellular MG levels are found to be more than four times higher than plasma MG levels. There is a dynamic exchange of the membrane-permeable MG between intracellular and extracellular compartments [43]. Seeing that MG is generated both exogenously and endogenously, both high sugar and high fat diets, as well as diseased states including dysfunctional MG metabolism, high glucose flux, or obesity-induced glyceroneogenesis inevitably lead to the increment of systemic MG levels accompanying the accumulation of intracellular MG [47].

The pathology of MG may involve its high reactivity, as evidenced by the fact that in the presence of protein (e.g., albumin), only 1% of MG was in the free form, whereas more than 90% was bound to proteins [51]. MG is capable of covalently modifying DNA and protein to form various types of advanced glycation end products (AGEs), and MG is considered one of the most important precursors of AGEs *in vivo* [43]. Within proteins, MG irreversibly modifies arginine and lysine residues forming adducts like hydroimidazolone *N*δ-(5-hydro-5-methyl-4-imidazolon-2-yl)-ornithine (MG-H1) and carboxyethyllysine (CEL), respectively [51,52]; while in DNA, MG modifies deoxyguanosine (dG) to form N^2-(1-carboxyethyl)-2'-deoxyguanosine (CEdG) [52]. These covalent MG-adducts on protein directly alter their structure and function, and may also activate inflammatory pathways and generate oxidative stress via activation of the receptor for advanced glycation end products (RAGE), contributing to the pathogenesis of diabetes and its related complications [52,54]. Among the intracellular protein glycation by MG which has been reported to cause pathological changes in particular include proteins such as haemoglobin, lens proteins, mitochondrial proteins, and histones [43]. Small increases of modifications of mitochondrial proteins by MG have been linked to a two- to three-fold increase in oxidative stress, and overexpression of *Glo1* which encodes the MG

metabolic enzyme, Glyoxalase (GLO)-1, prevented hyperglycaemia-induced formation of MG as well as oxidative stress in a rat model of diabetes, confirming the link between MG and oxidative stress [43,55].

Under normal conditions, more than 99% of MG within the cell is detoxified primarily by the GLO system (**Fig. 1-3**), which consists of GLO1, the rate limiting enzyme in MG metabolism which catalyses the formation of D-lactoylglutathione from hemithioacetal (formed non-enzymatically from MG and reduced glutathione) and GLO2, which hydrolyses D-lactoylglutathione to D-lactate [43,56]. As the half-life of the permeability of MG across cell membranes is less than 15 minutes, detoxification of extracellular MG is expected to occur as and when the metabolite enters the cells [57]. This is observed by a nearly directly proportional conversion of MG to D-lactate by the cytosolic GLO system when MG is added to cells in culture; and when intra- and extracellular concentrations of MG decrease as the enzymatic detoxification of MG is increased [58]. However, despite the efficiency of the GLO system, a minor fraction of MG that is not metabolized still proceeds to react with proteins and DNA to form AGEs.

High fat and high sugar diets not just promote ectopic lipid accumulation and increase blood glucose levels which, if left unchecked, leads to obesity and diabetes; these diets also

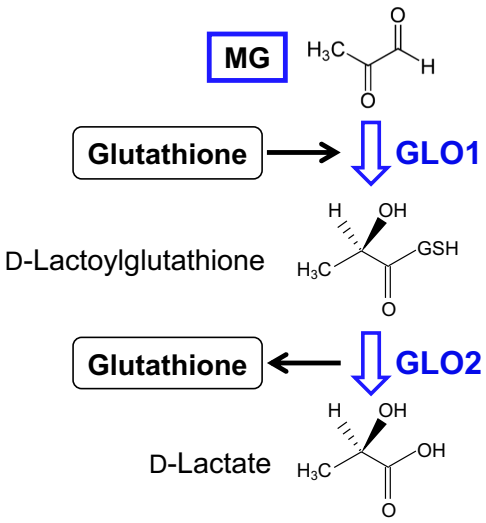

Figure 1-3. The glyoxalase system.

fuel the generation of endogenous MG. On the other hand, obesity and diabetes are associated with increased inflammation, hypoxia, and hyperglycaemia, and these conditions have been reported to invoke increased glycolysis which consequently increases MG formation [43]. Furthermore, decreased *Glo1* expression and activity are also associated with obesity and diabetes [43,56], further implying the involvement of MG in the pathogenesis of T2D under obese conditions. In spite of current knowledge that MG is associated with adipose tissue dysfunction and subsequent insulin resistance, the mechanism by which MG provokes these phenomena at the cellular level, i.e., in adipocytes, is still not sufficiently investigated.

Objectives of this study

To summarise the above, obesity is highly correlated with T2D, especially when adipocyte dysfunction is involved. Typical plasma levels of MG in healthy individuals are at ~60–250 nM [43], but 1.5–6-fold higher systemic MG levels have been reported in both obese and diabetic conditions [41,43,44], where disease severity corresponded with higher levels of systemic MG. It has also been reported that Western diet, i.e., a diet high in sugar and fat, is a major contributor to systemic MG levels [52]. This is because both high sugar and high fat diets feed the MG-producing glycolytic and the glyceroneogenic metabolic processes respectively. Although MG accumulation has been implicated in the impairment of adipose tissue metabolic function leading to systemic glucose and lipid metabolic dysregulation and the development of T2D, the underlying molecular mechanism behind MG's involvement in adipocyte dysfunction during metabolic disorders is still not clearly understood.

Adipocytes contribute to the regulation of systemic energy homeostasis by exhibiting acute metabolic responses to hormonal stimulation, such as glucose uptake which is followed by increased glucose metabolism upon insulin stimulation; as well as lipid catabolism which is followed by FFA release and initiation of thermogenesis by increased *Ucp1* expression upon

catecholamine stimulation. These hormone-stimulated adipocyte metabolic responses are brought about through a variety of cellular signalling, and dulled adipocyte metabolic responses to hormones due to diminished hormone-induced cellular signalling can be one cause of adipocyte metabolic dysfunction. Meanwhile, MG has been implicated in the activation of several cellular signalling transduction pathways such as the inflammatory and oxidative stress pathways [52,54], and these pathways are known to contribute towards the pathophysiology of metabolic disorders like obesity and diabetes [16,17,30,31,43]. This involvement of MG in initiating cellular signalling transduction pathways underscores the possibility that MG may provoke adipocyte metabolic dysfunction through asserting a negative influence on hormone-induced cellular signalling transduction pathways that are crucial in regulating adipocyte metabolism.

In this study, to elucidate the molecular mechanisms by which MG contributes to the dysregulation of adipocyte glucose and lipid metabolism, the author investigated the effects of MG on the acute metabolic responses of adipocytes to hormones. More specifically, the effects of MG on hormone-induced metabolic signalling pathways in adipocytes were explored. Since MG accumulation has been implicated in impaired glucose metabolism through adipose tissue insulin resistance, Chapter 1 of this study focuses on investigating the pathological effect of MG on insulin-induced glucose uptake via elucidating its effects on the insulin signalling pathway (**Fig. 1-4** (left)). On the other hand, since metabolic disorders have also been attributed to the impairment of lipid catabolism, Chapter 2 of this study focuses on investigating the pathological effect of MG on lipid catabolism by focusing on β-adrenergic receptor-stimulated FFA release as well as *Ucp1* expression. To elucidate the involvement of MG on the metabolic signalling pathways involved in lipid catabolism, the effects of MG on the PKA signalling pathway will be explored (**Fig. 1-4** (right)). Altogether, the findings of this study may elucidate

the potential of MG as a pathological metabolite which is capable in contributing towards the pathophysiology of metabolic disorders such as diabetes and obesity.

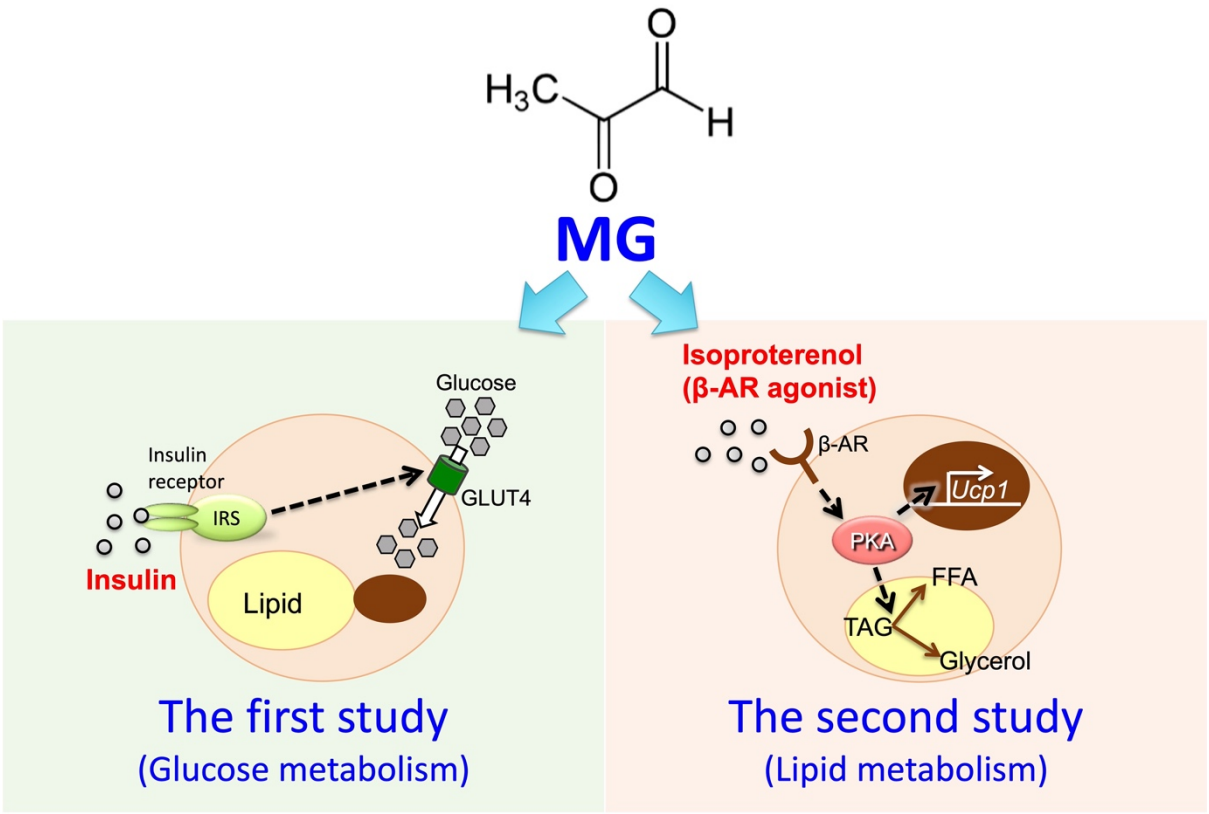

Figure 1-4. The objective of this study is to investigate the effects of MG on metabolic responses of adipocytes by focusing on: the effect of MG on insulin-stimulated glucose uptake (The first study; left) as well as the effect of MG on isoproterenol-induced FFA release and *Ucp1* expression (The second study; right).

β-AR, β-adrenergic receptor; FFA, free fatty acid; GLUT, glucose transporter; IRS, insulin receptor substrate; PKA, protein kinase A; TAG, triacylglycerol; Ucp1, uncoupling protein 1

Chapter 2

The first study: The effect of methylglyoxal on insulin-stimulated glucose uptake in adipocytes

Introduction

Some metabolites produced during energy metabolism are not merely metabolic intermediates, but also affect cellular functions. MG is a natural metabolite derived from glycolysis and is mainly formed from the triose-phosphate isomerase reaction [59]. MG is a highly reactive carbonyl compound that non-enzymatically forms various kinds of AGEs such as MG-H1 and CEL [51,52,60]. The accumulation of these AGEs, among others, is associated with accelerated aging and various chronic degenerative diseases, such as diabetes and Alzheimer's disease [61,62]. For example, plaques extracted from the brains of patients with Alzheimer's disease show a three-fold increase in AGE content compared to age-matched healthy individuals [61]. MG detoxification is mainly carried out by the glyoxalase system, where MG is metabolized by GLO1 and GLO2 to D-lactate in a glutathione-dependent manner (**Fig. 1-3**) [56,63]. MG has been shown to negatively influence metabolism by inducing glucose intolerance, insulin resistance, and diabetic complications [64,65,66,67]. Plasma and tissue MG levels are 1.5–6-fold higher in patients with diabetes than in healthy individuals [41,42,43]. Additionally, functional genome analyses revealed the association between glyoxalase system

---

*The content described in this chapter was originally published in *Biochemical Journal*. Su-Ping Ng, Wataru Nomura, Haruya Takahashi, Kazuo Inoue, Teruo Kawada, Tsuyoshi Goto and Yoshiharu Inoue (2022). Methylglyoxal induces multiple serine phosphorylation in insulin receptor substrate 1 via the TAK1–p38–mTORC1 signaling axis in adipocytes. *Biochem J.* 479(21):2279-2296. doi: 10.1042/BCJ20220271.

deficiency and the development of diabetic complications [47,48,68]. These observations suggest that MG plays a role in the development and progression of diabetic complications.

Adipocytes play an important role in the metabolism of lipids and glucose, and several hormones and cytokines, such as catecholamines, insulin, and TNFα, modulate their metabolic functions by activating intracellular signalling pathways [69,70,71]. Insulin activates the insulin signalling pathway by targeting the IR tyrosine kinase and regulating the IRS [72]. Since the activation of the insulin signalling pathway promotes glucose uptake into cells and modulates the metabolism of glucose and lipids, defects in its activation (i.e. insulin resistance) are closely associated with the development and progression of T2D [72]. Prolonged exposure of adipocytes to AGEs formed by synthetic MG derivatives of a single protein induces insulin resistance [73], suggesting that MG attenuates the insulin-stimulated activation of insulin signalling. However, the molecular mechanisms linking MG to insulin resistance are not yet fully understood.

MG is associated with the regulation of intracellular signalling pathways, including inflammatory and oxidative stress signalling pathways [74,75,76,77], indicating that MG functions as a signalling molecule that activates signal transduction. As MG increases the levels of intracellular reactive oxygen species (ROS) [78,79,80], ROS production is suggested to be involved in MG-induced activation of signalling pathways in some cell lines [78,79,80]. Meanwhile, the mTOR is a Ser/Thr protein kinase that controls cell growth and metabolism by forming two distinct complexes: mTORC1 and mTORC2 [81]. In the insulin signalling pathway, mTORC2 contributes to Akt activation in response to insulin stimulation, and mTORC1 is up-regulated via Akt activation [82]. It has previously been reported that MG activates mTORC2 signalling and increases Akt phosphorylation in 3T3-L1 adipocytes [83]. mTORC2 signalling was activated within 30 minutes following treatment of cells with MG, strongly suggesting that MG acts as an initiator of mTORC2 signalling [83].

To further understand the molecular mechanisms linking MG to insulin resistance, the physiological and molecular details of MG as a signalling molecule will be explored in this chapter. The effect of MG on the insulin signalling pathway involving IRS and mTOR was investigated in adipocytes. MG was demonstrated to activate mTORC1 signalling, increasing the phosphorylation of p70 S6K1 and IRS-1 at various serine residues which are downstream effectors of mTORC1, in 3T3-L1 adipocytes. Akt activation by mTORC2 was not required for MG-induced activation of mTORC1. Instead, it was found that activation of p38 MAPK via the transforming growth factor-β-activated kinase 1 (TAK1), which is an indispensable signalling intermediate in proinflammatory signalling [84], was involved in MG-induced activation of mTORC1. Furthermore, it was found that MG-induced activation of the TAK1–p38–mTORC1 signalling axis negatively regulated IRS-1 via multiple serine phosphorylation. Activation of the inflammatory pathway in response to proinflammatory cytokines, such as TNFα, is known to promote insulin resistance [85]. It was shown that the TAK1–p38–mTORC1 signalling axis identified in this study also contributed to TNFα-induced IRS-1 multiple serine phosphorylation, which may provoke insulin resistance.

Materials and Methods

Materials

Dulbecco's modified Eagle's medium (DMEM)-high glucose (Cat. No. 08458-16), penicillin-streptomycin mixed solution (Cat. No. 26253-84), 3-isobutyl-1-methylxanthine (IBMX) (Cat. No. 19624-31), dexamethasone (Cat. No. 50-02-2), dimethyl sulfoxide (Cat. No. 08904-14), 2-deoxyglucose (2-DG) (Cat. No. 10722-11), dihydroxyacetone (DHA) (Cat. No. 12438-62), and all chemicals used to prepare phosphate-buffered saline (PBS), lysis buffer, sample buffer, immunoprecipitation buffer, and Krebs Ringer Phosphate HEPES (KRPH) buffer were purchased from Nacalai Tesque (Kyoto, Japan). Foetal bovine serum (FBS) (Cat.

No. 10270-106) was purchased from Gibco (CA, U.S.A.). Insulin (Cat. No. 097-06474), SB203580 (IUPAC name: 4-[4-(4-fluorophenyl)-2-(4-methylsulfinylphenyl)-1H-imidazol-5-yl]pyridine; Cat. No. 199-16551), *N*-acetyl-L-cysteine (NAC) (Cat. No. 017-05131), H_2O_2 (Cat. No. 084-07441) and cytochalasin B (Cat. No. 034-17554) were purchased from Wako Pure Chemical Industries (Osaka, Japan). MG (Cat. No. 67028), rapamycin (Cat. No. R0395), and S-p-bromobenzylglutathione cyclopentyl diester (BBGC) (Cat. No. SML1306) were purchased from Sigma-Aldrich (MO, U.S.A.). AKT Inhibitor VIII (AKTi) (IUPAC name: 3-[1-[[4-(6-phenyl-8H-imidazo[4,5-g]quinoxalin-7-yl)phenyl]methyl]piperidin-4-yl]-1H-benzimidazol-2-one; Cat. No. 124018) was purchased from Calbiochem (CA, U.S.A.). BIRB796 (IUPAC name: 1-[5-tert-butyl-2-(4-methylphenyl)pyrazol-3-yl]-3-[4-(2-morpholin-4-ylethoxy)naphthalen-1-yl]urea; Cat. No. ab142166) was purchased from Abcam (Cambridge, U.K.). SP600125 (IUPAC name: 14,15-diazatetracyclo[7.6.1.02,7.013,16]hexadeca-1(15),2,4,6,9(16),10,12-heptaen-8-one; Cat. No. BML-EI305) was purchased from Enzo Life Sciences (NY, U.S.A.), while (5*Z*)-7-oxozeaenol (IUPAC name: (4S,6Z,9S,10S,12E)-9,10,18-trihydroxy-16-methoxy-4-methyl-3-oxabicyclo[12.4.0]octadeca-1(14),6,12,15,17-pentaene-2,8-dione; Cat. No. 17459) was purchased from Cayman Chemical Company (MI, U.S.A.). TNF-α (Cat. No. 410-MT) was purchased from R&D Systems (MN, U.S.A.).

Cell Culture

The 3T3-L1 cells were purchased from American Type Culture Collection (VA, U.S.A.). These cells were maintained in a humidified 5% CO_2 atmosphere at 37°C in basic medium (DMEM-high glucose supplemented with 10% (v/v) FBS, 100 units/ml penicillin, and 100 μg/ml streptomycin). To differentiate the pre-adipocytes into mature adipocytes, two days post-confluent cells were stimulated with 0.5 mM IBMX, 0.25 μM dexamethasone, and 10 μg/ml insulin in basic medium for 48 hours. The medium was then replaced with a growth

medium (basic medium with 5 μg/ml insulin). This step was repeated every two days until the adipocytes reached the sixth day after the induction of differentiation. Unless indicated, the six days post-differentiated adipocytes were incubated in a serum-free medium for three–five hours before the start of the experiment.

Cell Viability Assay

Cell viability was determined by using CellTiter 96® AQueous One Solution Cell Proliferation Assay by Promega, WI, USA (Cat. No. G3581) according to manufacturer's instructions. Briefly, 1/5 the volume of cell culture medium of MTS (3-(4,5-dimethylthiazol-2-yl)-5-(3-carboxymethoxyphenyl)-2-(4-sulfophenyl)-2H-tetrazolium) assay solution was added to the wells. The plate was then incubated at 37°C for two hours in a humidified, 5% CO_2 atmosphere before the absorbance at 490 nm was obtained using iMark™ Microplate Absorbance Reader (Bio-Rad, CA, USA).

Determination of Cellular Glucose Uptake

The cell culture medium of six days post-differentiated adipocytes was either changed to FBS-free medium after serum starvation of three–five hours, or to basic medium with or without 20 nM rapamycin or 0.5 μM (5*Z*)-7-oxozeaenol. The cells were incubated with the inhibitors for 30 minutes before treatment with 2.5 mM MG for 24 hours. Then, the glucose concentration of the cell culture medium was determined using a glucose detection kit, Glucose CII Test (Cat. No. 439-90901) from Wako Pure Chemical Industries, following the manufacturer's instructions. Absorbance levels were determined using a microplate reader (iMark; Bio-Rad, CA, U.S.A.) at a main wavelength of 490 nm and sub-wavelength of 600 nm for the bichromatic assay. The amount of glucose taken into the cells was calculated by subtracting the remaining glucose in the cell culture medium at 24.5 hours timepoint from that

in the medium at time zero and normalized to the corresponding cell lysate protein concentration.

Glucose Uptake Assay

Six days post-differentiated adipocytes were first starved of serum for three–five hours. Then, they were washed with warm KRPH buffer (1.2 mM KH_2PO4, 1.2 mM $MgSO_4$, 1.3 mM $CaCl_2$, 118 mM NaCl, 5 mM KCl, 30 mM HEPES, pH 7.5) thrice before being incubated at 37°C in KRPH buffer containing 2% bovine serum albumin with either 20 nM rapamycin or 0.5 μM (5*Z*)-7-oxozeaenol for 30 minutes. The cells were treated with 2.5 mM MG for four hours prior to stimulation with 1 μM insulin for 18 minutes. The cells were then incubated with 1 mM 2-DG in KRPH buffer for 20 minutes, allowing for cellular 2-DG uptake. Cellular 2-DG uptake was stopped by washing the cells with ice-cold PBS containing 50 μM cytochalasin B. Cells were collected in 1× sample diluent buffer and lysed via sonication. The cell lysates were then heated at 80°C for 15 minutes before centrifugation at 15 000×g for 20 minutes at 4°C. The supernatants were collected, and the 2-DG uptake value was determined by the levels of intracellular 2-DG 6-phosphate using the Glucose Cellular Uptake Measurement Kit (Cat. No. MBR-PMG-K01) from Cosmo Bio (Tokyo, Japan), according to the manufacturer's instructions. Fluorescence levels were measured using a Tecan Infinite F-200 microplate reader at excitation/emission wavelengths of 540/590 nm. These values were normalized to the corresponding cell lysate protein concentration.

Western Blotting

Cells were washed with PBS and lysed with lysis buffer containing 20 mM Tris-HCl buffer (pH 7.5), 1% (v/v) Triton X-100, 10% (v/v) glycerol, 137 mM NaCl, 2 mM EDTA (pH 8.0), a phosphatase inhibitor cocktail (Nacalai Tesque; Cat. No. 07575-51), and a protease inhibitor cocktail (Nacalai Tesque; Cat. No. 03696-21). The lysate was centrifuged at 16,700×g

for 10 minutes and the resulting supernatant was collected. Protein concentration was measured using the DC Protein Assay (Bio-Rad, Hercules, CA, USA; Cat. No. 500016) according to the manufacturer's protocol. Protein loading samples were prepared by homogenising four parts of the lysate supernatant with one part of 5x concentrated sample buffer containing 250 mM Tris-HCl (pH 6.8), 10% (w/v) sodium dodecyl sulphate (SDS), 25% (w/v) sucrose, 0.02 % (w/v) bromophenol blue (BPB), and 10% β-mercaptoethanol. 10 μg protein load per sample was separated by SDS-polyacrylamide gel electrophoresis (PAGE) and transferred to a polyvinylidene difluoride transfer (PVDF) membrane (Millipore, Burlington, MA, U.S.A.; Cat. No. IPVH00010). The membrane was then blocked, washed, and incubated with appropriate dilutions of the primary antibodies. The primary antibodies used in this study are listed in **Table 1-1** below. All primary antibodies were purchased from Cell Signaling Technology, MA, U.S.A., except for anti-phosphotyrosine PY20 which was purchased from ICN Biomedicals (CA, U.S.A.). Immunoreactive bands were detected using either anti-rabbit horseradish peroxidase (HRP) secondary antibody, (Cat. No. NBP1-75297) from Novus Biologicals (CO, U.S.A.), or anti-mouse HRP secondary antibody, (Cat. No. sc-2005) from Santa Cruz Biotechnology (TX, U.S.A.) with Immobilon Western Chemiluminescent HRP Substrate (Millipore; Cat. No. WBKLS0100) and an LAS-4000 mini-imaging system (Fujifilm, Tokyo, Japan). All antibodies were used at a dilution of 1:4000.

Table 1-1. Primary antibodies used in this study.

Primary antibody	Catalog number (manufacturer)
Phosphotyrosine PY20	#69-137 (ICN Biomedicals)
Phospho-IRS-1 (Ser307)	#2381 (Cell Signaling)
Phospho-IRS-1 (Ser318)	#5610 (Cell Signaling)
Phospho-IRS-1 (Ser612)	#3203 (Cell Signaling)

IRS-1	#3407 (Cell Signaling)
Phospho-Akt (Ser473)	#4060 (Cell Signaling)
Akt	#4691 (Cell Signaling)
Phospho-p70 S6K (Thr389)	#9234 (Cell Signaling)
p70 S6K	#2708 (Cell Signaling)
Phospho-TSC2 (Thr1462)	#3617 (Cell Signaling)
TSC2	#4308 (Cell Signaling)
Phospho-CREB (Ser133)	#9198 (Cell Signaling)
CREB	#9197 (Cell Signaling)
Phospho-p38 (Thr180/Tyr182)	#9215 (Cell Signaling)
p38	#9212 (Cell Signaling)
Phospho-JNK (Thr183/Tyr185)	#9251 (Cell Signaling)
JNK	#9252 (Cell Signaling)
Phospho-ERK (Thr202/Tyr204)	#9101 (Cell Signaling)
ERK	#9102 (Cell Signaling)

Immunoprecipitation

Cells were washed with PBS (137 mM NaCl, 2.7 mM KCl, 10 mM Na_2HPO4, and 1.8 mM KH_2PO_4) and lysed with immunoprecipitation buffer containing 25 mM Tris–HCl buffer (pH 7.5), 150 mM NaCl, 1% (v/v) NP-40, 0.1% SDS, 1 mM EDTA (pH 8.0) and the same phosphatase inhibitor cocktail and protease inhibitor cocktail from Nacalai Tesque as written above. The lysate was centrifuged at 16 700×g for ten minutes, and the resulting supernatant, that is, the protein extract, was collected. Approximately 800 μg of the protein extract was immunoprecipitated with an anti-IRS-1 antibody for 30 minutes before incubation with protein A/G PLUS-Agarose (Cat. No. sc-2003) immunoprecipitation reagent from Santa Cruz

Biotechnology (TX, U.S.A.) for 90 minutes. Immunoprecipitated proteins were then denatured, and western blotting was performed as mentioned above. Membranes were incubated with anti-phosphotyrosine PY20 or anti-phospho-IRS-1 Ser307 antibodies and then stripped and reblotted with an anti-IRS-1 antibody for total protein (**Table 1-1**).

Intracellular ROS Assay

Intracellular ROS levels were determined using the fluorescent probe, 2',7'-dichlorofluorescein diacetate (DCFDA; Cat. No. D6883) from Thermo Fisher Scientific (MA, U.S.A.). The three–five-hour serum-starved, six days post-differentiated adipocytes were incubated with 2 μM DCFDA in either the presence or absence of 10 mM NAC for 30 minutes at 37°C in the dark, followed by treatment with either 500 μM H_2O_2 for 30 minutes or 2.5 mM MG for one hour. Fluorescence levels were then measured in the fluorescence reader, Tecan Infinite F-200 microplate reader (Tecan Inc., Maennedorf, Switzerland) with excitation/emission at 485/535 nm. These values were normalized to the cell number of the corresponding samples, as indicated by fluorescence levels from 30 minutes of 2 μg/ml of Hoechst 33342 (Nacalai Tesque; Cat. No. 23491-52-3) staining with excitation/emission at 360/465 nm.

RNA Preparation and Quantification of Gene Expression

Total RNA was isolated from cultured cells using Sepasol Super-I (Nacalai Tesque; Cat. No. 09379-84) following the manufacturer's protocol. Total RNA was reverse-transcribed using M-MLV reverse transcriptase (Promega; Cat. No. M1708) according to the manufacturer's instructions using a thermal cycler (Takara PCR Thermal Cycler SP, Takara, Shiga, Japan). mRNA expression was quantified by real-time PCR using the SYBR® Green I assay system performed with a LightCycler (Roche Diagnostics, Mannheim, Germany). The

protocol for amplification was as follows: denaturation at 95°C for 15 seconds, annealing at 60°C for 15 seconds, and extension at 72°C for 45 seconds. The expression levels of these genes were normalized to those of *Rplp0*. The primer sequences are listed in **Table 1-2**.

Table 1-2. Oligonucleotide primers used for mRNA analysis in this study.

Gene	Forward Primer (5'→3')	Reverse Primer (5'→3')
Rplp0	TCCTTCTTCCAGGCTTTGGG	GACACCCTCCAGAAAGCGAG
Pai1	CGCCTTCATTTGGACGAAACT	CAGGGAGAAGGCTCGCTATTG
Ptgs2	CAGTTTTTCAAGACAGATCATAAGCG	TGCTCCTGGTTGAGTATGTCG
Il6	CTGATGCTGGTGACAACCAC	TTTTCTGCAAGTGCATCATCGT
Ccl2	GACCCCAAGAAGGAATGGGT	ACCTTAGGGCAGATGCAGTT

Statistical Analysis

Statistical analyses were performed using the GraphPad Prism software (version 9.3.1; CA, U.S.A.). Statistical significance was determined using one-way analysis of variance followed by Tukey's multiple comparison test. Differences were considered statistically significant at $P < 0.05$.

Results

MG reduced insulin-stimulated glucose uptake and attenuated insulin signalling

Adipocytes play a crucial role in the regulation of physiological energy balance, and its dysfunction results in the onset of diabetes. This makes it a suitable cell model to study the involvement of MG in diabetes. Insulin is a major endocrine hormone which plays a major role in the regulation of glucose metabolism in adipocytes, increasing the rate of glucose transport across the cell membrane from two to ten-fold as well as increasing the rate of glycolysis via the enhancement of glycolytic enzymes such as hexokinase and 6-phosphofructokinase activity [86,87]. To investigate if MG contributes to insulin resistance via its effect on adipocytes, the changes to adipocyte glucose uptake and insulin response upon exposure to MG was investigated. Prior to the start of that investigation, MTS assay was first performed under short-term (two hours) and long-term (24 hours) MG treatment at different doses to determine the maximum dose by which MG did not affect adipocyte viability. This was to ease the assessment of the effects of MG on adipocyte physiology. As can be observed by the results in **Fig. 2-1(A)** and **Fig. 2-1(B)**, the maximum concentration of MG which posed no significant threat to cell viability after both short (two hours) and long (24 hours) term treatments was at 2.5 mM. Therefore, the concentration of MG for treatment of adipocytes was set at 2.5 mM. Next, to investigate the effect of MG on adipocyte glucose metabolism, the effect of MG on adipocyte glucose uptake was assessed by measuring the remaining glucose in the cell culture medium after adipocytes were incubated with MG in FBS-free medium or basic medium under normal culture conditions for 24 hours. FBS already contains insulin, and additional insulin did not increase glucose uptake into the cells (**Fig. 2-1(C)**). Meanwhile, cells incubated in basic medium which contains FBS exhibited significantly increased glucose uptake compared to those incubated in FBS-free medium (**Fig. 2-1(D)**). On the other hand, it was found that adipocytes incubated in basic medium with MG present had significantly reduced glucose

uptake compared to the control FBS group (**Fig. 2-1(D)**), suggesting that MG inhibited insulin-stimulated glucose uptake. However, this inhibitory effect of MG on insulin-stimulated glucose uptake was found to be not permanent, but was instead reversible. This was observed through adipocytes that were first incubated with MG in FBS-free medium for four hours before culture in basic medium in the absence of MG for 24 hours. Unlike the result observed in **Fig. 2-1(D)**, the adipocytes previously treated with MG showed no significant decrease in glucose uptake when compared to the control group when both were cultured in basic medium (**Fig. 2-1(E)**). Although glucose uptake did not seem to be completely recovered in MG-treated adipocytes, this phenomenon suggests that adipocytes are capable of reverting back to a more insulin-sensitive state upon the removal of MG.

Next, to further confirm that MG induced a decrease in adipocyte glucose uptake (**Fig. 2-1(D)**) through its negative effects on insulin-stimulation, insulin-induced glucose uptake was tested using a glucose cellular uptake measurement kit which utilizes 2-DG as a means to identify glucose uptake into the cells. Since serum contains insulin, mature 3T3-L1 adipocytes were first starved of serum for three–five hours to completely remove insulin as well as its remaining metabolic effects on the adipocytes. Only then were the adipocytes pre-treated with MG before stimulation by insulin and subsequent assay for cellular glucose uptake. As seen by the results in **Fig. 2-1(F)**, while insulin induced a cellular 2-DG uptake of approximately two times in the adipocytes, pre-treatment with MG completely abolished insulin-induced 2-DG uptake as the adipocytes exhibited a 2-DG uptake that did not significantly differ from the unstimulated control. This result confirmed the results in **Fig. 2-1(D)** that MG exerted negative effects on the insulin signalling pathway in adipocytes.

Many insulin responses require IRS-1 and IRS-2 to regulate metabolism [88]. The IRS proteins, IRS-1 and IRS-2 are one of the major targets of insulin receptor tyrosine kinase and are necessary for hormonal control of glucose metabolism due to its role as the primary

mediator of the insulin signalling pathway. Because IRS-1 plays an important role in the metabolic actions of insulin and insulin-like growth factor (IGF)-1 mainly in adipose tissues and skeletal muscles, as opposed to IRS-2 which plays an important role in the metabolic actions of these hormones in the liver [89], IRS-1, rather than IRS-2, is the main focus in this research. During insulin stimulation, IRS-1 is phosphorylated by the insulin receptor tyrosine kinase on several tyrosine residues which induces the activation of the insulin signalling pathway, leading to the activation of downstream proteins such as Akt. Akt is yet another key effector within the insulin signalling pathway as it mediates critical metabolic processes, such as glucose and lipid metabolism, in insulin-responsive tissues. Specifically, Akt is responsible in promoting glucose uptake via activation of its direct target, a substrate of 160 kDa (AS160), also known as TBC1 domain family member (TBC1D)-1, a Rab-GTPase activating protein implicated in insulin-stimulated glucose transporter 4 (GLUT4) translocation for increasing cellular glucose uptake [90]. In addition, Akt is also responsible for increased conversion of glucose to glucose 6-phosphate by its stimulatory effect on hexokinase in intracellular compartments [90]. Phosphorylation of Akt at Ser473 is considered crucial for the full activation of Akt [91]. Hence, to examine the effect of MG on the insulin signalling pathway in adipocytes, the insulin-stimulated phosphorylation levels of both IRS-1 tyrosine residues as well as Akt at Ser473 were examined in serum-starved 3T3-L1 adipocytes that were pre-treated with MG. Insulin-stimulation increased the phosphorylation levels of IRS-1 tyrosine residues and Akt at Ser473, by approximately three-fold (**Fig. 2-1(G)**) and five-fold (**Fig. 2-1(H)**), respectively, when compared with the unstimulated control. However, in the MG pre-treatment group, insulin-induced phosphorylation of these sites was attenuated at two-fold for IRS-1 tyrosine residues (**Fig. 2-1(G)**), and 2.5-fold for Akt at Ser473 (**Fig. 2-1(H)**), upon comparison with the basal control. Meanwhile, MG did not seem to have a significant impact on basal levels of IRS-1 tyrosine phosphorylation (**Fig. 2-1(G)**). By these results, MG negatively

affected the insulin signalling pathway as hypothesised, evidenced by significantly reduced levels of insulin-stimulated IRS-1 multiple tyrosine phosphorylation (**Fig. 2-1(G)**) and Akt phosphorylation (**Fig. 2-1(H)**). Altogether, these results imply that the negative influence that MG had exerted on glucose uptake (**Fig. 2-1(D)**), and by extension, glucose metabolism, is attributed to the negative regulatory effects of MG on the insulin signalling pathway (**Fig. 2-1(G–H)**) and subsequent insulin-stimulated glucose uptake (**Fig. 2-1(F)**).

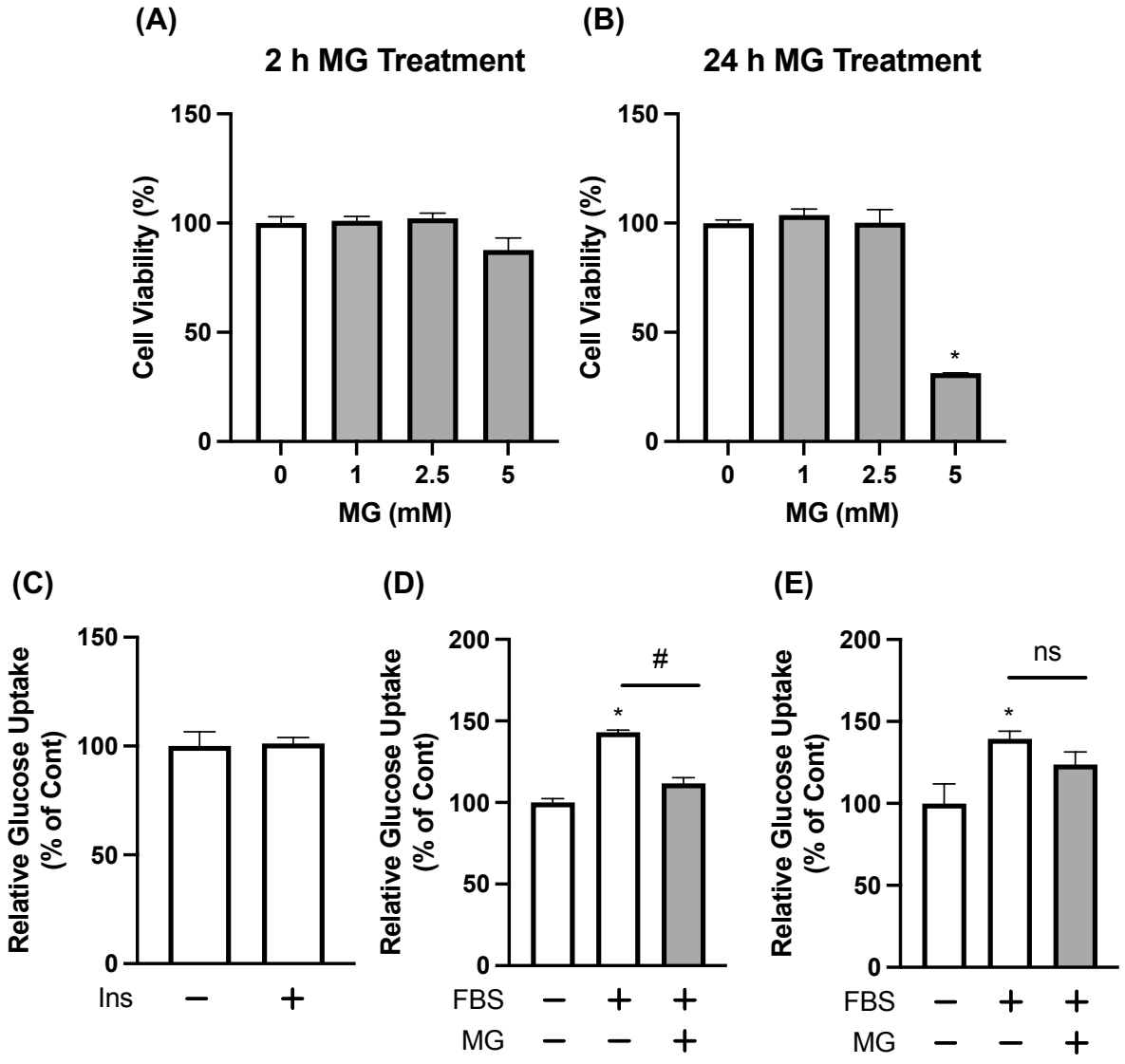

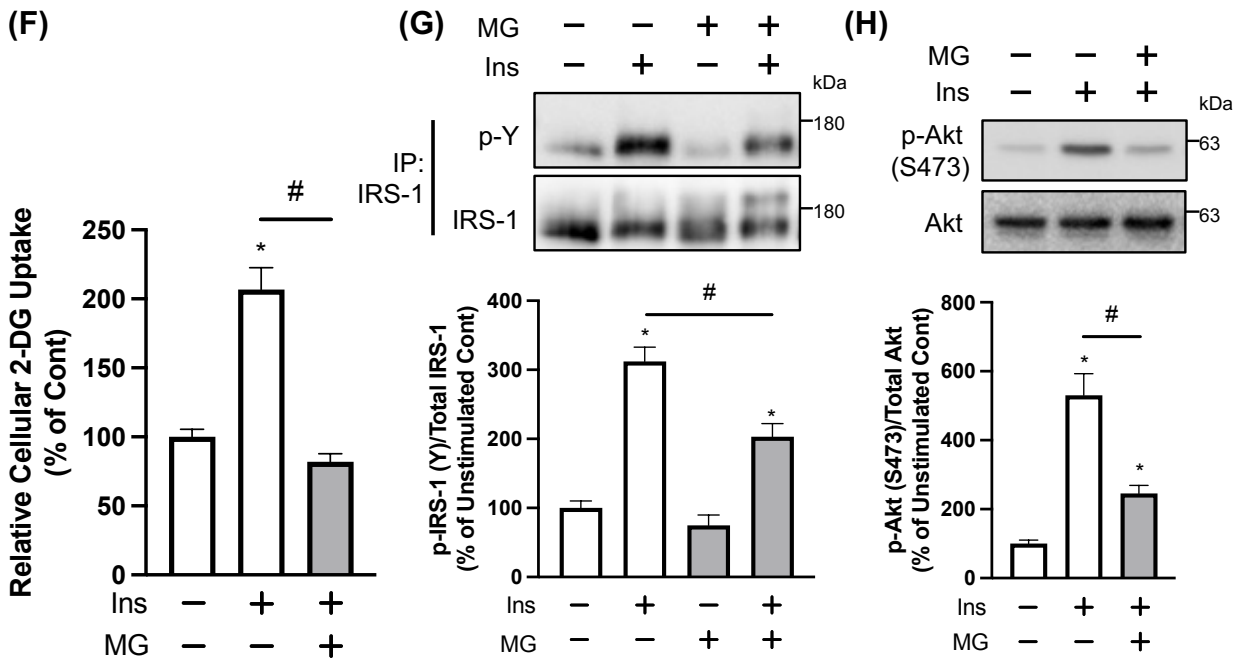

Figure 2-1. MG reduced insulin-stimulated glucose uptake and attenuated insulin signalling **(A-B)** 3T3-L1 adipocytes were treated with 1, 2.5, or 5 mM MG for 2 h **(A)** or 24 h **(B)**. MTS assay was then conducted. **(C–E)** 3T3-L1 adipocytes were incubated under ordinary cell culture conditions in basic medium with or without 0.86 μM insulin (Ins) for 48 h **(C)**, or in either FBS-free medium or basic medium with or without 2.5 mM MG for 24 h **(D)**, or in FBS-free medium with or without 2.5 mM MG for 4 h before switching to basic medium without MG for 24 h **(E)**. Glucose uptake into the cells was then determined by measuring glucose remaining in the cell culture medium. **(F)** 3T3-L1 adipocytes were treated with or without 2.5 mM MG for 4 h before glucose cellular uptake assay was then conducted. **(G)** 3T3-L1 adipocytes were treated with or without 2.5 mM MG for 4 h. The cells were then stimulated with 1 μM Ins for 15 min before immunoprecipitation (IP) was conducted with monoclonal antibodies against IRS-1. **(H)** Adipocytes were treated with 2.5 mM MG for 30 min before 30 min of 10 nM Ins stimulation. Levels of phosphorylated tyrosine (p-Y) and IRS-1 **(G)**; phosphorylated Akt (p-Akt) and Akt **(H)** were determined using anti-phosphotyrosine, anti-IRS-1, anti-phospho Akt Ser473 and anti-Akt antibodies, respectively. p-IRS-1 and p-Akt levels were quantified by measuring the intensity of the immunoreactive bands using the ImageJ software. The ratio of p-IRS-1/IRS-1 and p-Akt/Akt in the non-treated vehicular control group was assigned a relative value of 100. Quantitative data are presented as the mean ± standard error of the mean (SEM) (error bars), with n = 3 **(A,B)**, 4 **(D,F)**, 5 **(G)** or 6 **(C,E,H)** per group. Student's *t*-test **(C)** or one-way ANOVA followed by Tukey's post-hoc test was conducted to determine the statistical significance **(A–F)**. *, $P < 0.05$ between the non-treated vehicular control group and respective groups. #, $P < 0.05$ between the indicated groups. ns, non-significant differences between the indicated groups.

MG caused multiple serine phosphorylation on IRS-1

While multiple tyrosine phosphorylation IRS proteins is required to activate several downstream effectors of the insulin signalling, multiple serine or threonine phosphorylation leads to the impairment of insulin response and insulin resistance [72,92]. This negative regulation of IRS proteins may involve the phosphorylation of more than 50 serine/threonine residues within the IRS proteins, with different serine/threonine sites being phosphorylated by different serine/threonine kinases which respond to different stimuli [72,92]. Stimuli such as TNFα, FFAs and cellular stress activate IRS serine/threonine kinases including JNK, protein kinase C (PKC), mTOR, S6K, IKK, ERK that phosphorylate the IRS proteins on their corresponding serine or threonine residues which inhibits IRS activity. Depending on the phosphorylation status of serine/threonine at particular sites, or the combination of simultaneous phosphorylation of a number of specific serine/threonine residues, IRS is negatively regulated by different mechanisms, which may involve tyrosine dephosphorylation of IRS, IRS dissociation from the insulin receptor, IRS intracellular localisation and eventual degradation [72,92]. However, neither the role of serine/threonine phosphorylation, nor molecular mechanisms responsible for their activation are fully understood. As observed in **Fig. 2-1(D,F)**, MG significantly reduced levels of insulin-stimulated IRS-1 multiple tyrosine phosphorylation, suggesting that MG may play a role in its inhibition by affecting IRS-1 serine/threonine phosphorylation. Since IRS is regulated by multiple phosphorylation, and that proteins exhibit a phosphorylation dependent electrophoretic mobility shift (PDEMS) in SDS-PAGE [93], the possibility that MG affects IRS-1 serine/threonine phosphorylation was first investigated by observing if PDEMS can be observed in IRS-1 from adipocytes treated by MG. Treatment of 3T3-L1 adipocytes with MG increased PDEM of IRS-1, starting at 15 minutes, and peaking by 60 minutes (**Fig. 2-2(A)**). Investigation into the phosphorylation of relatively well-investigated negative regulatory serine sites of IRS1 such as Ser307, 318 and 612 revealed

that MG treatment significantly increased the phosphorylation of all those sites (**Fig. 2-2(B–D)**). These results imply that MG attenuated insulin-stimulated glucose uptake (**Fig. 2-1(D,F)**) via its negative effect on insulin-induced IRS-1 activity.

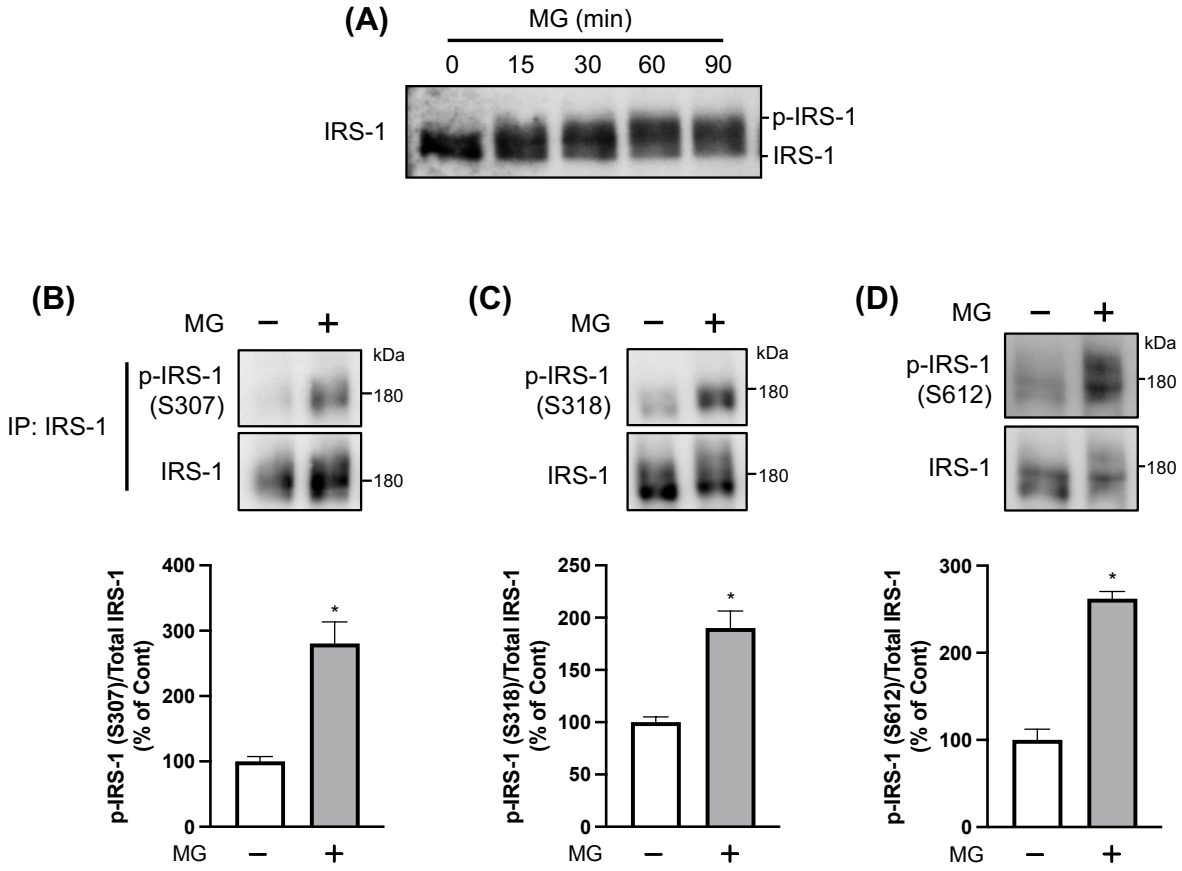

Figure 2-2. MG caused multiple serine phosphorylation on IRS-1
(A) The 3T3-L1 adipocytes were treated with 2.5 mM MG for the indicated durations. **(B-D)** Cells treated with 2.5 mM MG for 60 min. Immunoprecipitation (IP) was conducted with monoclonal antibodies against IRS-1 **(B)**. Levels of phosphorylated IRS-1 (p-IRS-1) at the serine residues-307 **(B)**, 318 **(C)**, and 612 **(D)**; and IRS-1 were determined using anti-phospho IRS-1 Ser307, Ser318, Ser612 and anti-IRS-1 antibodies, respectively. p-IRS-1 levels were quantified by measuring the intensity of the immunoreactive bands using the ImageJ software, the ratio of p-IRS-1/IRS-1 in the non-treated vehicular control group being assigned a relative value of 100. Quantitative data are presented as the mean ± SEM (error bars), with n = 6 **(B–D)** per group. Welch's **(B–C)** or Student's **(D)** *t*-test were conducted to determine the statistical significance. *, $P < 0.05$ between the non-treated vehicular control group and respective groups.

MG activated the mTORC1 signalling pathway

As aforementioned, various stimuli could activate IRS serine/threonine kinases to negatively regulate it. Apart from extracellular stimuli, the insulin signalling pathway, itself is also structured to terminate its own activation to prevent prolonged activation. This is mainly done via the activation of Akt in response to insulin, which simultaneously propagates insulin signalling while also activating the negative feedback loop which promotes the phosphorylation of IRS1 on serine residues in order to terminate continuous insulin signalling. In more detail, the negative feedback loop of the insulin signalling pathway involves the control of Akt over Rheb GTPase activity via regulation of the Tuberous Sclerosis Complex (TSC)-1–TSC2 complex, a GTPase-activating protein (GAP) [81], and it is this activation of the Rheb GTPase which induces mTORC1 activity, subsequently contributing towards the negative regulation of IRS-1 by phosphorylation its serine/threonine residues. Since mTORC2 is a direct modulator upstream of Akt, mTORC2 is also a component of the insulin signalling pathway involved in the regulation of mTORC1 activity; in other words, mTORC1 is one of the downstream effectors of mTORC2 signalling [81]. It has previously been reported that MG activates mTORC2 signalling and enhances the phosphorylation levels at Ser473 of Akt in 3T3-L1 adipocytes [83]. Therefore, the effect of MG on the negative feedback loop of the insulin signalling pathway, mTORC1 signalling, was first examined by monitoring the phosphorylation levels of the mTORC1 effector, p70 S6K1, as an indicator. The phosphorylation levels at Thr389 of p70 S6K1 in 3T3-L1 adipocytes were enhanced within 60 min of the addition of 2.5 mM MG (**Fig. 2-3(A)**), and this MG-induced increase in phosphorylation levels of p70 S6K1 within 60 min of MG treatment was found to start at MG concentrations of 0.5 mM, suggesting that MG induced mTORC1 activity at concentrations from as low as 0.5 mM (**Fig. 2-3(B)**). Furthermore, this effect of MG on the phosphorylation

levels of p70 S6K1 was completely abolished by rapamycin, an mTORC1 inhibitor, confirming that MG activated mTORC1 signalling (**Fig. 2-3(C)**).

The phosphorylation of serine residues on IRS-1 at Ser307, 318, and 612 are also modulated by mTORC1 and its effector, p70 S6K1 [72,92,94,95,96]. Upon further investigation to see if the MG-induced phosphorylation on IRS-1 at these serine residues were nullified by mTORC1 inhibition, it was found that rapamycin pre-treatment in MG treated-adipocytes also exhibited significantly reduced phosphorylation of all three of those serine residues (**Fig. 2-3(D–E)**). Hence, the MG-induced multiple serine phosphorylation of IRS-1 as seen in **Figs. 2-2; 2-3(D–E)**, at least pertaining to the IRS-1 serine residues of Ser307, 318, and 612, could be attributed to MG-induced mTORC1 activation.

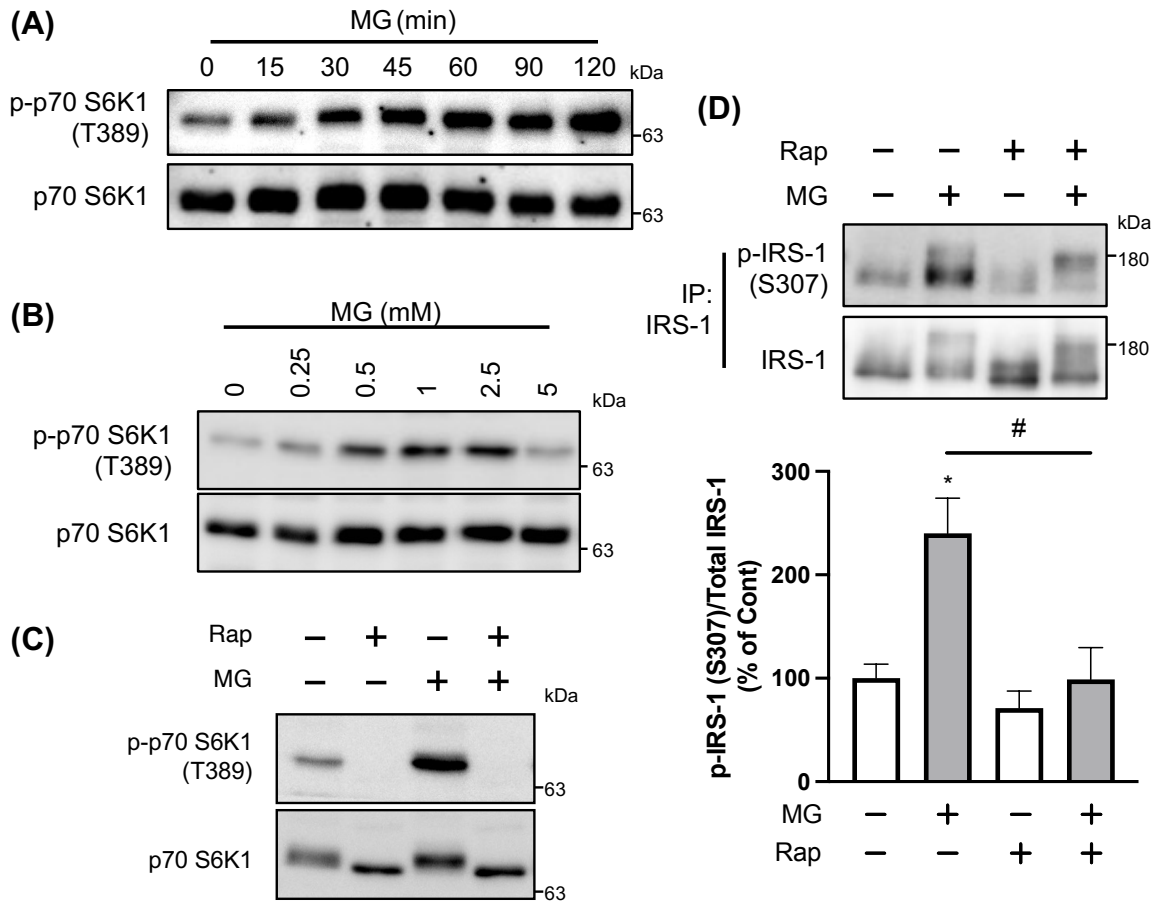

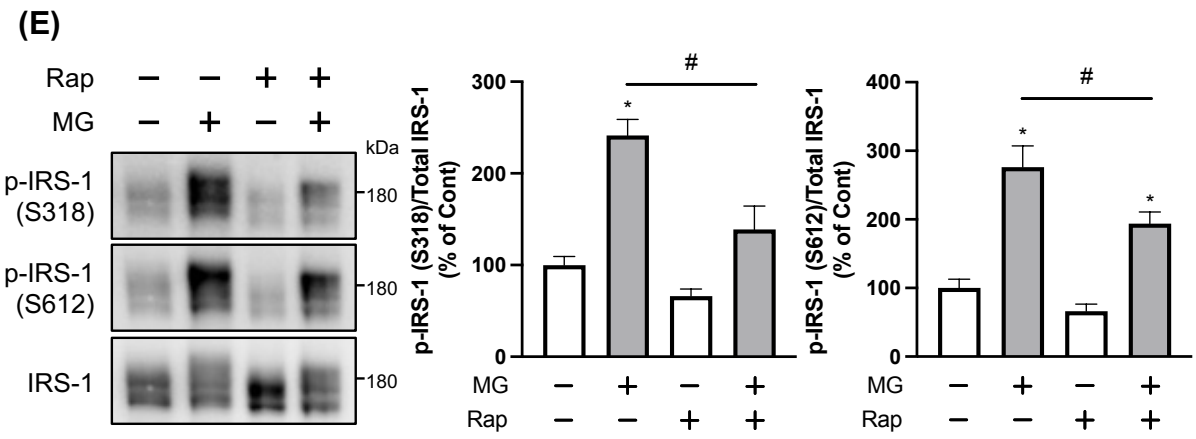

Figure 2-3. MG activated the mTORC1 signalling pathway

(A) The 3T3-L1 adipocytes were treated with 2.5 mM MG for the indicated durations. **(B)** The adipocytes were treated with the indicated concentrations of MG for 60 min. **(C-E)** The adipocytes were treated with or without 20 nM rapamycin (Rap) for 30 min, followed by treatment with 2.5 mM MG for 60 min. Immunoprecipitation (IP) was also conducted with monoclonal antibodies against IRS-1 **(D)**. Phosphorylated p70 S6K1 (p-p70 S6K1) and p70 S6K1 **(A-C)**; phosphorylated IRS-1 (p-IRS-1) at the serine residues-307 **(D)**, 318 and 612 **(E)** and IRS-1 were determined using the anti-phospho p70 S6K Thr389 and anti-p70 S6K; anti-phospho IRS-1 Ser307, Ser318, Ser612, and anti-IRS-1 antibodies, respectively. p-p70 S6K1 and p-IRS-1 levels were quantified by measuring the intensity of the immunoreactive bands using the ImageJ software, the ratio of p-p70 S6K1/ p70 S6K1 and p-IRS-1/IRS-1 in the non-treated vehicular control group being assigned a relative value of 100. Quantitative data are presented as the mean ± SEM (error bars), with n = 4 **(D–E)** per group. One-way ANOVA followed by Tukey's post-hoc test was conducted to determine the statistical significance **(D–E)**. *, $P < 0.05$ between the non-treated vehicular control group and respective groups. #, $P < 0.05$ between the indicated groups.

mTORC1 inhibition recovered MG-inhibited insulin signalling and glucose uptake

Seeing that inhibition of mTORC1 by rapamycin could suppress multiple phosphorylation on IRS-1 serine residues (**Fig. 2-3(D–E)**), the investigation proceeded towards whether or not pre-treatment of adipocytes with rapamycin could recover the attenuated insulin signalling as well as reduced glucose uptake that was caused by MG treatment (**Fig. 2-1**). Pre-treatment of 3T3-L1 adipocytes with rapamycin not just completely recovered the inhibited insulin-induced IRS-1 multiple tyrosine phosphorylation in the MG-treated group (**Fig. 2-4(A)**), it also returned the inhibited insulin-induced phosphorylation levels of Akt at Ser473 back to phosphorylation levels that is comparable to that of the stimulated control (**Fig. 2-4(B)**). The magnitude of increase in insulin-stimulated phosphorylation levels of Akt at Ser473 in adipocytes pre-treated with rapamycin alone (**Fig. 2-4(C)**) did not compare to the magnitude of increase in insulin-stimulated phosphorylation levels of Akt at Ser473 in adipocytes pre-treated with both rapamycin and MG (**Fig. 2-4(B)**). This suggests that insulin signalling attenuated by MG that was recovered through rapamycin pre-treatment was not due to the isolated positive effects of rapamycin to insulin signalling.

Next, the effect of mTORC1 inhibition on MG-inhibited insulin-stimulated cellular glucose uptake was assessed. Contrary to expectations, pre-treatment of adipocytes with rapamycin had no effect on the inhibition of MG on insulin-stimulated cellular 2-DG uptake (**Fig. 2-4(D)**). However, upon measuring glucose uptake after 24 hours of incubation with MG under normal cell culture conditions, pre-treatment of adipocytes with rapamycin could recover glucose uptake that was inhibited by MG treatment back to levels that was similar to the untreated group (**Fig. 2-4(E)**). Therefore, despite unexpected results on insulin-stimulated cellular glucose uptake, these data suggest that inhibition of mTORC1 could recover MG-inhibited insulin signalling and glucose uptake.

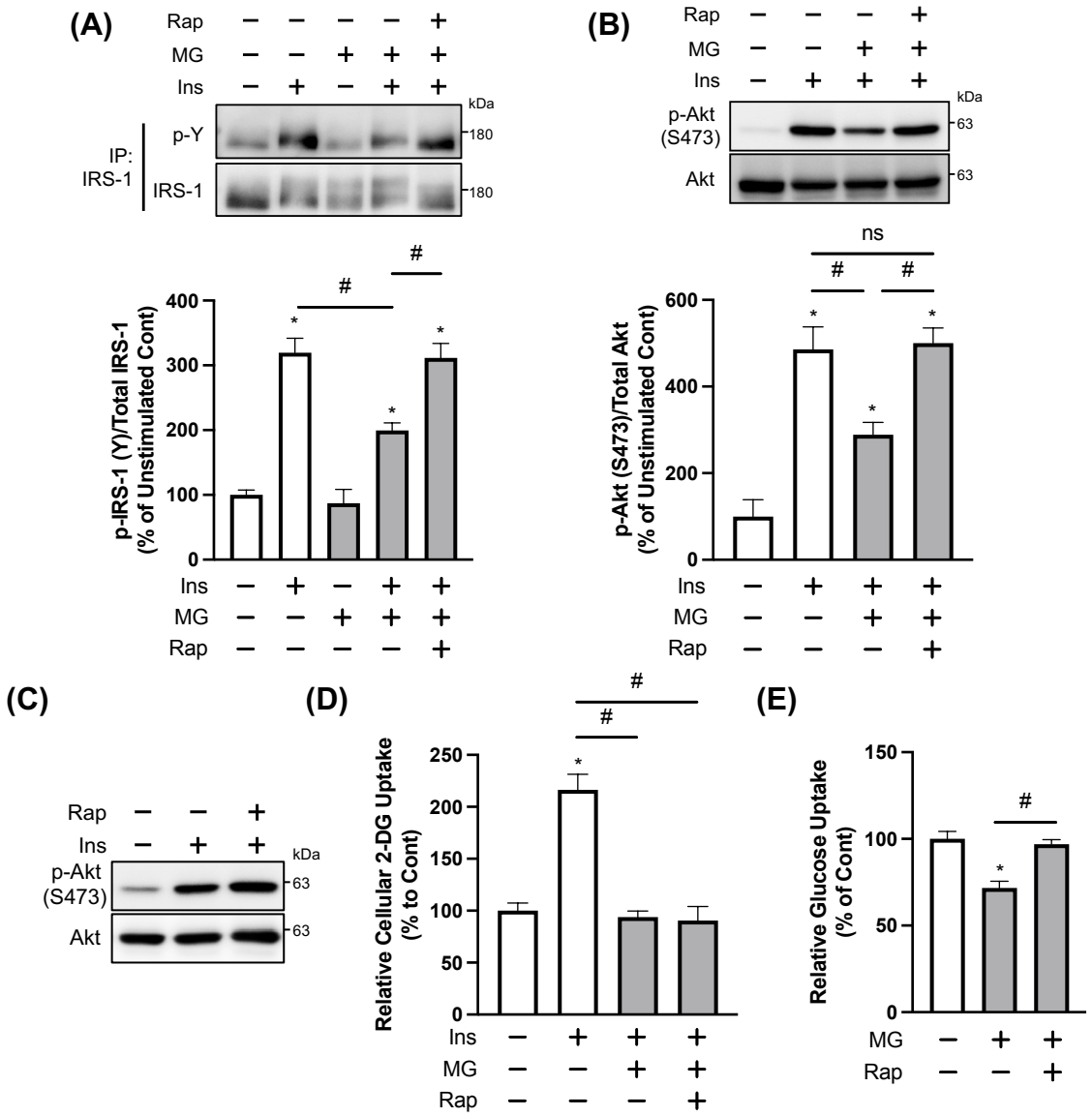

Figure 2-4. mTORC1 inhibition recovered MG-inhibited insulin signalling and glucose uptake **(A)** 3T3-L1 adipocytes were treated with or without 20 nM rapamycin (Rap) for 30 min, followed by treatment with 2.5 mM MG for 4 h. The cells were then stimulated with 1 μM insulin (Ins) for 15 min before immunoprecipitation (IP) was conducted with monoclonal antibodies against IRS-1. **(B–C)** Adipocytes were pre-treated with or without 20 nM Rap for 30 min, followed by treatment with or without 2.5 mM MG for 30 min. Then, the cells were stimulated by 10 nM Ins for 30 min. Levels of phosphorylated tyrosine (p-Y) and IRS-1 **(A)**; phosphorylated Akt (p-Akt) and Akt **(B–C)** were determined and quantified as described in the legend of **Figure 2-1**. **(D)** 3T3-L1 adipocytes were treated with or without 20 nM Rap for 30 min, followed by treatment with 2.5 mM MG for 4 h. Glucose cellular uptake assay was then conducted. **(E)** 3T3-L1 adipocytes were treated with or without 20 nM Rap for 30 min in basic medium, followed by treatment with 2.5 mM MG for 24 h. Glucose uptake into the cells was then determined by measuring glucose remaining in the cell culture medium. Quantitative data are presented as the mean ± SEM (error bars), with n = 3 **(A)** or 4 **(B,D,E)** per group. One-way ANOVA followed by Tukey's post-hoc test was conducted to determine the statistical significance **(A,B,D,E)**. *, $P < 0.05$ between the non-treated vehicular control group and respective groups. #, $P < 0.05$ between the indicated groups. ns, non-significant differences between the indicated groups.

MG induced mTORC1 activity independently of AKT

The negative feedback loop of the insulin signalling pathway involves the positive control of Akt over Rheb GTPase activity via the removal of the inhibitory action of TSC1–TSC2 complex [81] on Rheb GTPase. This Akt-dependent inhibition of TSC1–TSC2 complex activity activates Rheb GTPase which induces mTORC1 activity, subsequently contributing towards the negative regulation of IRS-1 by phosphorylation its serine/threonine residues. To examine whether Akt is necessary for MG-induced activation of mTORC1 signalling, the effect of an Akt inhibitor on the phosphorylation levels of p70 S6K1, as well as IRS-1 were determined. While Akt inhibitor inhibited the insulin-stimulated increase in mTORC1 activity, as evidenced by significantly reduced insulin-stimulated p70 S6K1 phosphorylation (**Fig. 2-5(A)**); unexpectedly, the Akt inhibitor neither abrogated the increased phosphorylation of p70 S6K1 nor the PDEMS on IRS-1 that were induced by MG treatment (**Fig. 2-5(B–C)**). Akt phosphorylates TSC2 at Thr1462 to inhibit its inhibitory activity on mTORC1 [97]; in other words, Akt phosphorylation of TSC2 induces mTORC1 activity. To further show that Akt is uninvolved in MG-induced mTORC1 activity, the phosphorylation status of TSC2 at Thr1462 was confirmed to show no significant increase upon MG treatment (**Fig. 2-5(D)**). These results altogether suggest that MG activates mTORC1 signalling through a pathway different from the Akt–mTORC1 axis.

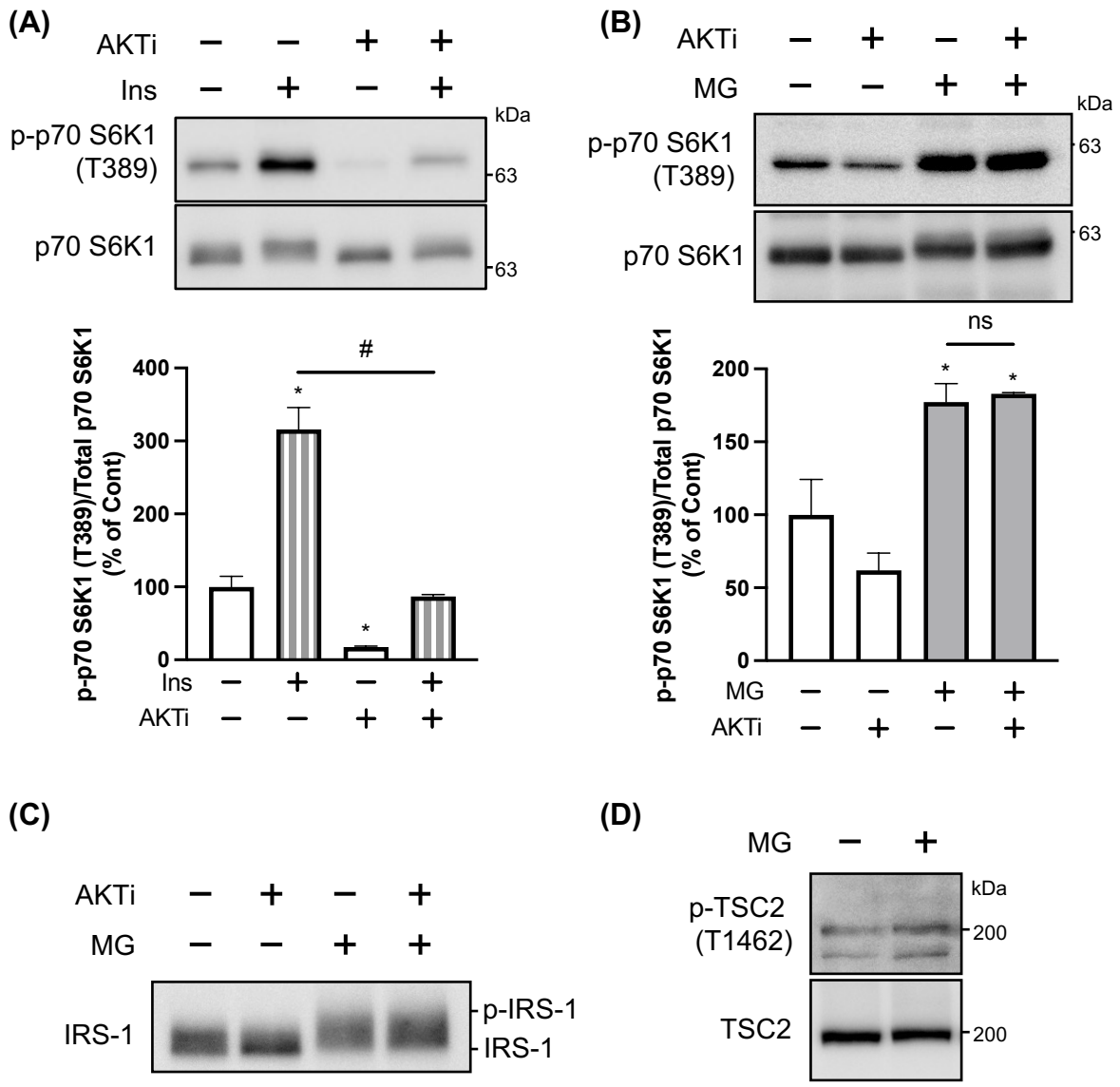

Figure 2-5. MG induced mTORC1 activity independently of Akt

(A) 3T3-L1 adipocytes were pre-treated with 5 μM AKT inhibitor VIII (AKTi) for 30 min before 15 min of 10 nM insulin (Ins) stimulation. **(B–D)** 3T3-L1 adipocytes were treated with or without 5 μM AKT Inhibitor VIII (AKTi) for 30 min, followed by treatment with 2.5 mM MG for 60 min. Phosphorylated p70 S6K1 (p-p70 S6K1) and p70 S6K1 **(A–B)**; IRS-1 **(C)**; and phosphorylated TSC2 (p-TSC2) and TSC2 **(D)** were determined using the anti-phospho p70 S6K Thr389, anti-p70 S6K, anti-IRS-1, anti-phospho TSC2 Thr 1462, and TSC2 antibodies, respectively. p-p70 S6K1 levels were quantified by measuring the intensity of the immunoreactive bands using the ImageJ software, and the ratio of p-p70 S6K1/p70 S6K1 in the non-treated vehicular control group being assigned a relative value of 100. Quantitative data are presented as the mean ± SEM (error bars), with n = 3 **(A–B)** per group. One-way ANOVA followed by Tukey's post-hoc test was conducted to determine the statistical significance **(A–B)**. *, $P < 0.05$ between the non-treated vehicular control group and respective groups. ns, non-significant differences between the indicated groups.

MG activated the mTORC1 signalling pathway via p38 MAPK

Next, the mechanism by which MG activated mTORC1 signalling, as observed in **Fig. 2-3**, was explored. In addition to TOR signalling, MG is known to induce the activation of the JNK, p38 MAPK, and extracellular receptor kinase (ERK) MAPK signalling pathways in various cultured cells [67,98,99,100]. MAPK signalling pathways are essential for regulating many cellular processes through the modulation of various target proteins. Several studies have shown that JNK, p38 MAPK, and ERK are involved in mTORC1 activation via direct or indirect machineries [101,102,103,104,105,106,107]. As shown in **Fig. 2-6(A)**, the phosphorylation levels of JNK and p38 MAPK increased following treatment with MG in 3T3-L1 adipocytes, although MG did not significantly affect ERK phosphorylation. Activation of JNK induces *Pai1* expression [108,109,110] while p38 MAPK activation leads to downstream CREB phosphorylation [111,112]. Both *Pai1* expression and CREB phosphorylation have been confirmed in MG-treated cells (**Fig. 2-6(B–D)**); and both *Pai1* expression and CREB phosphorylation were inhibited by their respective MAPK inhibitors, further showing that MG treatment increased JNK and p38 MAPK activity (**Fig. 2-6(B–D)**). After that, whether or not JNK and p38 MAPKs contribute to MG-induced activation of mTORC1 signalling were investigated using their respective inhibitors. SB203580, a selective inhibitor of p38 MAPK, attenuated MG-induced phosphorylation of p70 S6K1; this inhibitory effect was also confirmed with yet another p38 MAPK inhibitor, BIRB796 (**Fig. 2-6(E–F)**). However, SP600125, a selective inhibitor of JNK, did not attenuate the MG-induced phosphorylation of p70 S6K1 (**Fig. 2-6(G)**). Extending the investigation to MG-induced IRS-1 phosphorylation at the serine residues, Ser318 and 612, it was confirmed that p38 MAPK inhibition via SB203580 inhibited MG-induced phosphorylation at both serine sites on IRS-1 (**Fig. 2-6(H)**). Thus, these results suggest that MG activated the mTORC1–IRS-1 signalling via p38 MAPK activation, and not via JNK.

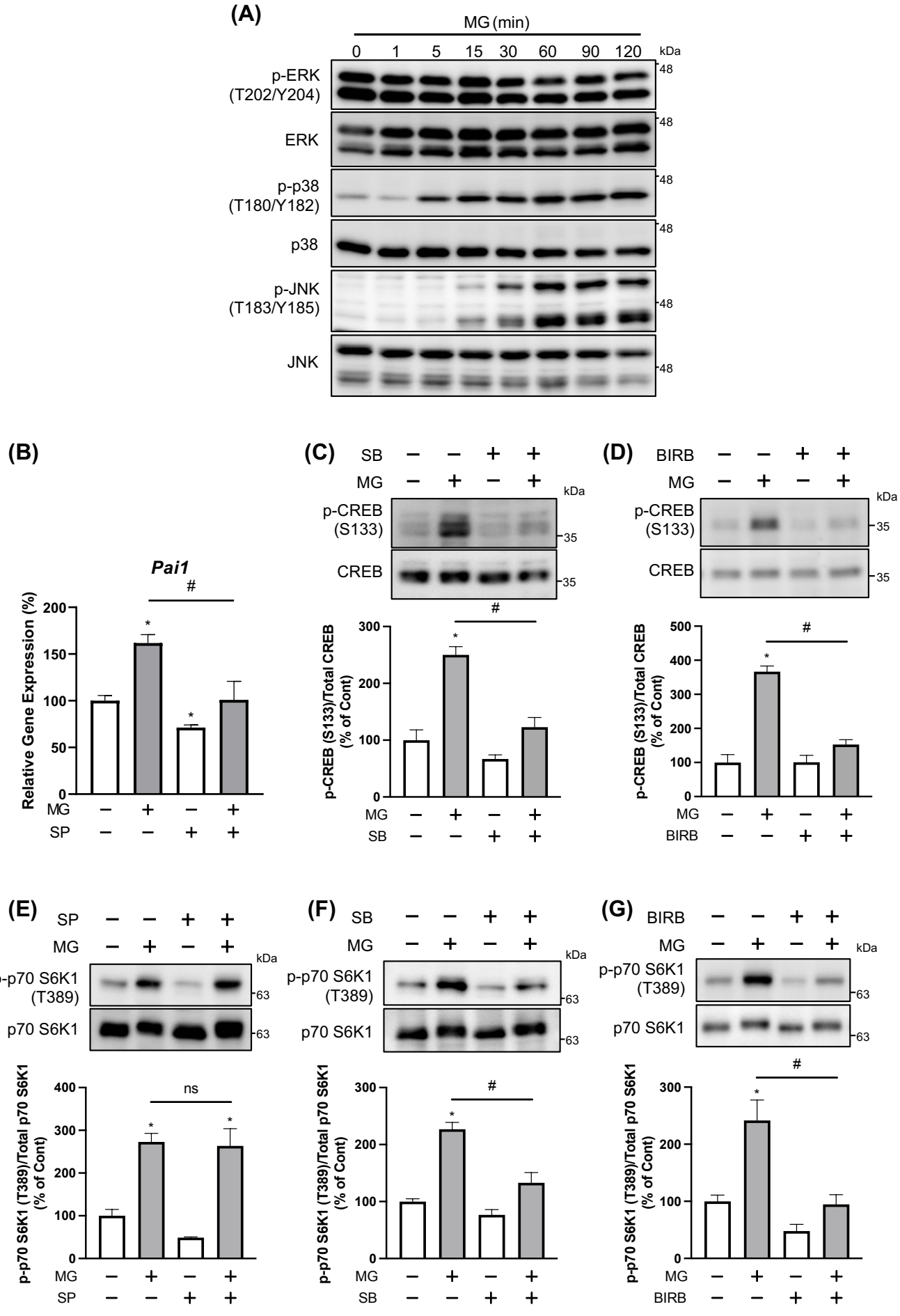
(A)
MG (min)
0 1 5 15 30 60 90 120 kDa
p-ERK (T202/Y204)
ERK
p-p38 (T180/Y182)
p38
p-JNK (T183/Y185)
JNK
48
(B)
Pai1
Relative Gene Expression (%)
MG
SP
(C)
SB
MG
p-CREB (S133)
CREB
35
p-CREB (S133)/Total CREB (% of Cont)
(D)
BIRB
MG
p-CREB (S133)
CREB
35
p-CREB (S133)/Total CREB (% of Cont)
(E)
SP
MG
p-p70 S6K1 (T389)
p70 S6K1
63
ns
p-p70 S6K1 (T389)/Total p70 S6K1 (% of Cont)
(F)
SB
MG
p-p70 S6K1 (T389)
p70 S6K1
63
p-p70 S6K1 (T389)/Total p70 S6K1 (% of Cont)
(G)
BIRB
MG
p-p70 S6K1 (T389)
p70 S6K1
63
p-p70 S6K1 (T389)/Total p70 S6K1 (% of Cont)

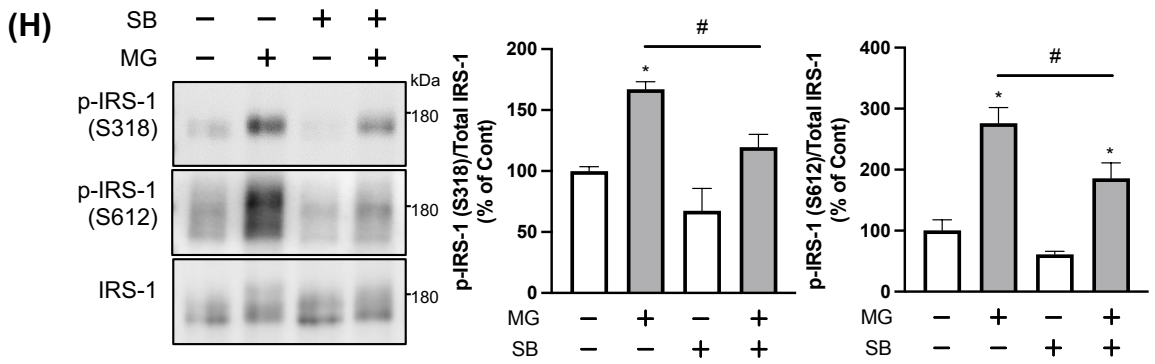

Figure 2-6. MG activated the mTORC1 signalling pathway via p38 MAPK

(A) The 3T3-L1 adipocytes were treated with 2.5 mM MG for the indicated durations. **(B)** 3T3-L1 adipocytes were pre-treated with 10 μM SP600125 (SP) for 30 min before 2 h of 2.5 mM MG treatment. mRNA expression levels of *Pai1* in the cells was then determined by real-time PCR. **(C–H)** The adipocytes were treated with or without 10 μM SB203580 (SB) **(C,F,H)**; 0.1 μM BIRB796 (BIRB) **(D,G)**; or 10 μM SP600125 (SP) **(E)** for 30 min, followed by treatment with 2.5 mM MG for 60 min. Levels of phosphorylated extracellular signal-regulated kinase (ERK) (p-ERK), ERK, phosphorylated p38 (p-p38), p38, phosphorylated JNK (p-JNK), and JNK **(A)**; and levels of phosphorylated CREB (p-CREB) and CREB **(C–D)**, were determined using anti-phospho ERK Thr202/Tyr204, anti-ERK, anti-phospho p38 Thr180/Tyr182, anti-p38, anti-phospho JNK Thr183/Tyr185, and anti-JNK **(A)**; and anti-phospho CREB Ser133 and anti-CREB antibodies **(C–D)**, respectively. Meanwhile, phosphorylated p70 S6K1 (p-p70 S6K1) and p70 S6K1 **(E-G)**; phosphorylated IRS-1 (p-IRS-1) at the serine residues- 318 and 612; and IRS-1 **(H)** were determined as described in the legend of **Figure 2-3**. p-CREB levels were quantified by measuring the intensity of the immunoreactive bands using the ImageJ software, and the ratio of p-CREB/CREB in the non-treated vehicular control group being assigned a relative value of 100. p-p70 S6K1 and p-IRS-1 levels were quantified as described in the legend of **Figure 2-3**. Data are presented as the mean ± SEM (error bars), with n = 3 **(C–D, F–G)**, 4 **(B)** or 5 **(E,H)** per group. One-way ANOVA followed by Tukey's post-hoc test was conducted to determine the statistical significance **(B–H)**. *, $P < 0.05$ between the non-treated vehicular control group and respective groups. #, $P < 0.05$; ns, non-significant differences between the indicated groups.

MG did not activate p38 MAPK via ROS production

An increase in ROS levels can adversely affect cellular function and homeostasis, leading to oxidative stress [113]. Small increases of modifications of mitochondrial proteins by MG have been linked to a two- to three-fold increase in oxidative stress [43], and in some cell lines, such as rat pheochromocytoma, human vascular endothelial, mouse glomerular mesangial, and pancreatic β-cells, MG has been reported to activate the JNK and p38 MAPK signalling pathways through ROS generation [78,79,80,114]. To determine if MG also increases ROS production in adipocytes, the effect of MG on intracellular ROS levels in 3T3-L1 adipocytes were examined. H_2O_2 treatment of 60 minutes could increase intracellular ROS levels and induce both p38 MAPK and p70 S6K1 phosphorylation in adipocytes (**Fig. 2-7(A–C)**). While short-term MG treatment of about 60 min was also sufficient to increase p38 MAPK and p70 S6K1 phosphorylation in adipocytes (**Fig. 2-6(A)**), the same duration of MG treatment in adipocytes had no significant effect on adipocyte intracellular ROS levels (**Fig. 2-7(A)**). The pre-treatment of cells with NAC, a ROS scavenger, significantly decreased the intracellular levels of ROS to below basal levels, regardless of subsequent H_2O_2 or MG treatment (**Fig. 2-7(A)**). However, while NAC attenuated H_2O_2-induced phosphorylation of both p38 MAPK and p70 S6K1, it was unable to attenuate MG-induced phosphorylation of both p38 MAPK and p70 S6K1 (**Fig. 2-7(B–C)**). These results suggest that in adipocytes, MG is not involved in ROS generation and therefore, the mechanism behind the MG-induced activation of p38 MAPK and mTORC1 did not involve ROS production.

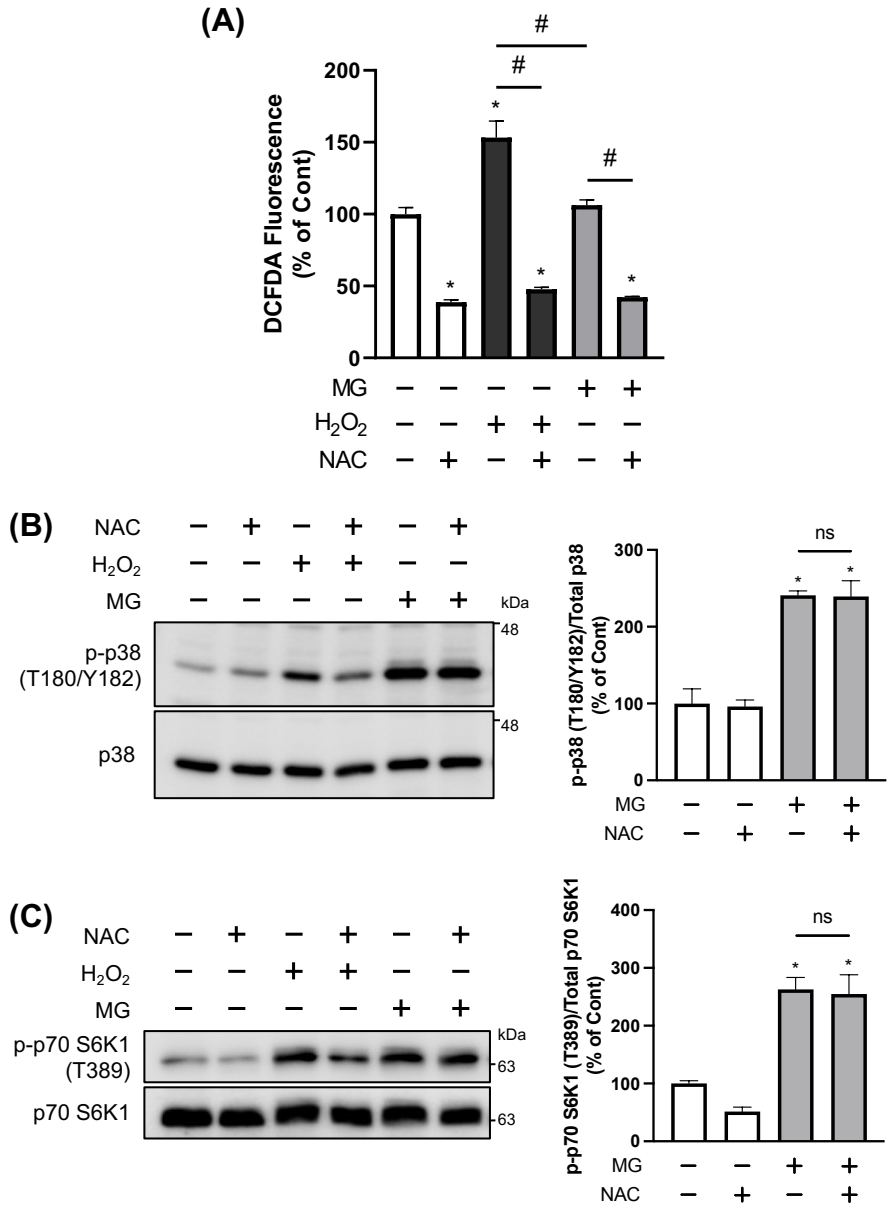

Figure 2-7. MG did not activate p38 MAPK via ROS production

(A) The 3T3-L1 adipocytes were pre-treated with 2 μM 2',7'-dichlorofluorescein diacetate (DCFDA) with or without 10 mM *N*-acetyl-L-cysteine (NAC) for 30 min, followed by treatment with either 500 μM H_2O_2 for 30 min or 2.5 mM MG for 60 min. Intracellular ROS assay was then performed. **(B–C)** adipocytes were pre-treated with or without 10 mM NAC for 30 min, followed by treatment with either 500 μM H_2O_2 for 30 min or 2.5 mM MG for 60 min. Levels of phosphorylated p38 (p-p38) and p38 **(B)**, phosphorylated p70 S6K1 (p-p70 S6K1) and p70 S6K1 **(C)** were determined as described in the legends of **Figure 2-6** and **Figure 2-3**, respectively. **(B–C)** p-p38 and p-p70 S6K1 levels were quantified by measuring the intensity of the immunoreactive bands using the ImageJ software, the ratio of p-p38/p38 as well as p-p70 S6K1/p70 S6K1 in the non-treated vehicular control group being assigned a relative value of 100. Data are presented as the mean ± SEM (error bars), with n = 4 **(A)** or 5 **(B–C)** per group. One-way ANOVA followed by Tukey's post-hoc test was conducted to determine the statistical significance **(A–C)**. *, $P < 0.05$ between the non-treated vehicular control group and respective groups. #, $P < 0.05$; ns, non-significant differences between the indicated groups.

MG activated p38 MAPK via TAK1

p38 MAPK and JNK are known to be activated through TAK1 in response to proinflammatory cytokines, such as TNFα and IL1β [84]. TAK1 is a member of the MAPK kinase kinase (MAPKKK) family and plays crucial roles in the development and homeostasis of multiple tissues, including adipose tissues [115,116]. MG has been reported to induce inflammatory responses in endothelial cells and adipose tissues [117,118]. In addition, dysfunction of MG metabolism is associated with a proinflammatory profile, as knockdown of GLO1 results in the up-regulation of several genes involved in the inflammatory pathway [74,119]. It was found that MG treatment in adipocytes also significantly increased inflammatory gene expression, and this increase in gene expression was suppressed by TAK1 inhibition by (5*Z*)-7-oxozeaenol, a selective inhibitor of TAK1 [120] (**Fig. 2-8(A)**). To examine if the proinflammatory signalling pathway is involved in the activation of p38 MAPK in response to MG, the effect of TAK1 inhibition on MG-induced phosphorylation of p38 MAPK was assessed. As shown in **Fig. 2-8(B–D)**, (5*Z*)-7-oxozeaenol attenuated MG-induced phosphorylation of p38 MAPK at Thr180 and Tyr 182 (**Fig. 2-8(B)**); this inhibitory effect was also confirmed in the case of p70 S6K1 phosphorylation at Thr389 (**Fig. 2-8(C)**) and IRS-1 serine phosphorylation at Ser318 and 612 (**Fig. 2-8(D)**). Therefore, these results show that the MG-induced activation of mTORC1–IRS-1 signalling is attributed to TAK1–p38 signalling. Finally, the effect of inhibition of the TAK1–p38–mTORC1–IRS-1 signalling axis on MG-suppressed glucose uptake was investigated. The use of the TAK1 inhibitor, (5*Z*)-7-oxozeaenol, was found to significantly recover glucose uptake that was inhibited by MG treatment to the extent that it did not significantly differ from the untreated control (**Fig. 2-8(E)**), confirming that the TAK1–p38–mTORC1 signalling axis is responsible for the inhibitory effect of MG on glucose uptake in adipocytes.

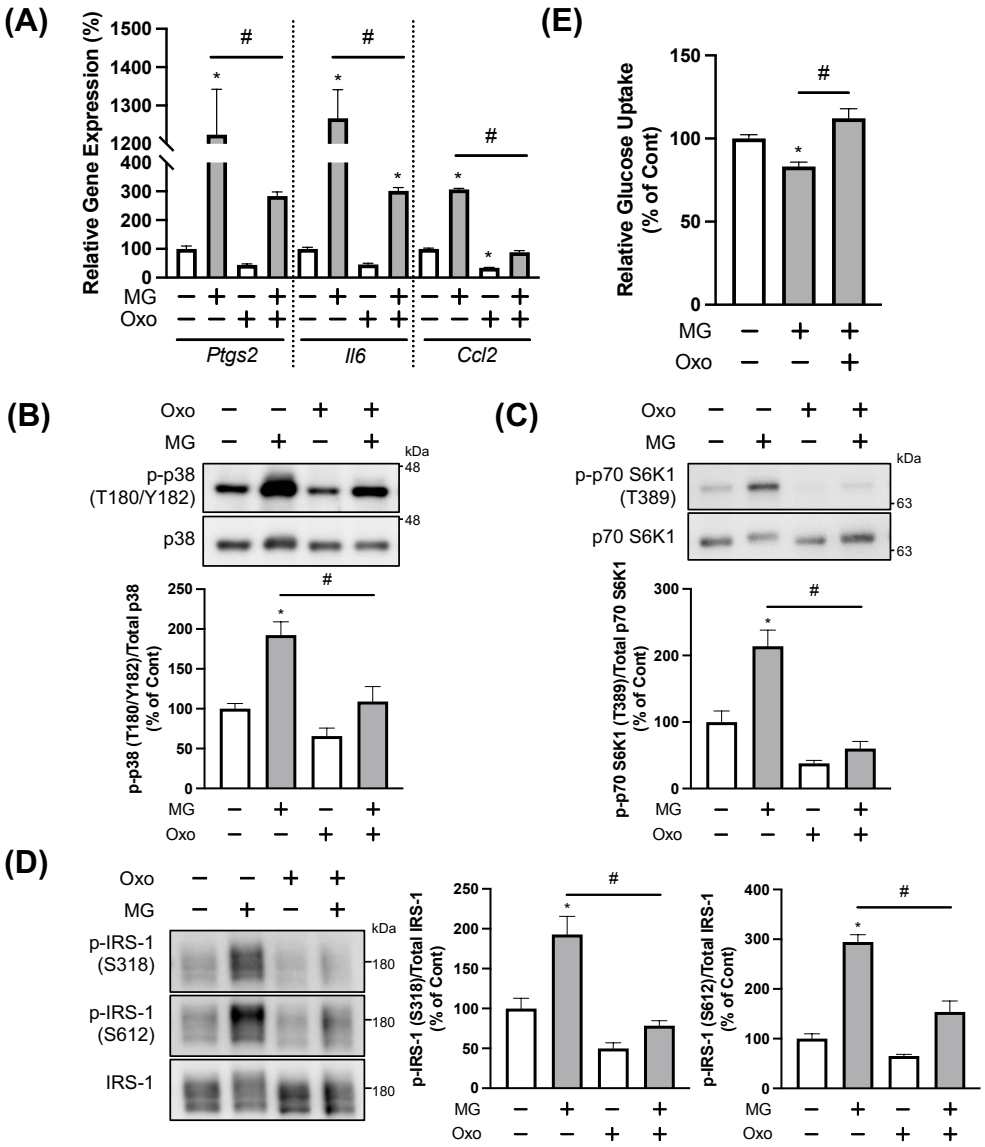

Figure 2-8. MG activated p38 MAPK via TAK1

(A) 3T3-L1 adipocytes were pre-treated with 0.5 μM (5*Z*)-7-oxozeaenol (Oxo) for 30 min before 2 h of 2.5 mM MG treatment. mRNA expression levels of *Ptgs2* (Gene encoding COX2), *Il6* and *Ccl2* (Gene encoding MCP1) in the cells were then determined by real-time PCR. **(B–E)** Adipocytes were pre-treated with or without 0.5 μM Oxo for 30 min, followed by treatment with or without 2.5 mM MG for 60 min. Levels of phosphorylated p38 (p-p38) and p38 **(B)**, phosphorylated p70 S6K1 (p-p70 S6K1) and p70 S6K1 **(C)**; phosphorylated IRS-1 (p-IRS-1) at the serine residues- 318 and 612; and IRS-1 **(D)** were determined as described in the legends of **Figure 2-6** and **Figure 2-3**. p-p38, p-p70 S6K1, p-IRS-1 levels were quantified by measuring the intensity of the immunoreactive bands using the ImageJ software. The ratio of p-p38/p38, p-p70 S6K1/p70 S6K1 and p-IRS-1/IRS-1 in the non-treated vehicular control group was assigned a relative value of 100. **(E)** 3T3-L1 adipocytes were treated with or without 0.5 μM Oxo for 30 min in basic medium, followed by incubation with 2.5 mM MG for 24 h under normal cell culture conditions. Glucose uptake into the cells was then determined by measuring glucose remaining in the cell culture medium. Data are presented as the mean ± SEM (error bars), with n = 4 **(A)**, 5 **(B–D)** or 6 **(E)** per group. One-way analysis of variance (ANOVA) followed by Tukey's post-hoc test was conducted to determine the statistical significance **(A–D)**. *, $P < 0.05$ between the non-treated vehicular control group and respective groups. #, $P < 0.05$ between the indicated groups.

MG enhanced the phosphorylation of IRS-1 at various serine residues

The main investigations up to this point focused on the effects of extracellular MG treatment on adipocytes. However, whether or not MG works extracellularly or intracellularly in these adipocytes to activate the TAK1–p38–mTORC1 signalling axis is not really known. MG has been reported to be fully membrane permeable [43,121], which hints at the possibility that MG diffuses across the cellular membrane to activate TAK1, which is localised in the cytosol. To confirm if endogenously produced intracellular MG could also induce the activation of the TAK1–p38–mTORC1 signalling axis, as seen in **Figs. 2-3–2-8**, the investigation then shifted to investigate if conditions of increased intracellular MG levels could also induce p38 MAPK and p70 S6K1 phosphorylation. GLO1 is the main metabolic enzyme for intracellular MG, and therefore the use of the cell permeable BBGC, an inhibitor of GLO1, increases the concentration of intracellular MG [122]. In addition to that, the concentration of intracellular MG can also be increased via the use of DHA, a metabolite which is non-enzymatically converted to MG within cells [123,124]. Usage of either BBGC or DHA on the adipocytes increased both p38 MAPK and mTORC1 activity, as seen by significantly increased p38 MAPK and p70 S6K1 phosphorylation, respectively (**Fig. 2-9(A–D)**); and pre-treatment of the cells with (5*Z*)-7-oxozeaenol to inhibit TAK1 significantly suppressed both BBGC and DHA-induced phosphorylation of both those proteins (**Fig. 2-9(A–D)**). Altogether, these data suggest that MG that has been generated intracellularly could activate the TAK1–p38–mTORC1 signalling axis in adipocytes.

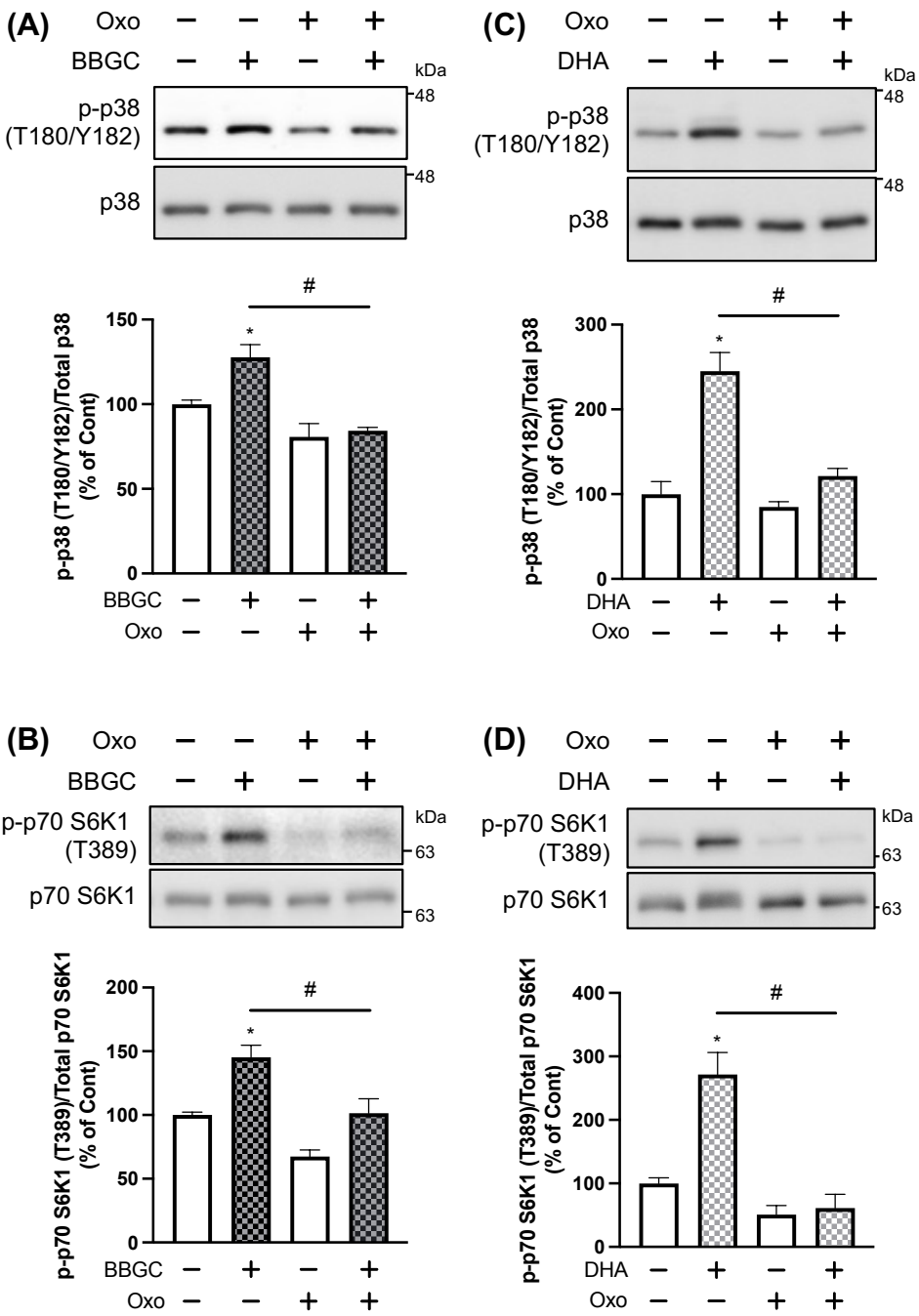

Figure 2-9. MG enhanced the phosphorylation of IRS-1 at various serine residues
(A–D) 3T3-L1 adipocytes were pre-treated with 0.5 μM (5*Z*)-7-oxozeaenol (Oxo) for 30 min, followed by treatment with 20 μM S-p-bromobenzylglutathione cyclopentyl diester (BBGC; **A–B**) or 200 mM dihydroxyacetone (DHA; **C–D**) for 2 h. Phosphorylated p38 (p-p38) and p38 **(A,C)**; phosphorylated p70 S6K1 (p-p70 S6K1) and p70 S6K1 **(B,D)** were determined as described in the legends of **Figure 2-6** and **Figure 2-3**, respectively. p-p38 and p-p70 S6K1 levels were quantified as described in the legend of **Figure 2-7**. Data are presented as the mean ± SEM (error bars), with n = 4 **(A–D)** per group. One-way ANOVA followed by Tukey's post-hoc test was conducted to determine the statistical significance **(A–D)**. *, $P < 0.05$ between the non-treated vehicular control group and respective groups. #, $P < 0.05$ between the indicated groups.

TNFα-induced IRS-1 phosphorylation is contributed by the TAK1–p38–mTORC1 signalling axis

Inflammation is well-known to be associated with metabolic dysregulation, including T2D [125,126]. Activation of the inflammatory pathway in response to proinflammatory cytokines induces insulin resistance, which is partly attributed to the negative regulation of IRS-1 [70,71]. Previous studies on 3T3-L1 adipocytes have shown that proinflammatory cytokines, such as TNFα, enhances the phosphorylation of serine residues (Ser307 and Ser636/639) in IRS-1 in a JNK- or ERK-dependent manner to impair insulin signalling [127,128,129]. The involvement of p38 MAPK in proinflammatory cytokine-induced IRS-1 phosphorylation is not well understood in adipocytes, while TNFα-induced activation of p38 MAPK contributes to the phosphorylation of serine residues in IRS-1 in skeletal muscle [130]. Seeing that the MG-induced TAK1–p38–mTORC1 signalling axis is elicited by the proinflammatory effect of MG (**Fig. 2-8**), whether or not this was a signalling axis unique to MG, or whether or not other proinflammatory cues could also activate the same signalling axis were investigated. Just as was observed under MG treatment in **Fig. 2-8(A)**, TNFα treatment significantly increased the gene expression of the proinflammatory cytokines, *Il6* and Ccl2 (which encodes MCP1 protein) (**Fig. 2-10(A–B)**). TNFα also increased the phosphorylation levels of p70 S6K1, which was attenuated by rapamycin, SB203580, or (5*Z*)-7-oxozeaenol, indicating that TNFα activated the TAK1–p38–mTORC1 signalling axis (**Fig. 2-10(C–E)**). Lastly, the effect of the TAK1–p38–mTORC1 signalling axis on the TNFα-induced phosphorylation levels of the Ser318 and 612 serine residues in IRS-1 was examined, both of which are regulated by mTORC1. The phosphorylation levels of Ser318 and Ser612 were enhanced following treatment with TNFα, and the enhanced phosphorylation at these serine residues were attenuated by rapamycin or (5*Z*)-7-oxozeaenol (**Fig. 2-10(F–G)**). These results

suggest that not just MG, but also TNFα induced the activation of the TAK1–p38–mTORC1 signalling axis which enhanced IRS-1 phosphorylation at various serine residues.

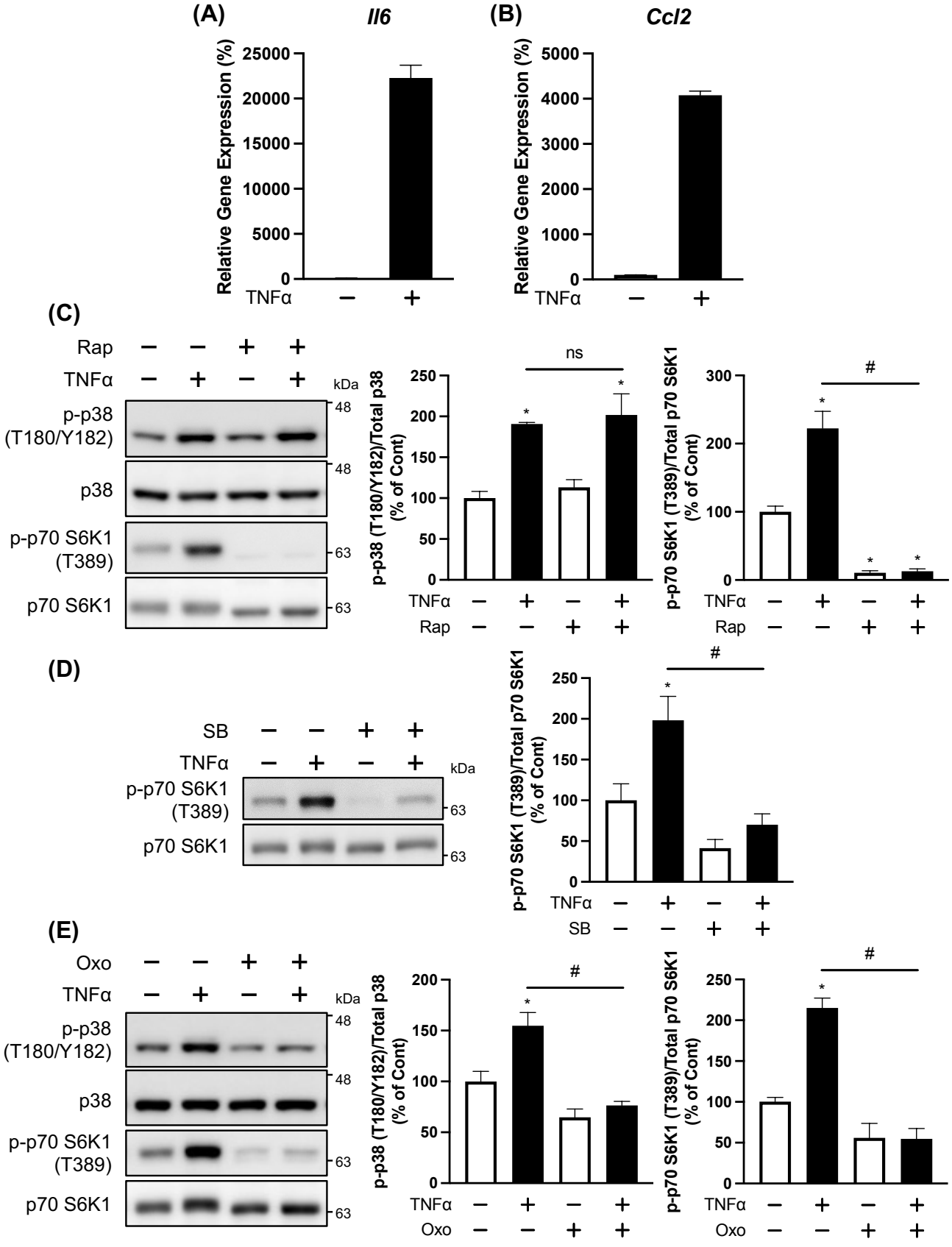

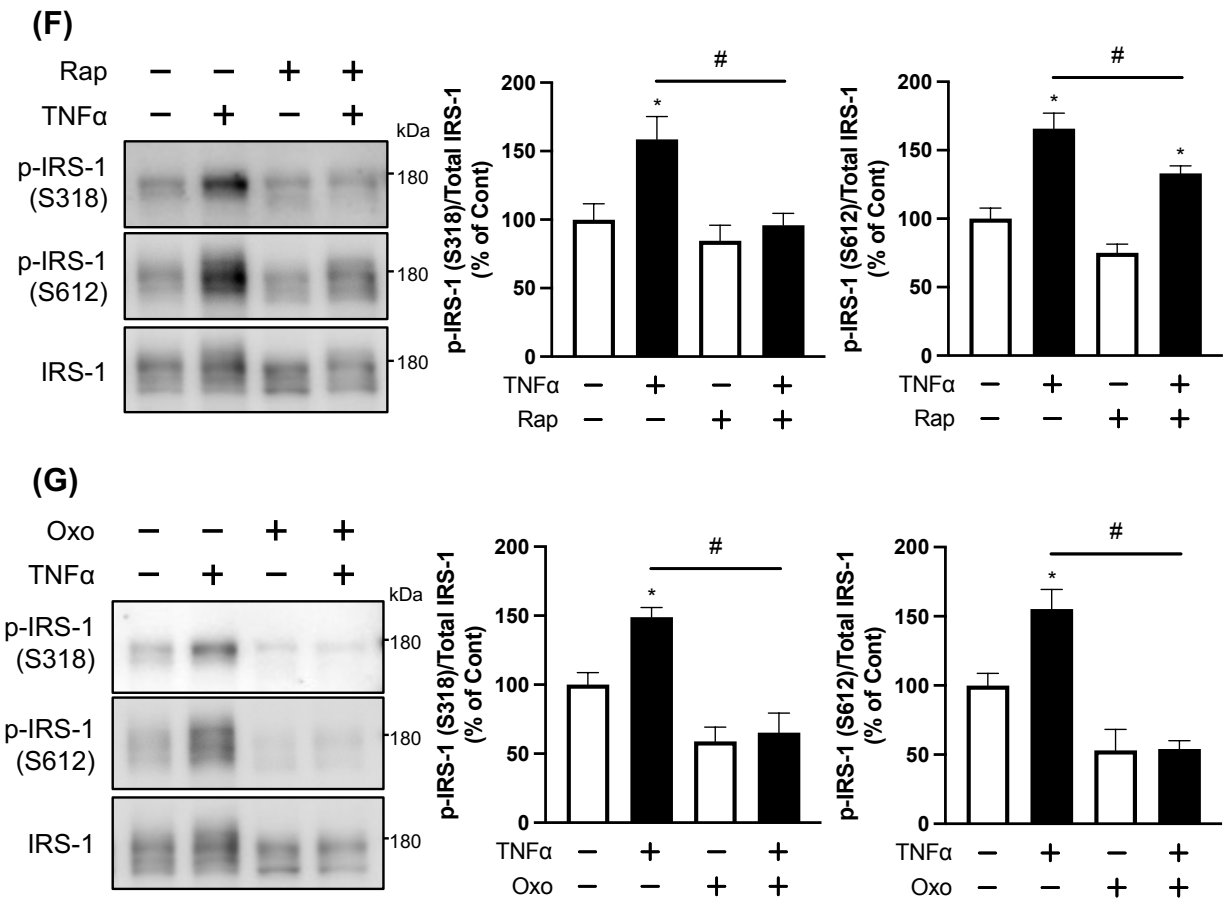

Figure 2-10. TNFα-induced IRS-1 phosphorylation is contributed by the TAK1–p38–mTORC1 signalling axis

(A–B) Adipocytes were treated with 50 ng/ml TNFα for 2 h. mRNA expression levels of *Il6* **(A)** and *Ccl2* **(B)** in the cells were then determined by real-time PCR. **(C–G)** The 3T3-L1 adipocytes were treated with or without 20 nM rapamycin (Rap) **(C,F)**, 10 μM SB203580 (SB) **(D)**, or 0.5 μM (5*Z*)-7-oxozeaenol (Oxo) **(E,G)** for 30 min, followed by treatment with 100 ng/ml of TNFα for 30 min. Levels of phosphorylated p38 (p-p38) and p38 **(C,E)**; phosphorylated p70 S6K1 (p-p70 S6K1) and p70 S6K1 **(C–E)** were determined and quantified as described in the legend of **Figure 2-7**; whereas levels of phosphorylated IRS-1 (p-IRS-1) at Ser318 and Ser612, and IRS-1 **(F–G)** were determined and quantified as described in the legend of **Figure 2-2**. Data are presented as the mean ± SEM (error bars), with n = 3 **(A–B)**, 4 **(C)** or 5 **(D–G)** per group. Welch's *t*-test **(A–B)** or one-way ANOVA followed by Tukey's post-hoc test **(C–G)** were conducted to determine the statistical significance. *, $P < 0.05$ between the non-treated vehicular control group and respective groups. #, $P < 0.05$; ns, non-significant differences between the indicated groups.

Discussion

The possible mechanism through which MG induces the TAK1–p38–mTORC1 signalling axis in adipocytes

Although MG is a dicarbonyl metabolite derived from glycolysis, it does not contribute to cellular energy production. Rather, MG contributes to aging and disease by inducing carbonyl stress when its concentrations increase beyond the typical concentrations of 50–250 nM in human plasma and 1–5 μM in cells [43,131]. In particular, MG is associated with the development and progression of diabetic complications in adipose tissues and kidneys, and the involvement of AGEs formed by MG may be a possible mechanism of action [43,52,54]. Since AGEs are produced by non-enzymatic glycation, which is a relatively slow process, via the Maillard reaction that targets arginine and lysine residues in proteins and peptides, the association of MG with diabetic complications is mainly focused on the chronic effects of MG. In the present study, which viewed MG as a signalling molecule that initiates signal transduction, the short-term effects of MG were focused on, and it was demonstrated that MG activated mTORC1–IRS-1 signalling in adipocytes within one hour of the addition of MG (**Figs. 2-2–2-3**) and within two hours of the addition of either BBGC or DHA, which have been reported to increase intracellular MG (**Fig. 2-9**). These results imply that MG activates the TAK1–p38–mTORC1 signalling axis intracellularly. Furthermore, since p38 MAPK and TAK1 were necessary for the MG-induced activation of mTORC1 signalling (**Figs. 2-6, 2-8, and 2-9**), the TAK1–p38–mTORC1 signalling axis was identified as a signalling pathway that enhances IRS-1 phosphorylation at serine residues, which negatively affects insulin signalling. It has been found recently that MG has the ability to form methylimidazole crosslink between proximal cysteine and arginine residues (MICA) in kelch-like ECH-associated protein (KEAP)-1 [132]. MICA modification in KEAP1 results in its dimerization at a region necessary for proper nuclear factor erythroid 2-related factor (NRF)-2 binding and ubiquitination, which

consequently removes the inhibitory effect of KEAP1 on NRF2 and allows NRF2 to accumulate and activate signalling [132]. Like other AGEs, the formation of MICA is unspecific, occurring in any protein with accessible proximal cysteine and arginine residues; and is formed rapidly, increasing by the hour [132,133]. There is a possibility that TAK1 itself, and/or upstream regulators of TAK1 also have susceptible amino acid residues that are key to their function that could be subjected to, and influenced by MG modification. One potential group of proteins upstream of TAK1 which may be influenced by MG through MICA modification of proteins is the tumour necrosis factor receptor-associated factor (TRAF) family of proteins which are E3 ubiquitin ligases that play a crucial role in immune signalling [134,135,136]. TRAF family members form trimers to become a functional unit of TRAF, and the really interesting new gene (RING) domain which is commonly associated with ubiquitin transfer can also dimerise to form a network of TRAF trimers [135,136]. The RING domain is conserved among different TRAF proteins, and dimerization of the RING domain is required for ubiquitin transfer by TRAF6 [135,136]. While Phe118 forms the core of the dimerization interface [135,136], Arg88 was also found to be necessary for RING domain dimerization [136]. Mutation of Arg88 to Ala disrupted TRAF6 dimerization and severely impaired polyubiquitin synthesis, leading to residual and delayed downstream IKK activation [136]. Located two, three, and five amino acids away from the arginine residue of the RING domain dimerization interface are cysteine residues, and these residues are conserved across TRAF2, 3, 5 and 6. It is likely that MG may promote dimerization of TRAF proteins through the formation of MICA at inter-protein RING domains. Dimerization of the RING domains through MICA formation may promote increased TRAF ubiquitin ligase activity, which consequently contributes to the activation of the downstream TAK1–p38–mTORC1 signalling axis.

In 3T3-L1 adipocytes, prolonged MG treatment (24 hours), which induces intracellular AGEs formation, has been reported to diminish insulin signalling with increased ROS

production [137]. Another study has also reported that AGEs increased the intracellular ROS generation in 3T3-L1 adipocytes, and the negative effects of AGEs on glucose uptake were completely reversed by the treatment with NAC [138]. In contrast, no significant increase in ROS production following treatment with MG was observed during the MG-treatment period in which the TAK1–p38–mTORC1 signalling axis was activated in this study (**Fig. 2-7**), and the MG-induced activation of the TAK1–p38–mTORC1 signalling axis was not affected by treatment with NAC (**Fig. 2-7**). Therefore, while there is a possibility that AGEs may have been formed in 3T3-L1 adipocytes during the one-hour MG treatment which activated the TAK1–p38–mTORC1 signalling axis, ROS generation as a result from AGEs production may not function as a signalling cue in the MG-induced activation of the TAK1–p38–mTORC1 signalling axis. A previous study about the involvement of MG in insulin resistance has shown that the insulin-stimulated activation of insulin signalling is attenuated by prolonged treatment (16 hours) with MG in an ERK-dependent manner in mouse aortic endothelial cells [66]. An increase in ERK phosphorylation following MG treatment in 3T3-L1 adipocytes was not observed in this study (**Fig. 2-6**). Thus, the mechanism by which MG induces insulin resistance may differ depending on the target cells and the duration of MG action.

The TAK1–p38–mTORC1 signalling axis may not be solely responsible for MG-induced IRS-1 serine phosphorylation

While the MG-activated TAK1–p38–mTORC1 signalling axis was identified as a signalling pathway which negatively affects insulin signalling by enhancing IRS-1 phosphorylation at serine residues, inhibition of mTORC1, p38 MAPK, or TAK1 via their respective inhibitors could not completely block MG-induced signalling to IRS-1 serine residues (**Figs. 2-3, 2-6, and 2-8**). This phenomenon could have occurred because these phosphorylation sites are not exclusive to mTORC1 phosphorylation, and other kinases such

as JNK [139], IKK [140], as well as several isoforms of PKC [141,142,143,144,145] have been reported to be also involved in their phosphorylation. Therefore, there remains the possibility that JNK and PKC signalling may also influence MG-induced IRS-1 multiple phosphorylation in 3T3-L1 adipocytes under our experimental conditions, and further investigations are necessary to examine the involvement of MG-induced serine phosphorylation of IRS-1 via signalling pathways other than the TAK1–p38–mTORC1 signalling axis in adipocytes.

Lower exogenous MG concentrations may also induce IRS-1 serine phosphorylation and inhibit glucose uptake in adipocytes

On the other hand, since MG induced p70 S6K1 phosphorylation from concentrations of 0.5 mM **(Fig. 2-3(B))**, it is likely that MG could also induce mTORC1 to increase IRS-1 serine phosphorylation at Ser307, 318, and 612 at that concentration, subsequently provoking resistance towards insulin-stimulated glucose uptake. However, additional experiments may be necessary to confirm if the MG concentration of 0.5 mM are also capable of affecting IRS-1 multiple serine phosphorylation and insulin-stimulated glucose uptake in adipocytes. Still, even if that were to be the case, it is thinkable that the MG-induced inhibition on glucose uptake would be shorter-lived at lower doses of MG than at higher doses, considering that the inhibitory effects of MG on glucose uptake were found to be reversible (**Fig. 2-1(E)**). More than 99% of MG within the cell is detoxified primarily by the GLO system, and it was observed that in 50% (v/v) red blood cell suspensions, there was a nearly directly proportional conversion rate of ~0.5 mmol/h/L to D-lactate when 0.5 mM MG was added to the culture [58]. Although the conversion rate of MG to D-lactate in adipocytes is not known, it can be expected that at lower concentrations of MG, insulin-stimulated glucose uptake would start to recover as soon as MG is completely metabolised and removed by the GLO system in adipocytes.

Negative IRS-1 regulation via the TAK1–p38–mTORC1 signalling axis may not be the sole contributor towards MG-inhibited glucose uptake

MG-induced repression of glucose uptake during acute stimulation with insulin was not cancelled by the mTORC1 inhibitor (**Fig. 2-3**), rapamycin, despite mTORC1 inhibition being able to attenuate MG-enhanced serine phosphorylations of IRS-1 (**Fig. 2-3**) as well as to restore insulin-stimulated tyrosine phosphorylation of IRS-1 in the presence of MG (**Fig. 2-4**). It was previously reported that MG attenuates the glucose uptake activity of human GLUT1 or rat GLUT4 in a system that exogenously expresses mammalian hexose transporters in yeast [146], suggesting that MG directly inhibits these transporters. The mechanism by which MG directly inhibits these hexose transporters may influence short-term insulin-stimulated glucose uptake. In contrast, the repression of glucose uptake under steady-state culture conditions in the presence of MG was cancelled by inhibition of the TAK1–p38–mTORC1 signalling axis (**Figs. 2-4, and 2-8**). The inhibitory effect of MG on hexose transporter activity is reversible, not irreversible [146]. Although the molecular mechanism of hexose transporter inhibition by extracellular MG is not clear, the inhibitory effect on hexose transporters may be exerted more under acute insulin stimulation than under steady-state culture conditions. Therefore, the contribution of MG-induced activation of the TAK1–p38–mTORC1 signalling axis on glucose uptake activity was also confirmed under steady-state culture conditions. However, while the inhibitory effect of MG on insulin-stimulated glucose uptake was also found to be reversible (**Fig. 2-1(E)**), more investigations into the mechanisms of how IRS-1 multiple serine phosphorylation caused by MG-induced TAK1–p38–mTORC1 signalling axis affects downstream IRS-1 signalling are necessary.

MG treatment may result in attenuated insulin-stimulated GLUT4 translocation, which is downstream of IRS-1 signalling, leading to inhibited glucose uptake

IRS-1 phosphorylation at multiple serine residues, which negatively affects insulin signalling, was found to be increased in MG-treated adipocytes via the TAK1–p38–mTORC1 signalling axis (**Figs. 2-3, 2-6, 2-8, and 2-9**). mTORC1 inhibition using rapamycin beforehand recovered insulin signalling that was inhibited in MG-treated adipocytes, as seen in **Fig. 2-4** which shows that both insulin-stimulated IRS-1 Tyr phosphorylation as well as Akt Ser473 phosphorylation were comparable to control adipocytes stimulated with insulin. However, whether or not insulin signalling at proteins most closely linked to glucose transport, such as TBC1D1; or better yet, whether or not GLUT4 translocation were affected by MG in the first place were not addressed in this study. Akt is responsible in promoting glucose uptake via direct activation of TBC1D1 which is implicated in insulin-stimulated GLUT4 translocation for increasing cellular glucose uptake [84], and since insulin-induced Akt phosphorylation was found to be reduced in MG-treated adipocytes, it is quite likely that the insulin-induced TBC1D1 activation was similarly reduced in MG-treated adipocytes in this study. In Chinese hamster ovary cells stably expressing IR and GLUT4 fused with green fluorescent protein, MG pre-treated cells were not just found to display a significant decrease in insulin-stimulated Akt phosphorylation, a phenomenon which was similar to was found in this study, these cells were also found to have impaired insulin-stimulated GLUT4 translocation to the cell membrane [147]. Therefore, it is quite likely that in the adipocytes used in this study, insulin-induced GLUT4 translocation to the cell membrane may have been impaired as well.

The possible mechanisms by which MG-induced p38 MAPK activation may regulate mTORC1 activity

Crosstalk between p38 MAPK and mTORC1 signalling exists, and it has been reported that p38 MAPK contributes to the activation of mTORC1 signalling. The involvement of the p38 MAPK-activated kinase, MAPK-activated protein kinase (MK)-2, which is also known as MAPKAPK2, and the direct involvement of p38 MAPK in mTORC1 activity have been proposed as activation mechanisms for the p38–mTORC1 signalling axis [103,104,105,106]. It has been suggested that MK2 which is activated by p38 MAPK in the presence of FBS phosphorylates TSC2 to negatively regulate its GAP function [103], whereas p38 MAPK has been proposed to directly phosphorylate raptor, a regulatory component of mTORC1, which subsequently activates mTORC1 in cells treated with arsenite [105]. As such, p38 MAPK may contribute to the activation of mTORC1 signalling via multiple mechanisms, depending on the signalling input. It would be interesting to further investigate the mechanism by which p38 MAPK regulates mTORC1 in the TAK1– p38–mTORC1 signalling axis identified in this study.

MG is a metabolite capable of modulating proinflammatory signalling in adipocytes

Both MG and TNFα induced a proinflammatory response, as seen by an increase in proinflammatory cytokine gene expression (**Figs. 2-8(A), 2-10(A–B)**). In addition to MG, increased phosphorylation of IRS-1 at serine residues via the TAK1–p38–mTORC1 signalling axis was observed when adipocytes were treated with the proinflammatory cytokine, TNFα (**Fig. 2-10**). TNFα and other proinflammatory stimuli activate TAK1, which is a central player in inflammatory signal transduction, thereby inducing inflammatory responses [84]. Adipose tissue inflammation in obesity is a factor that contributes to insulin resistance, and increased TNFα levels are related to the combined effects of obesity and diabetes [148,149]. It is known that TNFα-promotes insulin resistance, and the development of diabetic complications is

mediated by several kinases, such as JNK and IKKβ [85]; therefore, TNFα negatively regulates insulin signalling through various pathways. In this regard, the finding that the TAK1–p38–mTORC1 signalling axis activated by TNFα enhanced serine phosphorylations of IRS-1 suggests that the TAK1–p38–mTORC1 signalling axis contributes to the mechanisms of insulin resistance induced under inflammatory conditions. Meanwhile, it has been reported that GLO1 expression and its enzymatic activity are decreased under inflammatory conditions [125,126], suggesting an increase in intracellular MG levels. The initial inflammatory trigger in adipose tissues during obesity remains largely unknown [150]. The finding in this study that MG activates TAK1, an indispensable signalling intermediate in proinflammatory signalling, suggests that MG acts as a modulator of proinflammatory signalling, which provides insight into the association of MG with inflammation in adipocytes.

Chapter 3

The second study: The effect of methylglyoxal on isoproterenol-induced free fatty acid release and uncoupling protein 1 expression in adipocytes

Introduction

Adipocytes, which play an important role in lipid metabolism, are generally classified into white and brown adipocytes according to their function [151]. White adipocytes store excess energy in the form of TAGs and release the stored energy in the form of FFAs, while brown adipocytes are specialised in producing heat associated with energy consumption through the degradation of TAGs, which plays a vital role in regulating systemic metabolism and thermogenesis [151]. UCP1, a proton carrier located in the inner membrane of the mitochondria, is involved in the thermogenic function of brown adipocytes [152,153]. UCP1 activation causes dissipation of the electro-chemical proton gradient and a decrease in the proton motive force used to synthesize ATP. Proton leakage induced by UCP1 uncouples the proton gradient from ATP synthesis, releasing the free energy as heat [152,153]. Recently, some white adipocytes located in subcutaneous fat, such as the inguinal white adipose tissue (iWAT), have been shown to increase *Ucp1* gene expression under cold exposure or adrenergic stimulation (i.e., brown-like "beige" adipocytes) [154,155]. Beige adipocytes also expend energy through UCP1-mediated thermogenesis [154,155]. Therefore, the elucidation of the

*The content described in this chapter was originally published in *Biochemistry and Biophysics Reports*. Su-Ping Ng, Wataru Nomura, Haruya Takahashi, Kazuo Inoue, Teruo Kawada, and Tsuyoshi Goto (2021) Methylglyoxal attenuates isoproterenol-induced increase in uncoupling protein 1 expression through activation of JNK signaling pathway in beige adipocytes. *Biochem Biophys Rep*. 28:101127. doi: 10.1016/j.bbrep.2021.101127.

molecular mechanisms underlying the regulation of thermogenesis in both brown and beige adipocytes is of interest because it can provide novel insights into approaches to control and treat obesity and obesity-related metabolic diseases such as T2D and diabetic complications [154,155].

The metabolically unhealthy obese state is a state of chronic inflammation, which plays a role in negatively affecting adipocyte response towards hormonal stimulation such as catecholamines [30]. Inflammatory cytokine stimulation increases lipolysis [30,156], which increases circulatory FFA which continue to positively feed inflammation [156], creating a vicious cycle of FFA production and inflammatory response. Increased circulatory FFA during chronic inflammation not just mediates insulin resistance in other organs such as the muscle and pancreas [30,37], increased accumulation of intracellular fatty acids also causes catecholamine resistance via reduced adenylyl cyclase activity [36]. This resistance towards catecholamine stimulation represses energy expenditure processes such as lipolysis and thermogenesis under obese conditions, which may further exacerbate insulin resistance and contribute towards the development of T2D. This is especially when many studies have negatively correlated UCP1 activity to obesity and T2D [38,39,40]. Although the development of diabetes and its complications are the result of a highly complex process, the accumulation of AGEs, the synthesis of which is initiated by a non-enzymatic reaction between the aldehyde groups of glucose and amino groups of proteins, is recognized as one of the major factors linked to it [157]. MG is a ubiquitous 2-oxoaldehyde derived from glycolysis [56,67,158]. Although MG is a natural metabolite, it is highly reactive because it contains two carbonyl groups and has a higher potential than glucose to produce AGEs. Plasma and tissue MG levels are higher in patients with diabetes than in healthy individuals, suggesting that MG plays a role in the development and progression of diabetic complications [42,159,160]. MG is mainly metabolized to D-lactate within cells through a ubiquitous glutathione-dependent glyoxalase system

consisting of GLO1 and GLO2 (**Fig. 1-3**) [56,67]. Functional genome analyses suggest a relationship between a deficiency in this system, which implies increased MG and the development of diabetes and its complications [47,48,68]. Whilst MG is implied to function as a signalling molecule due to its association with the regulation of intracellular signalling pathways like inflammatory and oxidative stress signalling pathways [74,75,76,77], it remains to be determined if high MG levels are involved in the development of T2D via repressive effects on energy expending processes in adipocytes.

In this chapter, the effect of MG on lipolysis as well as *Ucp1* expression induced by treatment with the β-adrenergic receptor agonist, isoproterenol, were investigated in differentiated immortalized iWAT-derived pre-adipocytes. Although MG had no significant effect on isoproterenol-induced FFA and glycerol release, isoproterenol-induced expression of *Ucp1* was significantly inhibited by MG. Downregulation of the PKA pathway, which is the core regulator for *Ucp1* expression by isoproterenol, was not responsible for this inhibitory effect. Instead, it was found that MG enhanced the phosphorylation of JNK MAPK, and an inhibitor of JNK suppressed the inhibitory effect of MG on *Ucp1* expression. These results indicate that activation of JNK is necessary for the MG-induced inhibition of *Ucp1* expression. This inhibitory effect of MG on *Ucp1* expression and subsequent thermogenesis in adipocytes may contribute towards the provocation insulin resistance.

Materials and Methods

Materials

DMEM-high glucose (Cat. No. 044-29765), insulin (Cat. No. 097-06474), indomethacin (Cat. No. 093-02473), SB203580 (Cat. No. 199-16551), and NAC (Cat. No. 017-05131) were purchased from Wako (Osaka, Japan). FBS (Cat. No. 10270-106) was purchased from Gibco (FBS; Grand Island, NY, USA). Penicillin-Streptomycin mixed solution (Cat. No.

26253-84), IBMX (Cat. No. 19624-31), dexamethasone (Cat. No. 50-02-2), DHA (Cat. No. 12438-62), and all chemicals used to prepare PBS, lysis buffer, and sample buffer were purchased from Nacalai Tesque (Kyoto, Japan). Rosiglitazone (IUPAC name: 5-[[4-[2-[methyl(pyridin-2-yl)amino]ethoxy]phenyl]methyl]-1,3-thiazolidine-2,4-dione; Cat. No. R5773) was purchased from LKT Laboratories (Minneapolis, MN, USA). 3,3',5'-Triiodo-L-thyronine (T_3; Cat. No. T2877), BBGC (Cat. No. SML1306), MG (Cat. No. 67028), and isoproterenol (IUPAC name: 4-[1-hydroxy-2-(propan-2-ylamino)ethyl]benzene-1,2-diol; Cat. No. I6504-1G) were purchased from Sigma-Aldrich (MO, USA). SP600125 (Cat. No. BML-EI305) was purchased from Enzo Life Sciences (NY, USA).

Cell Culture

Immortalized primary pre-adipocytes from mouse iWAT were a kind gift from Dr. Shingo Kajimura (Harvard Medical School, MA, USA). C3H10T1/2 cells were purchased from the American Type Culture Collection (Manassas, VA, USA). These cells were maintained in a humidified 5% CO_2 atmosphere at 37°C in basic medium (DMEM-high glucose supplemented with 10% (v/v) FBS, 10,000 units/ml penicillin, and 10,000 μg/ml streptomycin). To differentiate the pre-adipocytes into mature adipocytes, cells were cultured to confluence before stimulation with 1 nM T_3, 5 μg/ml insulin, 0.5 μM rosiglitazone, 2 μg/ml dexamethasone, 0.5 mM IBMX, and 125 μM indomethacin in a basic medium for 48 hours. The medium was then replaced with a growth medium (basic medium supplemented with 1 nM T_3, 5 μg/ml insulin, and 0.5 μM rosiglitazone). This step was repeated every two days until the adipocytes reached the sixth day after the induction of differentiation. After six days of differentiation, the matured adipocytes were incubated in a serum-free medium for three–five hours before being subjected to 1 μM isoproterenol. The cells were pre-treated with either MG, BBGC or DHA in serum-free medium for 30 minutes before isoproterenol stimulation. The use of 10 μM

SP600125 (JNK inhibitor), 10 μM SB203580 (p38 inhibitor), or 10 mM NAC (ROS scavenger) precedes MG or BBGC treatment by 30 minutes.

Lipolysis Assay

Mature adipocytes (six days post-differentiation induction) were starved of serum for three–five hours before adrenergic stimulation with 1 μM isoproterenol in serum-free medium containing 2% bovine serum albumin (Nacalai Tesque; Cat. No. 08587-84) for three hours. FFA, also known as non-esterified fatty acids (NEFA), and glycerol levels within the cell culture medium were measured using NEFA C (Wako; Cat. No. 279-75401) and triglyceride E (Wako; Cat. No. 432-40201) assay kits, respectively. FFA and glycerol levels were then normalized to the cellular protein levels.

Western Blotting

Cells were washed with PBS and lysed with lysis buffer containing 20 mM Tris-HCl buffer (pH 7.5), 1% (v/v) Triton X-100, 10% (v/v) glycerol, 137 mM NaCl, 2 mM EDTA (pH 8.0), a phosphatase inhibitor cocktail (Nacalai Tesque; Cat. No. 07575-51), and a protease inhibitor cocktail (Nacalai Tesque; Cat. No. 03696-21). The lysate was centrifuged at 16,700×g for ten minutes and the resulting supernatant was collected. Protein concentration was measured using the DC Protein Assay (Bio-Rad, Hercules, CA, USA; Cat. No. 500016) according to the manufacturer's protocol. Protein loading samples were prepared by homogenising four parts of the lysate supernatant with one part of 5x concentrated sample buffer containing 250 mM Tris-HCl (pH 6.8), 10% (w/v) SDS, 25% (w/v) sucrose, 0.02 % (w/v) BPB, and 10% β-mercaptoethanol. 10 μg protein load per sample was separated by SDS-PAGE and transferred to a PVDF membrane (Millipore, Burlington, MA, U.S.A.; Cat. No. IPVH00010). The membrane was then blocked, washed, and incubated with the primary

antibodies listed in **Table 2-1** below. All primary antibodies were purchased from Cell Signaling Technology (Danvers, MA, USA) and used at a dilution of 1:5000. Immunoreactive bands were detected using 1:5000 diluted anti-rabbit HRP secondary antibody, Cat. No. NBP1-75297 (Novus Biologicals, CO, USA) with Immobilon Western Chemiluminescent Horseradish Peroxidase Substrate (Millipore; Cat. No. WBKLS0100) and an LAS-4000 mini-imaging system (Fujifilm, Tokyo, Japan).

Table 2-1. Primary antibodies used in this study.

Primary antibody	Catalog number (manufacturer)
Phospho-HSL (Ser660)	#4126 (Cell Signaling)
HSL	#4107 (Cell Signaling)
Phospho-PKA substrate	#9624 (Cell Signaling)
Perilipin	#9349 (Cell Signaling)
Phospho-CREB (Ser133)	#9198 (Cell Signaling)
CREB	#9197 (Cell Signaling)
Phospho-p38 (Thr180/Tyr182)	#9215 (Cell Signaling)
p38	#9212 (Cell Signaling)
Phospho-JNK (Thr183/Tyr185)	#9251 (Cell Signaling)
JNK	#9252 (Cell Signaling)
Phospho-ERK (Thr202/Tyr204)	#9101 (Cell Signaling)
ERK	#9102 (Cell Signaling)

RNA Preparation and Quantification of Gene Expression

Total RNA was isolated from cultured cells using Sepasol Super-I (Nacalai Tesque; Cat. No. 09379-84) following the manufacturer's protocol. Total RNA was reverse-transcribed

using M-MLV reverse transcriptase (Promega, WI, USA; Cat. No. M1708) according to the manufacturer's instructions using a thermal cycler (Takara PCR Thermal Cycler SP, Takara, Shiga, Japan). mRNA expression was quantified by real-time PCR using the SYBR® Green I assay system performed with a LightCycler (Roche Diagnostics, Mannheim, Germany). The protocol for amplification was as follows: denaturation at 95°C for 15 seconds, annealing at 60°C for 15 seconds, and extension at 72°C for 45 seconds. The expression levels of these genes were normalized to those of *Rplp0*. The primer sequences are listed in **Table 2-2**.

Table 2-2. Oligonucleotide primers used for mRNA analysis in this study.

Gene	Forward Primer (5'→3')	Reverse Primer (5'→3')
Ucp1	CAAAGTCCGCCTTCAGATCC	AGCCGGCTGAGATCTTGTTT
Rplp0	TCCTTCTTCCAGGCTTTGGG	GACACCCTCCAGAAAGCGAG
Fgf21	CACCGCAGTCCAGAAAGTCT	ATCCTGGTTTGGGGAGTCCT
Ppargc1α	CCCTGCCATTGTTAAGACC	TGCTGCTGTTCCTGTTTTC
Cidea	ATCACAACTGGCCTGGTTACG	TACTACCCGGTGTCCATTTCT
Dio2	AGCCCATGTAACCAGCACCGGA	CAGTCGCACTGGCTCAGGAC
Ccl2	GACCCCAAGAAGGAATGGGT	ACCTTAGGGCAGATGCAGTT
Il6	CTGATGCTGGTGACAACCAC	TTTTCTGCAAGTGCATCATCGT

Luciferase Reporter Assay

4.5 μg pUCP1-pro-Luc, a tk-LUC luciferase reporter plasmid containing the 3.8-kb portion of the 5'-flanking region of the mouse *Ucp1* gene [161], was transfected into 90% confluent C3H10T1/2 cells growing on a 100-mm culture dish along with 500 ng pGL4.74 (hRluc/TK) vector as an internal control using Lipofectamine 2000 (Thermo Fisher Scientific, MA, USA; Cat. No. 11668-019). Four hours after transfection, the cells were seeded in 96-

well-plates overnight. The next day, after three–five hours of serum starvation, cells were treated with 1 mM MG for 30 minutes before 1 μM isoproterenol stimulation for six hours. The cells were lysed and luciferase assay was performed using a Dual-Luciferase Reporter Gene Assay system (Promega, WI, USA) in accordance with the manufacturer's protocol. Luminescence was measured using the Centro XS3 LB 960 Microplate Luminometer (Berthold Technologies, Bad Wildbad, Germany).

Intracellular ROS Assay

The intracellular levels of ROS were detected using the fluorescent probe DCFDA (Thermo Fisher Scientific; Cat. No. D6883). The adipocytes were incubated with 2 μM of the dye in either the presence or absence of 10 mM NAC for 30 minutes at 37°C in the dark, followed by treatment with either 500 μM H_2O_2 (Wako; Cat. No. 084-07441) or 1 mM MG for three hours. Fluorescence levels were then measured in the fluorescence reader, Tecan Infinite F-200 microplate reader (Tecan Inc., Maennedorf, Switzerland) with excitation/emission at 485 nm/535 nm.

Statistical Analysis

Statistical analyses were conducted using GraphPad Prism (version 9.2; San Diego, CA, USA). Statistical significance was determined using one-way ANOVA followed by Sidak's or Dunnett's multiple comparison test, as indicated in the figure legends. Differences were considered significant at $P < 0.05$.

Results

MG did not affect isoproterenol-induced lipolysis

Stimulation of β-adrenergic receptors on adipocytes by adrenergic agonists increases the intracellular level of cAMP, which in turn activates PKA [162]. Activated PKA then directly phosphorylates its target proteins, including hormone-sensitive lipase (HSL) and perilipin (a protein located on the lipid droplet surface), which are crucial for the activation of lipolysis [163,164]. To assess if extracellular MG, or intracellularly generated MG had any effect on isoproterenol-induced lipolysis in adipocytes, differentiated immortalized iWAT-derived pre-adipocytes were pre-treated with either MG or BBGC, the inhibitor of the GLO1, the rate-limiting MG metabolic enzyme. Activation of PKA signalling by β-adrenergic agonists enhances adipocyte lipolysis and sequentially increases the release of FFA and glycerol into the medium [165]. Increased lipolytic activity was observed in this study when adipocytes were stimulated with the non-selective β-adrenergic receptor agonist, isoproterenol, as observed by markedly increased levels of both FFA (**Fig. 3-1(A)**) and glycerol within the cell culture medium (**Fig. 3-1(B)**). Pre-treatment of adipocytes with either MG or BBGC was not observed to significantly alter either FFA or glycerol levels in the cell culture medium (**Fig. 3-1(A–B)**). Isoproterenol induces the phosphorylation of PKA target proteins that are related to lipolysis, such as HSL at Ser660 [163], and perilipin at multiple sites, the phosphorylation levels of which can be detected using an anti-phospho-PKA substrate antibody [166,167]. Further assessment on isoproterenol-induced phosphorylation of HSL and perilipin after adipocytes were pre-treated with either MG or BBGC also did not yield any significant changes in phosphorylation levels compared to the stimulated control (**Fig. 3-1(C)**). These results illustrate that acute treatment of adipocytes with either MG or BBGC did not have any effect on isoproterenol-induced PKA activation of lipolytic proteins and subsequent FFA and glycerol release.

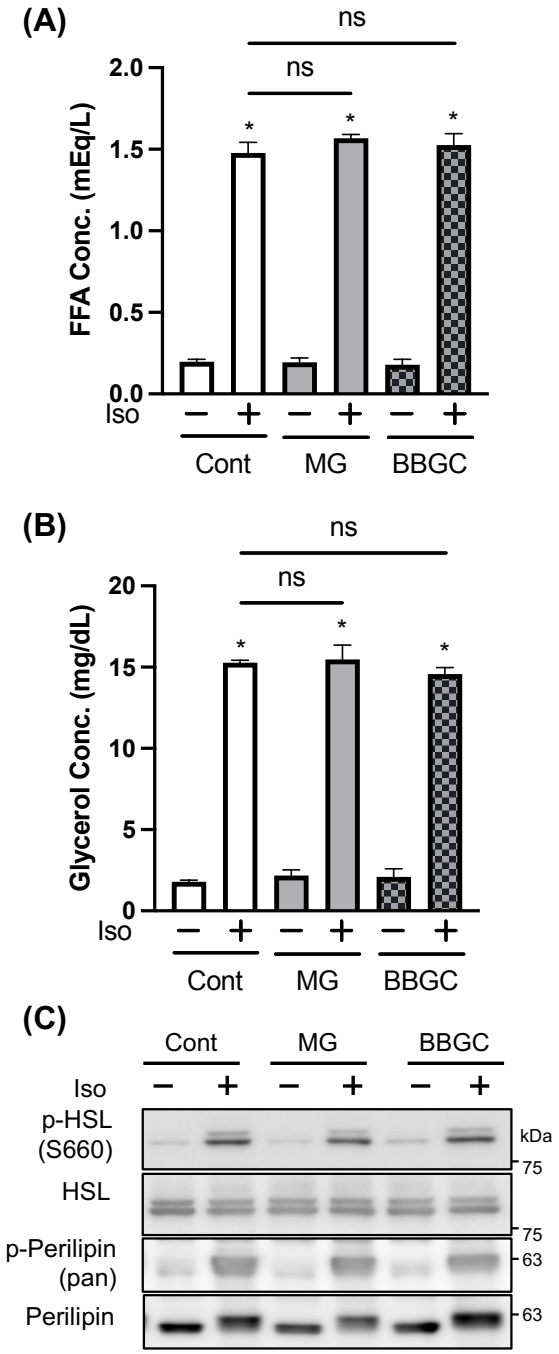

Figure 3-1. MG did not affect isoproterenol-induced lipolysis

(A–B) Adipocytes were treated with 1 mM MG or 20 μM BBGC for 30 min before stimulation with 1 μM isoproterenol (Iso) for 3 h. NEFA **(A)** and glycerol **(B)** levels in the culture medium were measured and normalized to cellular protein levels. **(C)** Adipocytes were treated with 20 μM BBGC or 1 mM MG for 30 min before stimulation with 1 μM isoproterenol (Iso) for 30 min. Phosphorylation of HSL (p-HSL), protein levels of HSL, phosphorylation of perilipin (p-perilipin) and protein levels of perilipin were determined using anti-phospho HSL Ser660, anti-HSL, anti-phospho-PKA substrate, and anti-perilipin antibodies respectively. Data are presented as the mean ± SEM (error bars), with n = 4 **(A–B)** per group. One-way ANOVA followed by Sidak's **(A–B)** post-hoc tests were done to determine statistical significance. *, $P < 0.05$ between the non-treated vehicular control group and respective groups. #, $P < 0.05$; ns, non-significant differences between the indicated groups.

MG attenuated the isoproterenol-induced expression of Ucp1

Other than lipolysis, the PKA signalling pathway is also the most classical pathway in thermogenesis and has been studied in depth. Like lipolysis, the expression of *Ucp1*, the protein considered the origin of adaptive thermogenesis, is regulated by β-adrenergic stimulation and subsequent PKA activation. However, after PKA, downstream thermogenic pathways differ from those of lipolysis in a manner whereby *Ucp1* expression is upregulated by PKA in a p38 MAPK-dependent manner [19]. p38 MAPK controls the expression of the *Ucp1* by activating two important downstream substrates which are also nuclear transcription factors, peroxisome proliferator-activated receptor gamma (PPARγ) coativator 1α (PGC1α, encoded by the *Ppargc1α* gene) and activating transcription factor-2 (ATF2), allowing their interactions with a cAMP response element and a PPAR response element that both reside within a critical enhancer motif of the *Ucp1* gene [18,19]. Independent from p38 MAPK activation, CREB is phosphorylated by PKA and binds with cAMP to directly promote *Ucp1* and *Ppargc1α* expression, promoting the occurrence of beige fat and enhancing thermogenesis [19]. To examine whether MG affects *Ucp1* expression, *Ucp1* expression was determined following stimulation by isoproterenol, in differentiated immortalized iWAT-derived pre-adipocytes. As shown in **Fig. 3-2(A)**, pre-treatment with MG decreased *Ucp1* expression induced by three hours of isoproterenol treatment. Using the range of 0–2 mM MG that was found to not affect cell viability (**Fig. 2-1(A–B)**), the inhibitory effect of MG on the isoproterenol-induced *Ucp1* expression was found to be dose-dependent (**Fig. 3-2(B)**). In addition, usage of a luciferase reporter system show that MG significantly decreased the luciferase activity of the mouse *Ucp1* gene promoter reporter plasmid under isoproterenol stimulation, which suggests that MG attenuates the isoproterenol-induced expression of *Ucp1* through decreasing its promoter activity (**Fig. 3-2(C)**). Treatment with BBGC, an inhibitor of GLO1, the main metabolic enzyme for MG, increases the concentration of intracellular MG [122]. It was confirmed that

BBGC pre-treatment also negatively affected the isoproterenol-induced expression of *Ucp1* (**Fig. 3-2(D)**). DHA is the smallest ketotriose that is utilized by many organisms as an energy source. It has been previously reported that DHA is non-enzymatically converted to MG [123], and intracellular MG levels in yeast are increased by cultivation under presence of DHA [124]. It was also confirmed that the isoproterenol-induced expression of *Ucp1* was attenuated by treatment with DHA (**Fig. 3-2(E)**). These results suggest that intracellular MG negatively influences the expression of *Ucp1* induced by adrenergic stimulation. Next, the mechanism by which intracellular MG affects *Ucp1* expression was then examined.

MG did not affect isoproterenol-induced activation of CREB

As stated above, the PKA signalling pathway is one of the major contributors towards the increased gene expression of *Ucp1* which is induced by adrenergic stimulation via activation of the transcription factor, CREB, by phosphorylation at Ser133 in adipocytes [168]. Since MG inhibited isoproterenol-induced *Ucp1* promoter activity, the phosphorylation levels of CREB at Ser133 was examined to validate if MG negatively affected the activation of PKA signalling. As shown in **Fig. 3-3(A)**, the isoproterenol-stimulated increase in the phosphorylation levels of CREB was not significantly decreased by pre-treatment with MG or BBGC. Interestingly, MG and BBGC pre-treatment was instead observed to significantly increase basal levels of CREB phosphorylation (**Fig. 3-3(A)**). Isoproterenol stimulation not only increases the expression of *Ucp1*, but also genes related to beige adipocyte function including *Fgf21*, *Ppargc1α*, *Cidea*, and *Dio2* by activating PKA signalling [169,170,171,172]. As shown in **Fig. 3-3(B)**, MG did not significantly decrease the isoproterenol-induced expression of these genes. This observation is consistent with the analysis of PKA signalling activity by western blotting in **Fig. 3-3(A) and Fig. 3-1(C)**, suggesting that MG may specifically inhibit *Ucp1* expression without affecting PKA signalling in response to isoproterenol stimulation.

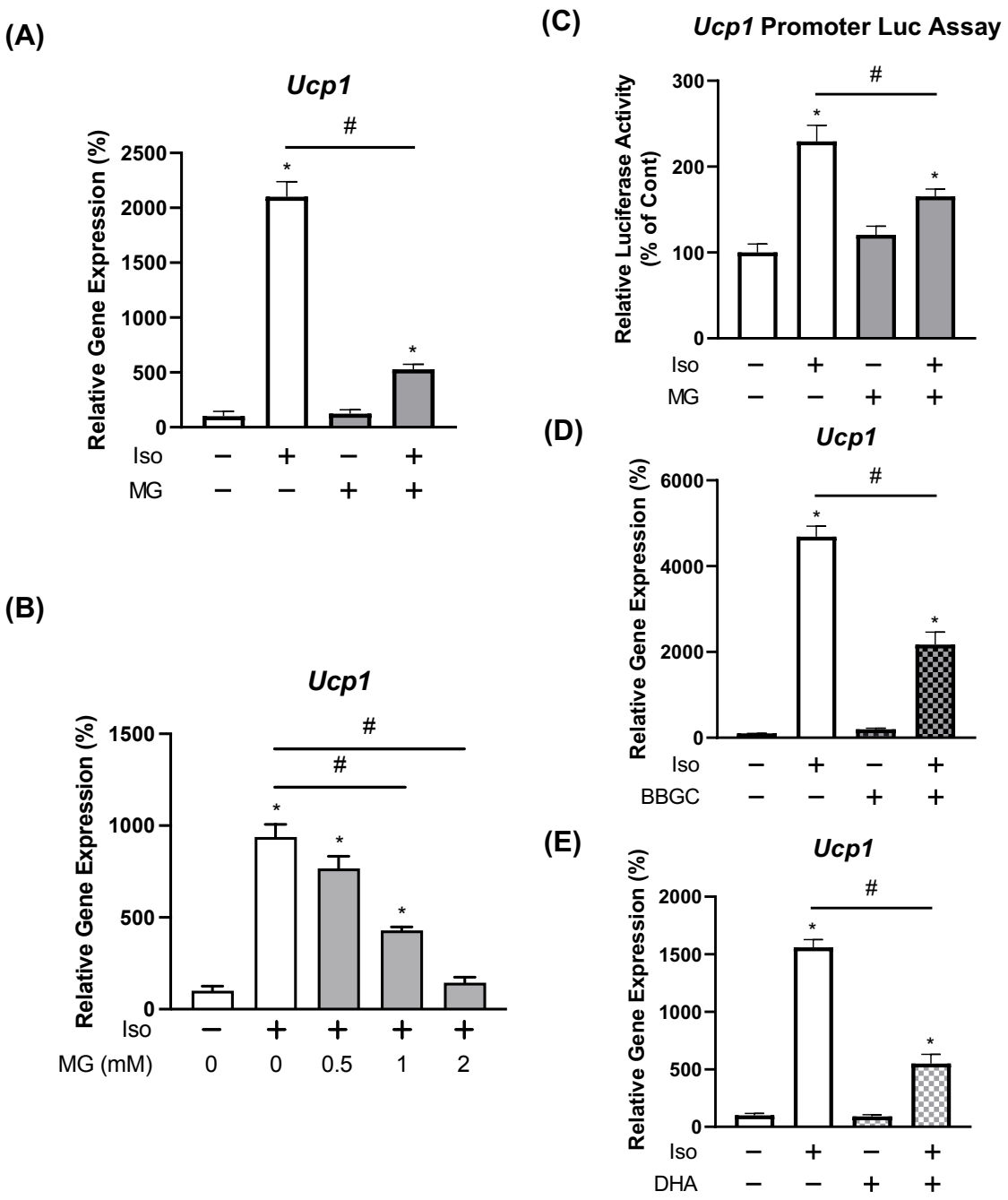

Figure 3-2. MG attenuated the isoproterenol-induced expression of *Ucp1*

(A–B) Adipocytes were treated with 1 mM MG **(A)** or 0.5, 1, or 2 mM MG **(B)** for 30 min, followed by stimulation with 1 μM isoproterenol (Iso) for 3 h. mRNA expression levels of *Ucp1* in the cells were then determined by real-time PCR. **(C)** C3H10T1/2 fibroblasts were transfected with the *Ucp1* promoter reporter plasmid, pUCP1-pro-Luc. After that, the cells were treated with 1 mM MG for 30 min, followed by stimulation with 1 μM isoproterenol for 6 h. Cells were lysed and luciferase assay was then performed. **(D–E)** 20 μM BBGC **(C)**, or 25 mM DHA **(D)** were pre-treated in adipocytes for 30 min, followed by stimulation with 1 μM isoproterenol for 3 h. Then, mRNA expression levels of *Ucp1* in the cells were determined by real-time PCR. Data are presented as the mean ± SEM (error bars), with n = 4 **(A,B,E)**, 3-4 **(D)**, or 5 **(C)** per group. One-way ANOVA followed by Dunnett's **(A,D)** or Sidak's **(B,C,E)** post-hoc tests were done to determine statistical significance. *, $P < 0.05$ between the non-treated vehicular control group and respective groups. #, $P < 0.05$ differences between the indicated groups.

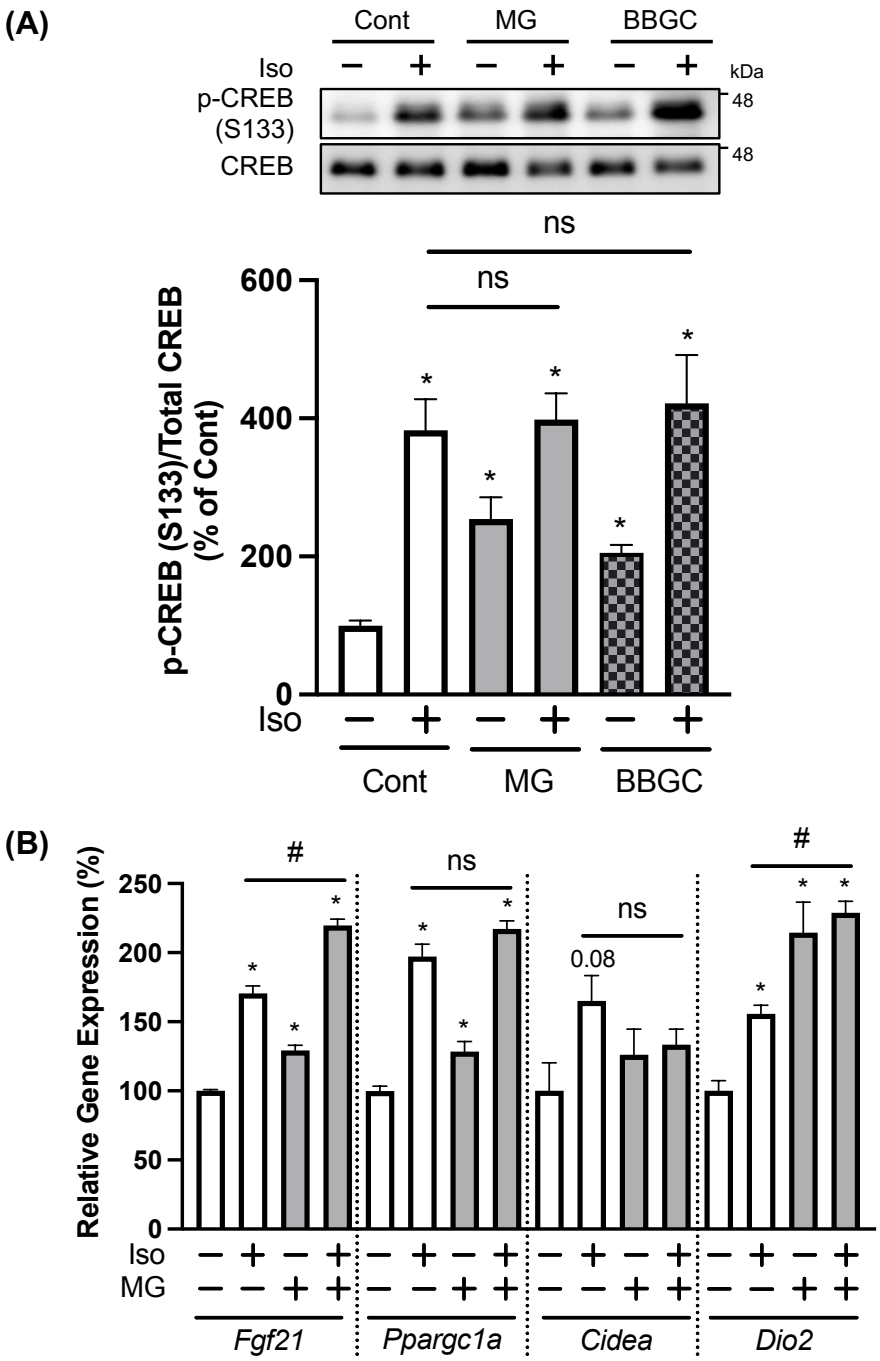

Figure 3-3. MG did not affect isoproterenol-induced activation of CREB

(A) Adipocytes were treated with 20 μM BBGC or 1 mM MG for 30 min before stimulation with 1 μM isoproterenol (Iso) for 30 min. Phosphorylation of CREB (p-CREB) and protein levels of CREB were determined using anti-phospho CREB Ser133 and anti-CREB, respectively. Levels of p-CREB were quantified by measuring the intensity of the immunoreactive bands using ImageJ. The ratio of p-CREB/CREB in the non-stimulated vehicular control group was assigned a relative value of 100. **(B)** Expression levels of thermogenic genes (*Fgf21*, *Ppargc1a*, *Cidea* and *Dio2*) in cells treated with 1 mM MG for 30 min before stimulation with 1 μM Iso for 3 h. Data are presented as mean ± SEM (error bars), with n = 5 **(A)** or 4 **(B)** per group. One-way ANOVA followed by Dunnett's **(A)** or Sidak's **(B)** post-hoc tests were done to determine statistical significance. *, $P < 0.05$ between the non-treated vehicular control group and respective groups. #, $P < 0.05$; ns, non-significant differences between the indicated groups.

TAK1 inhibition did not recover MG-induced inhibition of Ucp1 expression

The results seen in Chapter 1 show that MG treatment significantly increased proinflammatory gene expression (**Fig. 2-8(A)**). In the study for this chapter, differentiated immortalized iWAT-derived pre-adipocytes were used instead of the 3T3-L1 adipocytes that were used in Chapter 1. However, they also display a similar phenotype to what can be observed in **Fig. 2-8(A)**, i.e., MG treatment in these adipocytes also elicited an inflammatory response, as evidenced by increased expression of the proinflammatory genes, *Ccl2* (gene encoding MCP1) and *Il6*, upon MG treatment as shown in **Fig. 3-4(A–B)**. However, the extent of the increase in expression of these genes after MG treatment was not as high when compared to what can be observed in **Fig. 2-8(A)** (less that 1.5-fold increase for both *Ccl2* and *Il6* in **Fig. 3-4(A–B)** compared to ~three-fold increase for *Ccl2* and ~12.5-fold increase for *Il6* in **Fig. 2-8(A)**). Still, the increased expression of proinflammatory cytokines suggests that TAK1 was activated in these adipocytes as well. Inflammation has been reported to negatively regulate β-adrenergic stimulated *Ucp1* expression [36]. To examine if the proinflammatory signalling pathway is involved in the suppression of isoproterenol-induced *Ucp1* expression that was caused by both MG as well as BBGC treatment, TAK1 in these differentiated immortalized iWAT-derived pre-adipocytes were first inhibited via pre-treatment using the same TAK1 inhibitor, (5*Z*)-7-oxozeaenol, as had been used in **Fig. 2-8(A)**, before subsequent MG or BBGC treatment. This is later followed by isoproterenol stimulation. Despite inhibition of TAK1 by (5*Z*)-7-oxozeaenol, the suppressed isoproterenol-induced *Ucp1* expression by either MG or BBGC treatment did not recover (**Fig. 3-4(C)**). This result suggests that MG-induced activation of TAK1 may not be involved in the decrease in isoproterenol-induced *Ucp1* expression that was caused by either exogenous or endogenous MG.

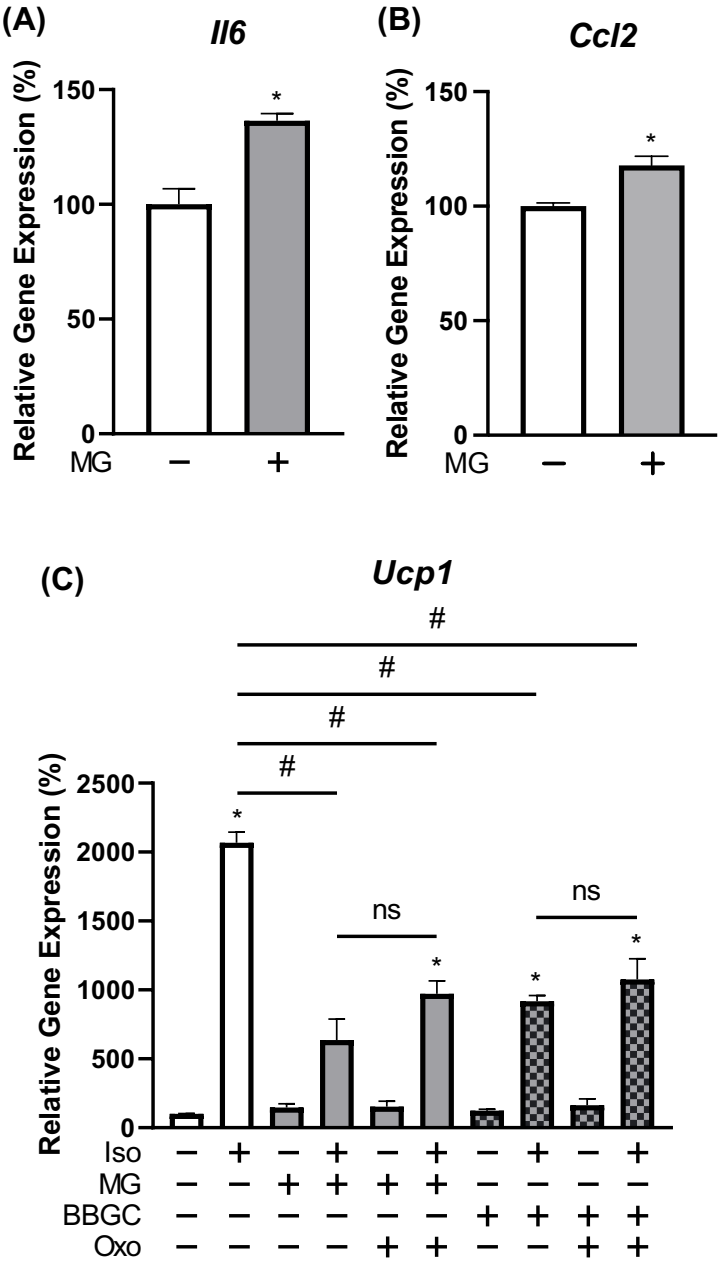

Figure 3-4. TAK1 inhibition did not recover MG-induced inhibition of *Ucp1* expression
(A–B) Adipocytes were treated with 1 mM MG for 3 h. mRNA expression levels of *Il6* **(A)** and *Ccl2* **(B)** in the cells were then determined by real-time PCR. **(C)** Adipocytes were pre-treated with 0.5 μM Oxo for 30 min. The cells were then treated with either 1 mM MG or 20 μM BBGC for an additional 30 min before stimulation with 1 μM isoproterenol (Iso) for 3 h. mRNA expression levels of *Ucp1* in the cells was determined by real-time PCR. Data are presented as the mean ± SEM (error bars), with n = 4 **(A–C)** per group. Student's *t*-test **(A–B)** or one-way ANOVA followed by Dunnet's post-hoc test **(C)** was done to determine statistical significance. *, $P < 0.05$ between the non-treated vehicular control group and respective groups. #, $P < 0.05$; ns, non-significant differences between the indicated groups.

MG attenuated Ucp1 expression through the activation of JNK signalling pathway

Although TAK1 MAPKKK was found to not be involved in the isoproterenol-induced *Ucp1* expression that was suppressed by MG, the downstream ERK, JNK and p38 MAPKs have been reported to modulate *Ucp1* expression [18,19,173,174,175,176,177]. MG is involved in the activation of signalling pathways as a signalling molecule in diverse organisms from yeast to mammalian cells [56,67]. This extends to cultured cells *in vitro*, where MG has been reported to induce the activation of ERK, JNK, and p38 MAPK signalling pathways [98,99,100]. As has been observed in 3T3-L1 cells in **Fig. 2-6(A–D)** in Chapter 1, MG treatment in differentiated immortalized iWAT-derived pre-adipocytes also enhanced phosphorylation of the stress activated protein kinases (SAPKs), JNK and p38 MAPKs (**Fig. 3-5(A)**). An increase in the phosphorylation levels of JNK and p38 MAPK was also observed following treatment with BBGC, the inhibitor of the MG metabolic enzyme, GLO1 (**Fig. 3-5(B)**). In contrast, ERK phosphorylation levels were not significantly affected by either MG or BBGC treatment (**Fig. 3-5(A–B)**), and this result is also consistent with the ERK phosphorylation results found in **Fig. 2-6(A)** that was conducted in 3T3-L1 adipocytes.

To determine whether the activation of JNK and p38 MAPK participates in the negative effect of MG on *Ucp1* expression, the effect of the respective MAPK inhibitors on the MG-induced inhibition of *Ucp1* expression were examined. Although the p38 MAPK inhibitor, SB203580, did not affect the decrease in the isoproterenol-induced expression of *Ucp1* by MG or BBGC treatment, the JNK inhibitor, SP600125, recovered the isoproterenol-induced expression of *Ucp1* that was decreased by MG or BBGC treatment (**Fig. 3-5(C–D)**). These results suggest that MG attenuates the isoproterenol-induced expression of *Ucp1* through the activation of the JNK signalling pathway.

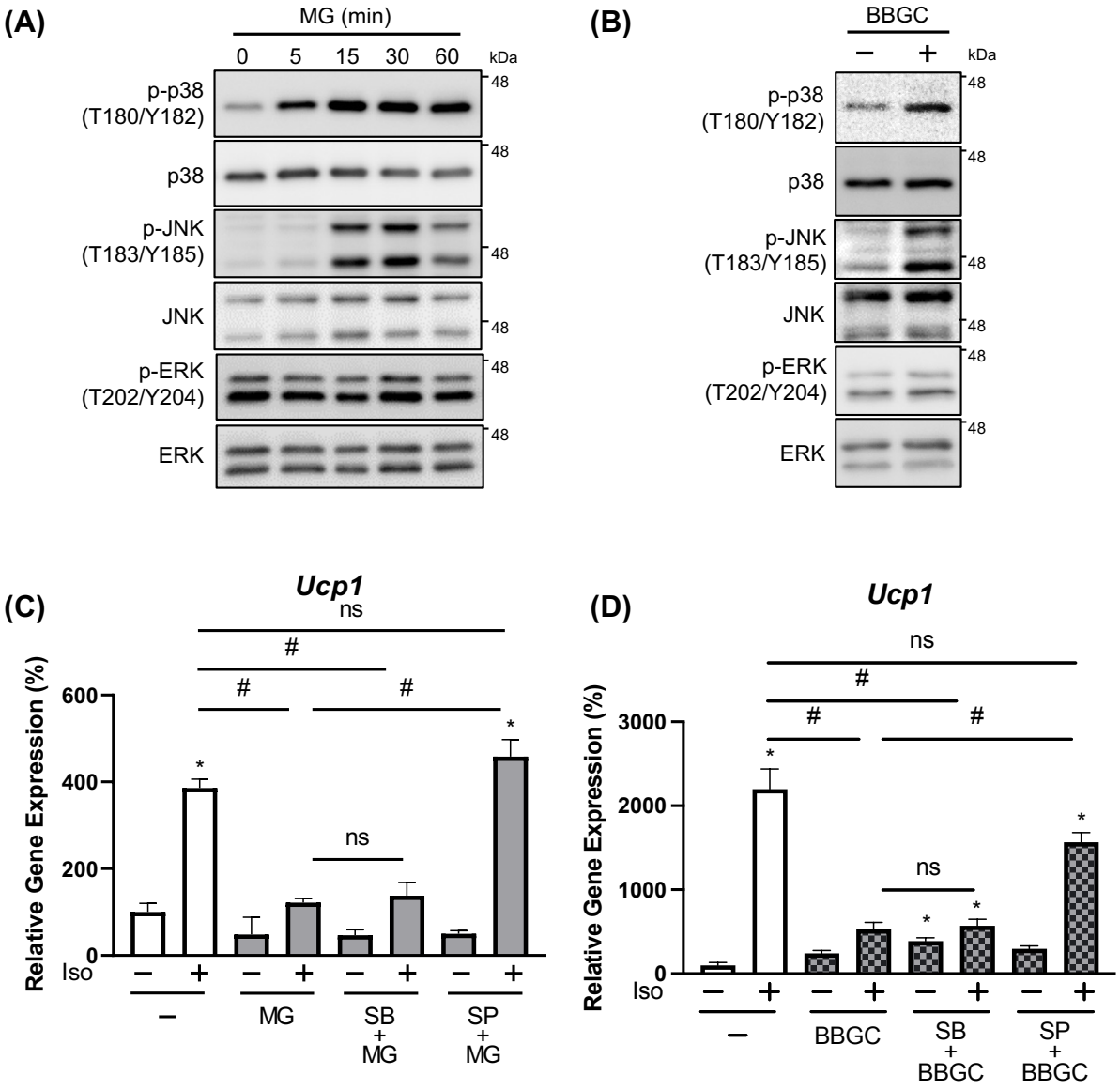

Figure 3-5. MG attenuated *Ucp1* expression through the activation of JNK signalling pathway **(A–B)** Adipocytes were treated with 1 mM MG for 5, 15, 30, or 60 min **(A)** or 20 μM BBGC for 30 min **(B)**. Phosphorylation of p38 (p-p38), protein levels of p38, phosphorylation of JNK (p-JNK), protein levels of JNK, phosphorylation of ERK (p-ERK), and protein levels of ERK were determined as described in the legend of **Figure 2-6**. **(C–D)** Adipocytes were pre-treated with 10 μM SB203580 (SB), a p38 inhibitor, or 10 μM SP600125 (SP), a JNK inhibitor, for 30 min. The cells were then treated with either 1 mM MG **(C)** or 20 μM BBGC **(D)** for an additional 30 min before stimulation with 1 μM isoproterenol (Iso) for 3 h. mRNA expression levels of *Ucp1* in the cells was determined by real-time PCR. Data are presented as the mean ± SEM (error bars), with n = 4 **(A–D)** per group. One-way ANOVA followed by Sidak's **(C)** or Dunnett's **(D)** post-hoc test was done to determine statistical significance. *, $P < 0.05$ between the non-treated vehicular control group and respective groups. #, $P < 0.05$; ns, non-significant differences between the indicated groups.

ROS generation was not involved in the MG-induced inhibition of Ucp1 expression

MAPKs react to diverse extracellular stimuli by eliciting intracellular responses which coordinately regulate multiple cellular programs such as cell proliferation, differentiation, motility, and survival [178]. An increase in ROS levels can adversely affect cell function and homeostasis, leading to oxidative stress which also activates certain MAPKs [178,179]. MG has been reported to increase the levels of intracellular ROS [78,79,80,114], and in some cell lines, such as human umbilical vascular endothelial cells and pancreatic β-cells, MG has been reported to activate the JNK signalling pathway through ROS generation [180,181]. Therefore, whether or not the MG-induced phosphorylation of JNK is due to ROS generation in differentiated immortalized iWAT-derived pre-adipocytes were examined using the ROS inhibitor, NAC. Similar to the other reported cell lines [180,181], three-hour treatment of differentiated immortalized iWAT-derived pre-adipocytes with MG also generate ROS, which could be inhibited by NAC pre-treatment, in the adipocytes (**Fig. 3-6(A)**). These results differ from the results found in **Fig. 2-7(A)** that was from 3T3-L1 adipocytes treated with MG for an hour. H_2O_2 treatment before isoproterenol stimulation significantly inhibits *Ucp1* expression, and pre-treatment with the ROS scavenger, NAC, prior to H_2O_2 treatment could recover the reduced isoproterenol-induced *Ucp1* expression that was caused by H_2O_2 treatment (**Fig. 3-6(B)**). In contrast, neither the MG-induced inhibition of isoproterenol-induced *Ucp1* expression (**Fig. 3-6(C)**), nor the increase in JNK phosphorylation following treatment with MG (**Fig. 3-6(D)**) could be significantly affected by the presence of NAC. These results suggest that while ROS was generated in differentiated immortalized iWAT-derived pre-adipocytes upon MG treatment, it was not involved in the MG-induced phosphorylation of JNK and the MG-inhibited isoproterenol-induced *Ucp1* expression.

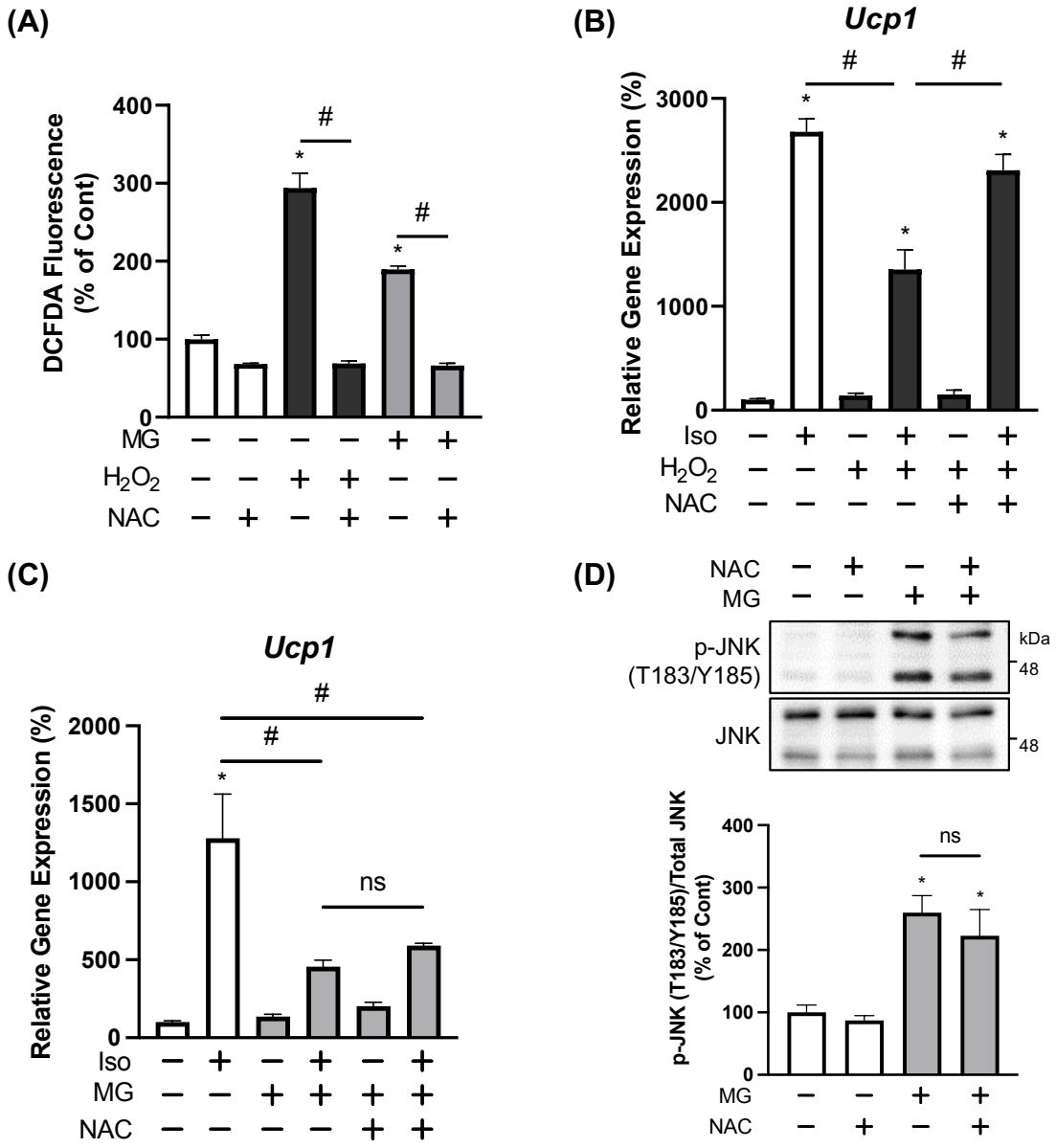

Figure 3-6. ROS generation was not involved in the MG-induced inhibition of *Ucp1* expression
(A) Adipocytes were pre-treated with 2 μM H2DCFDA with or without 10 mM NAC for 30 min, followed by treatment with either 500 μM H_2O_2 or 1 mM MG for 3 h. Intracellular ROS assay was then performed. **(B–C)** After pretreatment of cells with 10 mM NAC and 500 μM H_2O_2 **(B)** or 1 mM MG **(C)** for 30 min each, cells were stimulated with 1 μM isoproterenol (Iso) for 3 h, and mRNA expression levels of *Ucp1* was determined by real-time PCR. **(D)** Adipocytes were pre-treated with 10 mM NAC, a ROS inhibitor, for 30 min before treatment with 1 mM MG for 1 h. Phosphorylation of JNK (p-JNK) and protein levels of JNK were determined as described in the legend of **Figure 2-6**. Phosphorylation levels of JNK were quantified by measuring the intensity of the immunoreactive bands using ImageJ. The ratio of p-JNK/JNK in the non-stimulated vehicular control group was assigned a relative value of 100. Data are presented as the mean ± SEM (error bars), with n = 4 **(A–B)**, 3-4 **(C)**, or 6 **(D)** per group. One-way ANOVA followed by Sidak's **(A,C,D)** or Dunnet's **(B)** post-hoc test were done to determine statistical significance. *, $P < 0.05$ between the non-treated vehicular control group and respective groups. #, $P < 0.05$; ns, non-significant differences between the indicated groups.

Discussion

Acute MG treatment attenuated isoproterenol-stimulated Ucp1 expression without contributing towards catecholamine resistance

Many studies have shown that UCP1 activity is inversely correlated to obesity and T2D [38,39,40], and there is increasing evidence that proinflammatory signals directly alter thermogenic activity in brown and beige adipocytes [182]. Induction of inflammation by LPS or IL1β have been found to downregulate *Ucp1* expression in immortalized brown adipocytes [183]. Conversely, deletion of IKKε or interferon regulatory factor-3 (IRF3), which are among the main inflammation regulators in obesity, results in enhanced WAT browning with increased *Ucp1* expression and energy expenditure [184,185]. One possible explanation for this phenomenon of inflammation-suppressed *Ucp1* expression could be the provocation of catecholamine resistance, or dulled response towards adrenergic stimulation, during inflammation in adipocytes [34,35,36]. This is especially so when the main regulator of *Ucp1* expression is PKA signalling that has been activated by cAMP, whose levels increase during adrenergic stimulation [18,19]. MG is a dicarbonyl metabolite derived from glycolysis that contributes to aging and disease by inducing carbonyl stress when MG concentrations exceed typical concentrations of 50–250 nM in human plasma and 1–5 μM in cells [43,131]. It is also a metabolite that is associated with inflammation and oxidative stress [74,75,76,77], both of which have been demonstrated in this study (**Figs. 3-4(A–B), 3-6(A)**). In this study, it was found that both MG treatment and inhibition of MG metabolism via the use of the GLO1 inhibitor, BBGC, repressed isoproterenol-induced *Ucp1* expression due to reduced *Ucp1* transcription which can be observed from reduced *Ucp1* promoter activity when adipocytes were treated with exogenous MG (**Fig. 3-2**). However, despite an increment of proinflammatory gene expression induced by MG treatment (**Fig. 3-4(A–B)**), there was no effect on PKA signalling (**Figs. 3-1(C), 3-3(A)**) and subsequent FFA and glycerol release (**Figs.**

3-1(A–B)). As such, the suppressed isoproterenol-induced *Ucp1* expression in adipocytes by MG treatment in this study was not caused by catecholamine resistance. This absence of catecholamine resistance in the adipocytes in this study could perhaps be explained by the fact that the experiment system in this study focuses more on acute treatment of MG (total MG or BBGC treatment time is three–four hours), rather than chronic, meaning that the inflammation induced in this study is also acute inflammation, rather than chronic inflammation. Therefore, whether or not inflammation that is induced by MG is responsible for catecholamine resistance, or increased circulatory FFA [30] under conditions of chronic inflammation warrants another investigation using lengthier MG treatment durations.

The potential mechanism by which MG increased basal CREB phosphorylation and other thermogenic genes

Treatment of adipocytes with MG or BBGC increased basal levels of CREB phosphorylation (**Fig. 3-3(A)**). Ser133 in CREB is known as a phosphorylation target site of various kinases such as mitogen- and stress-activated protein kinase (MSK)-1 [111], TAK1 [186,187], and apoptosis signal-regulating kinase (ASK)-1 [188] in addition to PKA. Since MG did not activate PKA signalling, MG might have enhanced CREB phosphorylation through the activation of either of those kinases.

Meanwhile, apart from *Cidea*, MG treatment increases the expression of all other thermogenic marker genes (**Fig. 3-3(B)**). The p38 MAPK signalling pathway has been reported to lead to the upregulation of *Dio2* [196], as well as the phosphorylation of ATF2 [18] which promotes downstream target genes including *Ppargc1a* and *Fgf21* [197,198]. Therefore, the increment in most of the other thermogenic genes by MG treatment could be attributed to increased MG-induced p38 activity.

Possible molecular mechanisms underlying the JNK-dependent inhibition of isoproterenol-stimulated Ucp1 expression in MG-treated adipocytes

CREB and p38 phosphorylation is necessary for *Ucp1* expression. Despite increased phosphorylation of both CREB and p38 by MG treatment (**Figs. 3-3(A), 3-5(A–B)**), basal *Ucp1* expression was unaffected by either MG or BBGC treatment (**Fig. 3-2**). This may be due to the inhibitory effects of JNK-activated activator protein (AP)-1 complexes upon MG treatment, which competitively represses transcriptional activity at the CREB binding site at the proximal regulatory region near the transcription start site of *Ucp1* [170,177]. AP1 might also have contributed to the inhibition of isoproterenol-induced *Ucp1* expression under MG treatment as a transcriptional repressor. Nevertheless, further study is needed to elucidate if MG activates AP1 through JNK to inhibit *Ucp1* expression via inhibitory binding at the CREB binding site at the proximal regulatory region near the transcription start site of *Ucp1* under both basal and isoproterenol-stimulated conditions in adipocytes.

The number of mitochondria and UCP1 protein in beige adipocytes strongly depends on the activity of mitophagy [189,190], which is repressed in response to thermogenic activation [191,192]. Meanwhile, MG was recently shown to increase mitophagy in brain endothelial cells [193], and the involvement of JNK as an upstream regulator of mitophagy has been reported [194,195]. Hence, another one of the possible molecular mechanisms underlying the MG-induced inhibition of *Ucp1* expression may involve altered mitophagy activity through the activation of the JNK signalling pathway. However, further investigations of the involvement of alterations to mitochondria homeostasis by MG treatment are necessary.

Further studies are necessary to understand the effect of MG on UCP1 protein levels as well as its thermogenic functionality

Thermogenesis in adipose tissue is related to metabolic diseases such as obesity and T2D [40]. Thermogenesis mediated by UCP1 is an important component of total energy expenditure and contributes to the overall energy balance [40]. Based on the findings of this study, the analysis of MG on the thermogenic function in adipose tissues regarding the inhibitory effect of MG on *Ucp1* expression may lead to further understanding of the relationship between MG and diabetes mellitus. However, since this study especially focused on the regulatory mechanisms of *Ucp1* mRNA expression, further investigations into MG's effect on UCP1 protein levels as well as its thermogenic functionality are needed to understand the physiological functions on adipocytes.

The extent by which exogenous MG is incorporated intracellularly in adipocytes to reflect pathological levels found in obesity and diabetes

In both Chapter 1 and 2, the concentrations of MG used to treat the cells are beyond the physiological concentrations of MG, which has been reported to be 50–250 nM in human plasma if the method of quantification is by UPLC-MS/MS, and up to 400 μM if quantified by other methods [43,131]. Chapter 1 used a concentration of 2.5 mM, while Chapter 2 used a concentration of 1 mM, which can be up to 50000-fold and 20000-fold, respectively, of what is found physiologically in blood plasma when MG is quantification by UPLC-MS/MS. Intracellular levels of MG that is estimated at ~1–5 μM have been found to be higher than extracellular levels of MG found in the blood plasma [43]. Thus, for the increment of intracellular MG levels to match pathological cellular levels found in patients with obesity or diabetes, the addition of yet higher extracellular levels of MG may be necessary to increase MG accumulation within the cell. Within the cell, > 99% of MG is detoxified primarily by the

GLO system, and it was observed that 0.5 mM of extracellular MG had a nearly directly proportional conversion rate of ~0.5 mmol/h/L to D-lactate in 50% (v/v) red blood cell suspensions [58]. This suggests that MG is freely cell permeable, and at the concentration of 0.5 mM, most MG are metabolised to D-lactate within the hour in the case of erythrocytes. On the other hand, using radiolabelled MG added to the conditioned medium, only 3.1 ± 0.39% of the 2.5 mM of MG was found to be incorporated into L6 cells within 10–30 minutes [199]; while only 1.8% of the 160 μM MG was found to be incorporated into rat aortic smooth muscle cells after 15 minutes of extracellular MG addition [200]. This discrepancy between intracellular incorporation of MG into erythrocytes and muscle cells may perhaps be due to a difference in cell size, where a typical myotube diameter of up to 25 μm [201] is approximately three-fold larger than the typical red blood cell diameter of 8 μm [202]. This difference in cell size potentially affects the surface area for MG incorporation into the cell. Considering that the typical size for adipocytes has been reported to be up to 300 μm in diameter [203], which is 12-fold larger than the diameter of myotubes, it is implied that MG incorporation into adipocytes may be even lesser when compared to the 1.8–3.1% MG incorporation in muscle cells [199,200]. Therefore, taking into account the efficiency of the GLO system as well as the cell size of adipocytes, a supraphysiological concentration of extracellular MG may be necessary to increase intracellular levels in adipocytes to reflect pathological cellular levels of MG found in metabolic disorders. Decreased *Glo1* expression and activity have been associated with obesity and diabetes [43,56,125,126], so the use of the GLO1 inhibitor, BBGC, may have better reflected the pathophysiological state found in metabolic disorders, where endogenously produced MG are implied to accumulate intracellularly. The use of BBGC elicited similar p38 or JNK MAPK signalling to what was elicited after extracellular MG addition (**Figs. 2-6, 2-9(A), 3-5(A–B)**). Hence, although extracellular levels of MG used in this study were supraphysiological,

substantiation of the data with the more physiologically relevant BBGC data show that the findings in this study are physiologically plausible.

Other reactive dicarbonyl metabolites may also induce the same phenomena as MG in adipocytes

The dicarbonyl, methylglyoxal, which is derived from glycolysis was the main focus of this study. MG is up to 20,000-fold more reactive than glucose [50], and the pathology of MG may involve the modification of arginine, lysine, and/or cysteine amino acid residues to form products which include MG-H1, CEL [51,52], and the more recently discovered MICA [132,133]. The generation of these amino acid modifications are based on the high reactivity of the dicarbonyl group of MG. However, apart from MG, other highly reactive dicarbonyl metabolites such as glyoxal, 3-deoxyglucosone also provoke dicarbonyl stress in physiological systems [131]. Like MG, glyoxal reacts with arginine and cysteine residues to form *N*δ-(5-hydro-4-imidazolon-2-yl)ornithine (G-H1) and *N*ε-carboxymethyl-lysine (CML) respectively; glyoxal also reacts with dG in DNA to form N^2-carboxymethyl-deoxyguanosine (CMdG) [131]. Meanwhile, 3-deoxyglucosone also reacts with arginine to produce 3-deoxyglucosone-derived hydroimidazolone isomers (3DG-H) [131]. While MG is formed mainly from the degradation of G-3-P and DHAP in anaerobic glycolysis and glyceroneogenesis, glyoxal is formed mainly from lipid peroxidation and the degradation of glycated proteins; and 3-deoxyglucosone is formed mainly from the enzymatic repair of glycated proteins [131]. Like for MG, the GLO system is also the major metabolic system for glyoxal [131]. In the meantime, aldoketo reductases play the main role in metabolizing 3-deoxyglucosone [131]. Using UPLC-MS/MS, plasma levels of MG, glyoxal and 3-deoxyglucosone from patients with T2D vs healthy controls are measured to be as follows: 277 ± 9 vs 212 ± 8 nmol/L; 514 ± 49 vs 406 ± 26 nmol/L and 2217 ± 81 vs 1046 ± 37 nmol/L [204]; while plasma levels of MG and glyoxal

plasma levels from patients with T1D vs healthy controls determined using liquid chromatography-mass spectrophotometry were as follows: 841.7± 237.7 vs 439.2± 90.1 nmol/L and 1051.8± 515.2 vs 328.2± 207.5 nmol/L [205]. Like MG, it has been found that these elevated levels of glyoxal and 3-deoxyglucosone contribute towards the pathophysiology of diabetes [200,206,207,208]. MG and glyoxal differ only by MG possessing an additional methyl group compared to glyoxal, which causes a difference in reactivity. Despite that, considering that both of these metabolites react with the same amino acid residues in the same way, it is possible that glyoxal might also elicit similar phenomena in adipocytes as found in this study. This is especially so when both metabolites have been reported to induce the phosphorylation of both JNK and p38 MAPK in human endothelial cells [98]. Moreover, when taking into account that both MG and glyoxal are metabolised by the GLO system, there is a possibility that the data from BBGC (**Figs. 2-6, 2-9(A), 3-5(A–B)**) may also be due to the production of glyoxal during GLO1 inhibition. This is especially when glyoxal levels are found to be higher in plasma [204,205], and if like MG, glyoxal intracellular levels are higher than extracellular levels, it can be implied that GLO1 inhibition may lead to higher accumulation of intracellular levels of glyoxal compared to MG as well. However, at this point of time, there are no literature reporting the differences between the concentration of glyoxal extracellularly and intracellularly. Meanwhile, as for whether or not 3-deoxyglucosone may reproduce similar phenomena to the findings of this study, while there is a possibility, it may be lesser compared to glyoxal due to its smaller reactivity which causes it to react mostly with arginine residues only [131].

MG may affect different aspects of metabolism in adipocytes through the activation of different signalling pathways and cellular events

MG induced the phosphorylation of JNK and p38 MAPKs (**Figs. 2-6, 3-5(A–B)**). However, the inhibitory effect of MG on insulin-stimulated glucose uptake was dependent on p38, whilst the inhibitory effect of MG on catecholamine-stimulated *Ucp1* expression relied on JNK. This reliance of MG on different MAPKs for its inhibitory action may in a large part be due to the opposing functions of p38 MAPK during different hormone-stimulated adipocyte metabolic responses. In the context of insulin-stimulated glucose uptake, insulin stimulation in 3T3-L1 adipocytes was found to increase p38 phosphorylation, and human adipocytes from T2D subjects were found to exhibit increased phosphorylation of p38 which contributed towards the downregulation of GLUT4 expression [209]. These phenomena links p38 to the negative regulation of the insulin-stimulated glucose uptake response. Contrarily, p38 activation is necessary for facilitating catecholamine-stimulated thermogenesis as it actively partakes in the control of *Ucp1* gene expression [18,19]. Therefore, because of the differing effects of p38 MAPK on adipocyte physiology, i.e., an inhibitory effect on insulin-stimulated glucose uptake vs an activating effect on catecholamine-stimulated *Ucp1* gene expression, MG may work through different MAPKs to display inhibitory effects on hormone-induced metabolic responses of adipocytes. However, since MG is known to promiscuously modify proteins through accessible arginine, lysine and cysteine amino acid residues, it is entirely thinkable that MG may affect adipocyte physiology through means other than the cellular signalling pathways found in this study. For example, MG has been found to activate NRF2 signalling by directly affecting the NRF2-regulator, KEAP1 [132]. This MG-induced NRF2 signalling was also confirmed in *Caenorhabditis elegans*, but through transient receptor potential (TRP)A1-modulated MG-induced Ca^{2+} flux [210]. MG has also been found to modify histones, H2B, H3 and H4 in particular [211,212]. MG-induced glycation of histones disrupts

chromatin architecture and DNA accessibility especially at transcription start sites by affecting nucleosome core particle through histone-histone and histone-DNA cross-linking [211,212], suggesting that MG could affect epigenetic regulation as well. MG has additionally been implicated in mitochondrial dysfunction by means such as increasing mitophagy and decreasing the mitochondrial membrane potential which subsequently decreases intracellular ATP [193,213,214,215]. This MG-induced mitochondrial dysfunction may affect insulin-induced glucose uptake as the consequent increase in intracellular AMP may activate AMPK to trigger a phosphorylation cascade which culminates in cellular events that inhibits anabolic pathways [21,22]. The mitochondrial dysfunction induced by MG may also affect thermogenesis as mitochondrial dynamics have been implicated in the regulation of thermogenesis in adipocytes [189,190,191,192]. Therefore, while this study investigated the negative effects of MG on hormone-stimulated adipocyte metabolic responses by heavily focusing on the effects of MG on metabolic signalling pathways, it cannot be denied that the effects of MG on hormone-stimulated adipocyte metabolic responses may also be attributed to the potential effects of MG on other cellular events.

The biological function of MG in multicellular organisms remains unknown

Altogether the findings of this study show that MG, the metabolite derived mainly from glycolysis, is capable of negatively affecting adipocyte metabolic events. All cells inevitably generate MG as a product of glucose metabolism, and they possess the MG detoxifying GLO system to adapt to the resulting dicarbonyl stress. Despite MG being a metabolite that is generated in virtually all cells, limited studies have shown the functionality of MG. Due to the growth inhibitory nature of MG, situation-dependent MG production and tolerance have been reported to be a virulence mechanism utilised by bacteria to survive and proliferate in the infected host [216]. For example, MG production in Mycobacterial infection sites cause

apoptosis of the macrophages via activation of the JNK signalling [217]. On the other hand, *Brucella abortus* and *Salmonella Typhimurium* induce the expression of their respective lactoylglutathione lyase genes which confers tolerance to MG to aid the intracellular bacteria to survive and proliferate in macrophages [218,219]. While bacteria have utilised both MG production and metabolism for host-specific adaptation, the main role of MG in the biological system of multicellular organisms still remain a mystery, and questions such as whether a host cell environment has the ability to induce MG generation in intracellular pathogens, whether host cells themselves are capable of producing MG in order to curb microbial activities or their proliferation, and whether MG derived by bacterial pathogens has the ability to modulate host signalling remain unanswered. Instead, current knowledge regarding MG in multicellular organisms is its association with aging and disease [43,131]. Interestingly, despite the involvement of MG in disease pathogenesis, low doses of MG have also been reported to prolong lifespan in *Drosophila melanogaster* and *Caenorhabditis elegans* [47,220,221], suggesting a hormetic potential of MG. However, this hormetic potential of MG is also utilised by cancer cells to survive, grow and metastasise [222,223], indicating a pro-tumoural role of MG. Hence, whether or not MG is a metabolite that possesses particular functions or beneficial properties in multicellular organisms is still subjected to debate, and further investigations are necessary to determine and elucidate the functions of MG in organisms.

Chapter 4

Summary

Obesity is highly correlated with T2D, especially when adipocyte dysfunction is involved. In both obese and diabetic conditions, systemic levels of the glycolytic intermediate, MG, are 1.5–6-fold higher, and a diet high in sugar and fat is a major contributing factor to the significantly increased systemic MG levels. MG accumulation and its metabolic dysregulation have been implicated in adipose tissue dysfunction, leading to systemic metabolic dysfunction and the development of T2D, and the involvement of MG in insulin resistance could be one of the candidate mechanisms of action. Additionally, MG is linked to the activation of inflammatory and oxidative stress pathways, which are major determinants for metabolic dysfunction. In this study, the author has attempted to elucidate the underlying mechanism behind MG's involvement in dysfunction at the cellular level, i.e., in adipocytes.

The first study: The effect of methylglyoxal on insulin-stimulated glucose uptake in adipocytes

Insulin-stimulated glucose uptake is a physiological response of the insulin signalling pathway where IRS-1 is the primary mediator. MG-treated adipocytes show significantly inhibited glucose consumption and insulin-stimulated glucose uptake, and the insulin-induced IRS-1 tyrosine phosphorylation which is necessary for its activation of downstream signalling was found to be significantly reduced. IRS-1 is negatively regulated by serine phosphorylation via the negative feedback loop of the insulin signalling pathway which is regulated by mTORC1. MG was found to induce serine phosphorylation on IRS-1 through mTORC1; and the inhibition of mTORC1 recovered insulin-induced IRS-1 tyrosine phosphorylation and

glucose consumption in MG-treated adipocytes. Although Akt is the nodal point between insulin receptor and mTORC1 signalling, inhibition of Akt had no effect on MG-induced mTORC1 signalling, suggesting that MG activated mTORC1 independently of the insulin signalling pathway. Instead, MG was found to increase inflammatory gene expression via the activation of TAK1, which activates the SAPKs, p38 and JNK. Among them, only p38 inhibition neutralized MG-induced mTORC1 activation. This TAK1–p38–mTORC1 signalling axis is also recapitulated in proinflammatory cytokine, TNFα, treatment, suggesting that this signalling axis occurs during inflammation. Meanwhile, MG treatment in this study did not significantly increase oxidative stress in adipocytes. Altogether, these results indicate that MG negatively affects insulin-signalling and subsequent glucose consumption in adipocytes via inflammatory TAK1–p38–mTORC1 signalling, which induces insulin resistance and possibly contribute to the provocation of T2D. The schematic summary of this study is shown in **Fig. 4-1** (left).

The second study: The effect of methylglyoxal on isoproterenol-induced free fatty acid release and uncoupling protein 1 expression in adipocytes

Catecholamine-induced FFA release in adipocytes is mediated by the PKA pathway which activates multiple lipolytic proteins upon the binding of catecholamine to β-adrenergic receptors. Stimulation of MG-treated adipocytes with the β-adrenergic receptor agonist, isoproterenol, was found to not significantly affect the isoproterenol-induced phosphorylation of PKA-activated proteins as well as subsequent FFA and glycerol release, suggesting that MG has did not induce catecholamine resistance upon acute MG treatment as observed by the absence of any effect on isoproterenol-induced adipocyte lipolysis. Apart from lipolysis, PKA signalling also contributes to adipocyte thermogenesis which is conferred by increased expression of the *Ucp1* gene upon β-adrenergic receptor activation. MG-treatment significantly

reduced the isoproterenol-induced expression of *Ucp1* without affecting other thermogenic gene markers, confirming that MG suppressed isoproterenol-induced *Ucp1* expression independently of PKA. Inflammation has been reported to downregulate *Ucp1* expression, and the adipocytes used in this study also exhibited increased inflammatory gene expression. Among the SAPKs activated by MG, MG was found to suppress isoproterenol-stimulated *Ucp1* expression via JNK and not p38 MAPK. Altogether, these findings elucidate MG as a metabolite which is capable of modulating adipocyte *Ucp1* expression via JNK, possibly leading to reduced energy expenditure and eventual exacerbation of T2D symptoms. The schematic summary of this study is shown in **Fig. 4-1** (right).

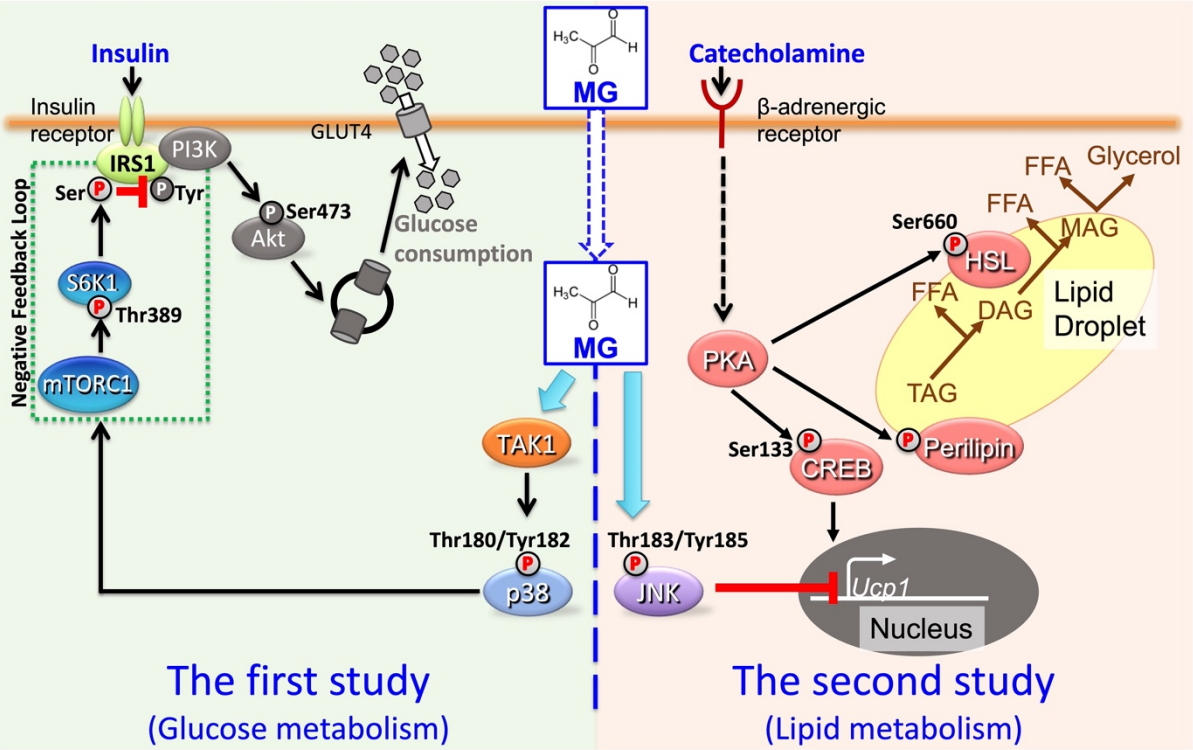

Figure 4-1. Schematic summary of the findings in this study.

References

1. NCD Risk Factor Collaboration. Trends in adult body-mass index in 200 countries from 1975 to 2014: a pooled analysis of 1698 population-based measurement studies with 19· 2 million participants. *Lancet*. 2016;**387**(10026):1377-1396. doi: 10.1016/S0140-6736(16)30054-X.
2. Lobstein T, Brinsden H, Neveux, M. World Obesity Atlas 2022. *World Obesity Federation*. 2022. Available at: http:// s3-eu-west-1.amazonaws.com/wof-files/World_Obesity_ Atlas_2022.pdf
3. Bramante CT, Lee CJ, Gudzune KA. Treatment of obesity in patients with diabetes. *Diabetes Spectr*. 2017;**30**(4):237-243. doi: 10.2337/ds17-0030.
4. Farag YM, Gaballa MR. Diabesity: an overview of a rising epidemic. *Nephrol. Dial. Transplant*. 2011;**26**(1):28-35. doi: 10.1093/ndt/gfq576.
5. Sun H, Saeedi P, Karuranga S, Pinkepank M, Ogurtsova K, Duncan BB, Stein C, Basit A, Chan JC, Mbanya JC, Pavkov ME, Ramachandaran A, Wild SH, James S, Herman WH, Zhang P, Bommer C, Kuo S, Boyko EJ, Magliano DJ. IDF Diabetes Atlas: Global, regional and country-level diabetes prevalence estimates for 2021 and projections for 2045. *Diabetes Res. Clin. Pract*. 2022;**183**:109119. doi: 10.1016/j.diabres.2021.109119.
6. Lin X, Xu Y, Pan X, Xu J, Ding Y, Sun X, Song X, Ren Y, Shan PF. Global, regional, and national burden and trend of diabetes in 195 countries and territories: an analysis from 1990 to 2025. *Sci. Rep*. 2020;**10**(1):14790. doi: 10.1038/s41598-020-71908-9.
7. Swift DL, Houmard JA, Slentz CA, Kraus WE. Effects of aerobic training with and without weight loss on insulin sensitivity and lipids. *PLoS One*. 2018;**13**(5):e0196637. doi: 10.1371/journal.pone.0196637.
8. Zhang L, Huang YJ, Sun JP, Zhang TY, Liu TL, Ke B, Shi XF, Li H, Zhang GP, Ye ZY, Hu J, Qin J. Protective effects of calorie restriction on insulin resistance and islet function in STZ-induced type 2 diabetes rats. *Nutr. Metab. (Lond)*. 2021;**18**(1):48. doi: 10.1186/s12986-021-00575-y.
9. Koliaki C, Liatis S, Le Roux CW, Kokkinos A. The role of bariatric surgery to treat diabetes: current challenges and perspectives. *BMC Endocr. Disord*. 2017;**17**(1):50. doi: 10.1186/s12902-017-0202-6.
10. Li Y, Yun K, Mu R. A review on the biology and properties of adipose tissue macrophages involved in adipose tissue physiological and pathophysiological processes. *Lipids Health Dis*. 2020;**19**(1):164. doi: 10.1186/s12944-020-01342-3.
11. Loskill P, Sezhian T, Tharp KM, Lee-Montiel FT, Jeeawoody S, Reese WM, Zushin PJH, Stahl A, Healy KE. WAT-on-a-chip: a physiologically relevant microfluidic system incorporating white adipose tissue. *Lab Chip*. 2017;**17**(9):1645-1654. doi: 10.1039/c6lc01590e.
12. Lenz M, Arts IC, Peeters RLM, de Kok TM, Ertaylan G. Adipose tissue in health and disease through the lens of its building blocks. *Sci. Rep*. 2020;**10**(1):10433. doi: 10.1038/s41598-020-67177-1.

13. Guilherme A, Rowland LA, Wang H, Czech MP. The adipocyte supersystem of insulin and cAMP signaling. *Trends Cell Biol*. 2022;**S0962-8924**(22)00190-8. doi: 10.1016/j.tcb.2022.07.009.
14. Wu J, Boström P, Sparks LM, Ye L, Choi JH, Giang AH, Khandekar M, Virtanen KA, Nuutila P, Schaart G, Huang K, Tu H, van Marken Lichtenbelt WD, Hoeks J, Enerbäck S, Schrauwen P, Spiegelman BM. Beige adipocytes are a distinct type of thermogenic fat cell in mouse and human. *Cell*. 2012;**150**(2):366-376. doi: 10.1016/j.cell.2012.05.016.
15. Saltiel AR, Kahn CR. Insulin signalling and the regulation of glucose and lipid metabolism. *Nature*. 2001;**414**(6865):799-806. doi: 10.1038/414799a.
16. Haeusler RA, McGraw TE, Accili D. Biochemical and cellular properties of insulin receptor signalling. *Nat. Rev. Mol. Cell Biol*. 2018;**19**(1):31-44. doi: 10.1038/nrm.2017.89.
17. Morigny P, Boucher J, Arner P, Langin D. Lipid and glucose metabolism in white adipocytes: pathways, dysfunction and therapeutics. *Nat. Rev. Endocrinol*. 2021;**17**(5):276-295. doi: 10.1038/s41574-021-00471-8.
18. Cao W, Daniel KW, Robidoux J, Puigserver P, Medvedev AV, Bai X, Floering LM, Spiegelman BM, Collins S. p38 mitogen-activated protein kinase is the central regulator of cyclic AMP-dependent transcription of the brown fat uncoupling protein 1 gene. *Mol. Cell Biol*. 2004;**24**(7):3057-3067. doi: 10.1128/MCB.24.7.3057-3067.2004.
19. Robidoux J, Cao W, Quan H, Daniel KW, Moukdar F, Bai X, Floering LM, Collins S. Selective activation of mitogen-activated protein (MAP) kinase kinase 3 and p38α MAP kinase is essential for cyclic AMP-dependent UCP1 expression in adipocytes. *Mol. Cell Biol*. 2005;**25**(13):5466-5479. doi: 10.1128/MCB.25.13.5466-5479.2005.
20. Inagaki T, Sakai J, Kajimura S. Transcriptional and epigenetic control of brown and beige adipose cell fate and function. *Nat. Rev. Mol. Cell Biol*. 2016;**17**(8):480-495. doi: 10.1038/nrm.2016.62.
21. Tatapudy S, Aloisio F, Barber D, Nystul T. Cell fate decisions: emerging roles for metabolic signals and cell morphology. *EMBO Rep*. 2017;**18**(12):2105-2118. doi: 10.15252/embr.201744816.
22. Marshall S. Role of insulin, adipocyte hormones, and nutrient-sensing pathways in regulating fuel metabolism and energy homeostasis: a nutritional perspective of diabetes, obesity, and cancer. *Sci. STKE*. 2006;**2006**(346):re7. doi: 10.1126/stke.3462006re7.
23. Feng T, Zhao X, Gu P, Yang W, Wang C, Guo Q, Long Q, Liu Q, Cheng Y, Li J, Cheung CKY, Wu D, Kong X, Xu Y, Ye D, Hua S, Loomes K, Xu A, Hui X. Adipocyte-derived lactate is a signalling metabolite that potentiates adipose macrophage inflammation via targeting PHD2. *Nat. Commun*. 2022;**13**(1):5208. doi: 10.1038/s41467-022-32871-3.
24. Zhu X, Tu Y, Chen H, Jackson AO, Patel V, Yin K. Micro-environment and intracellular metabolism modulation of adipose tissue macrophage polarization in relation to chronic inflammatory diseases. *Diabetes Metab. Res. Rev*. 2018;**34**(5):e2993. doi: 10.1002/dmrr.2993.

25. Petrus P, Lecoutre S, Dollet L, Wiel C, Sulen A, Gao H, Tavira B, Laurencikiene J, Rooyackers O, Checa A, Douagi I, Wheelock CE, Arner P, McCarthy M, Bergo MO, Edgar L, Choudhury RP, Aouadi M, Krook A, Rydén M. Glutamine links obesity to inflammation in human white adipose tissue. *Cell Metab*. 2020;**31**(2):375-390.e11. doi: 10.1016/j.cmet.2019.11.019.
26. Wang TJ, Larson MG, Vasan RS, Cheng S, Rhee EP, McCabe E, Lewis GD, Fox CS, Jacques PF, Fernandez C, O'donnell CJ, Carr SA, Mootha VK, Florez JC, Souza A, Melander O, Clish CB, Gerszten RE. Metabolite profiles and the risk of developing diabetes. *Nat. Med*. 2011;**17**(4):448-453. doi: 10.1038/nm.2307.
27. Long J, Yang Z, Wang L, Han Y, Peng C, Yan C, Yan D. Metabolite biomarkers of type 2 diabetes mellitus and pre-diabetes: A systematic review and meta-analysis. *BMC Endocr. Disord*. 2020;**20**(1):174. doi: 10.1186/s12902-020-00653-x.
28. Blüher M. Metabolically healthy obesity. *Endocr. Rev*. 2020;**41**(3):bnaa004. doi: 10.1210/endrev/bnaa004.
29. Smith GI, Mittendorfer B, Klein S. Metabolically healthy obesity: facts and fantasies. *J. Clin. Invest*. 2019;**129**(10):3978-3989. doi: 10.1172/JCI129186.
30. Guilherme A, Virbasius JV, Puri V, Czech MP. Adipocyte dysfunctions linking obesity to insulin resistance and type 2 diabetes. *Nat. Rev. Mol. Cell Biol*. 2008;**9**(5):367-377. doi: 10.1038/nrm2391.
31. Li Z, Gurung M, Rodrigues RR, Padiadpu J, Newman NK, Manes NP, Pederson JW, Greer RL, Vasquez-Perez S, You H, Hioki, KA, Moulton Z, Fel A, De Nardo D, Dzutsev AK, Nita-Lazar A, Trinchieri G, Shulzhenko N, Morgun A. Microbiota and adipocyte mitochondrial damage in type 2 diabetes are linked by $Mmp12^{+}$ macrophages. *J. Exp. Med*. 2022;**219**(7):e20220017. doi: 10.1084/jem.20220017.
32. Zand H, Morshedzadeh N, Naghashian F. Signaling pathways linking inflammation to insulin resistance. *Diabetes Metab. Syndr*. 2017;**11 Suppl 1**:S307-S309. doi: 10.1016/j.dsx.2017.03.006.
33. Chen L, Chen R, Wang H, Liang F. Mechanisms linking inflammation to insulin resistance. *Int. J. Endocrinol*. 2015;**2015**:508409. doi: 10.1155/2015/508409.
34. Mowers J, Uhm M, Reilly SM, Simon J, Leto D, Chiang SH, Chang L, Saltiel AR. Inflammation produces catecholamine resistance in obesity via activation of PDE3B by the protein kinases IKKε and TBK1. *Elife*. 2013;**2**:e01119. doi: 10.7554/eLife.01119.
35. Valentine JM, Ahmadian M, Keinan O, Abu-Odeh M, Zhao P, Zhou X, Keller MP, Gao H, Ruth TY, Liddle C, Downes M, Zhang J, Lusis AJ, Attie AD, Evans RM, Rydén M, Saltiel AR. β3-Adrenergic receptor downregulation leads to adipocyte catecholamine resistance in obesity. *J. Clin. Invest*. 2022;**132**(2):e153357. doi: 10.1172/JCI153357.
36. Mottillo EP, Granneman JG. Intracellular fatty acids suppress β-adrenergic induction of PKA-targeted gene expression in white adipocytes. *Am. J. Physiol. Endocrinol. Metab*. 2011;**301**(1):E122-E131. doi: 10.1152/ajpendo.00039.2011.
37. Sears B, Perry M. The role of fatty acids in insulin resistance. *Lipids Health Dis*. 2015;**14**:121. doi: 10.1186/s12944-015-0123-1.
38. Dong C, Lv Y, Xie L, Yang R, Chen L, Zhang L, Long T, Yang H, Mao X, Fan Q, Chen X, Zhang H. Association of UCP1 polymorphisms with type 2 diabetes mellitus

and their interaction with physical activity and sedentary behavior. *Gene*. 2020;**739**:144497. doi: 10.1016/j.gene.2020.144497.
39. Brondani LDA, Assmann TS, Duarte GCK, Gross JL, Canani LH, Crispim D. The role of the uncoupling protein 1 (UCP1) on the development of obesity and type 2 diabetes mellitus. *Arq. Bras. Endocrinol. Metabol*. 2012;**56**(4):215-225. doi: 10.1590/s0004-27302012000400001.
40. Jia JJ, Tian YB, Cao ZH, Tao LL, Zhang X, Gao SZ, Ge CR, Lin QY, Jois M. The polymorphisms of UCP1 genes associated with fat metabolism, obesity and diabetes. *Mol. Biol. Rep*. 2010;**37**(3):1513-1522. doi: 10.1007/s11033-009-9550-2.
41. Kong X, Ma MZ, Huang K, Qin L, Zhang HM, Yang Z, Li XY, Su Q. Increased plasma levels of the methylglyoxal in patients with newly diagnosed type 2 diabetes. *J. Diabetes*. 2014;**6**(6):535-540. doi: 10.1111/1753-0407.12160.
42. McLellan AC, Thornalley PJ, Benn, Sonksen PH. Glyoxalase system in clinical diabetes mellitus and correlation with diabetic complications. *Clin. Sci. (Lond)*. 1994;**87**(1):21-29. doi: 10.1042/cs0870021.
43. Schalkwijk CG, Stehouwer CDA. Methylglyoxal, a highly reactive dicarbonyl compound, in diabetes, its vascular complications, and other age-related diseases. *Physiol. Rev*. 2020;**100**(1):407-461. doi: 10.1152/physrev.00001.2019.
44. Lu J, Randell E, Han Y, Adeli K, Krahn J, Meng QH. Increased plasma methylglyoxal level, inflammation, and vascular endothelial dysfunction in diabetic nephropathy. *Clin. Biochem*. 2011;44(4):307-311. doi: 10.1016/j.clinbiochem.2010.11.004.
45. Jia X, Wu L. Accumulation of endogenous methylglyoxal impaired insulin signaling in adipose tissue of fructose-fed rats. *Mol. Cell Biochem*. 2007;**306**(1-2):133-139. doi: 10.1007/s11010-007-9563-x.
46. Rodrigues T, Matafome P, Sereno J, Almeida J, Castelhano J, Gamas L, Neves C, Gonçalves S, Carvalho C, Arslanagic A, Wilcken E, Fonseca R, Simões I, Conde SV, Castelo-Branco M, Seiça R. Methylglyoxal-induced glycation changes adipose tissue vascular architecture, flow and expansion, leading to insulin resistance. *Sci. Rep*. 2017;**7**(1):1698. doi: 10.1038/s41598-017-01730-3.
47. Moraru A, Wiederstein J, Pfaff D, Fleming T, Miller AK, Nawroth P, Teleman AA. Elevated levels of the reactive metabolite methylglyoxal recapitulate progression of type 2 diabetes. *Cell Metab*. 2018;**27**(4):926-934.e8. doi: 10.1016/j.cmet.2018.02.003.
48. Lodd E, Wiggenhauser LM, Morgenstern J, Fleming TH, Poschet G, Büttner M, Tabler CT, Wohlfart DP, Nawroth PP, Kroll J. The combination of loss of glyoxalase1 and obesity results in hyperglycemia. *JCI Insight*. 2019;**4**(12):e126154. doi: 10.1172/jci.insight.126154.
49. Prevenzano I, Leone A, Longo M, Nicolò A, Cabaro S, Collina F, Panarese I, Botti G, Formisano P, Napoli R, Beguinot F, Miele C, Nigro C. Glyoxalase 1 knockdown induces age-related β-cell dysfunction and glucose intolerance in mice. *EMBO Rep*. 2022;**23**(7):e52990. doi: 10.15252/embr.202152990.
50. Thornalley PJ, Dicarbonyl intermediates in the Maillard reaction. *Ann. N. Y. Acad. Sci*. 2005;**1043**:111-117. doi: 10.1196/annals.1333.014.
51. Nemet I, Varga-Defterdarović L, Turk Z. Methylglyoxal in food and living organisms. *Mol. Nutr. Food Res*. 2006;**50**(12):1105-1117. doi: 10.1002/mnfr.200600065.

52. Hernandez-Castillo C, Shuck SC. Diet and obesity-induced methylglyoxal production and links to metabolic disease. *Chem. Res. Toxicol*. 2021;**34**(12):2424-2440. doi: 10.1021/acs.chemrestox.1c00221.
53. Degen J, Hellwig M, Henle T. 1, 2-Dicarbonyl compounds in commonly consumed foods. *J. Agric. Food Chem*. 2012;**60**(28):7071-7079. doi: 10.1021/jf301306g.
54. Daffu G, Del Pozo CH, O'Shea KM, Ananthakrishnan R, Ramasamy R, Schmidt AM. Radical roles for RAGE in the pathogenesis of oxidative stress in cardiovascular diseases and beyond. *Int. J. Mol. Sci*. 2013;**14**(10):19891-19910. doi: 10.3390/ijms141019891.
55. Brouwers O, Niessen PM, Ferreira I, Miyata T, Scheffer PG, Teerlink T, Schrauwen P, Brownlee M, Stehouwer CD, Schalkwijk CG. Overexpression of glyoxalase-I reduces hyperglycemia-induced levels of advanced glycation end products and oxidative stress in diabetic rats. *J. Biol. Chem*. 2011;**286**(2):1374-1380. doi: 10.1074/jbc.M110.144097.
56. Inoue Y, Maeta K, Nomura W. Glyoxalase system in yeasts: structure, function, and physiology. *Semin. Cell Dev. Biol*. 2011;**22**(3):278-284. doi: 10.1016/j.semcdb.2011.02.002.
57. Rae C, Berners-Price SJ, Bulliman BT, Kuchel PW. Kinetic analysis of the human erythrocyte glyoxalase system using 1H NMR and a computer model. *Eur. J. Biochem*. 1990;**193**(1):83-90. doi: 10.1111/j.1432-1033.1990.tb19307.x.
58. Phillips SA, Thornalley PJ. Formation of methylglyoxal and D-lactate in human red blood cells *in vitro*. *Biochem. Soc. Trans*. 1993;**21**(2):163S. doi: 10.1042/bst021163s.
59. Phillips SA, Thornalley PJ. The formation of methylglyoxal from triose phosphates: investigation using a specific assay for methylglyoxal. *Eur. J. Biochem*. 1993;**212**(1):101-105. doi: 10.1111/j.1432-1033.1993.tb17638.x.
60. Gaens KH, Stehouwer CD, Schalkwijk CG. Advanced glycation end products and its receptor for advanced glycation endproducts in obesity. *Curr. Opin. Lipidol*. 2013;**24**(1):4-11. doi: 10.1097/MOL.0b013e32835aea13.
61. Chaudhuri J, Bains Y, Guha S, Kahn A, Hall D, Bose N, Gugliucci A, Kapahi P. The role of advanced glycation end products in aging and metabolic diseases: bridging association and causality. *Cell Metab*. 2018;**28**(3):337-352. doi: 10.1016/j.cmet.2018.08.014.
62. Zhu JL, Cai YQ, Long SL, Chen Z, Mo ZC. The role of advanced glycation end products in human infertility. *Life Sci*. 2020;**255**:117830. doi: 10.1016/j.lfs.2020.117830.
63. Thornalley, PJ. The glyoxalase system in health and disease. *Mol. Aspects Med*. 1993;**14**(4):287-371. doi: 10.1016/0098-2997(93)90002-u.
64. Dhar A, Desai KM, Wu L. Alagebrium attenuates acute methylglyoxal-induced glucose intolerance in Sprague-Dawley rats. *Br. J. Pharmacol*. 2010;**159**(1):166-175. doi: 10.1111/j.1476-5381.2009.00469.x.
65. Dhar A, Dhar I, Jiang B, Desai KM, Wu L. Chronic methylglyoxal infusion by minipump causes pancreatic beta-cell dysfunction and induces type 2 diabetes in Sprague-Dawley rats. *Diabetes*. 2011;**60**(3):899-908. doi: 10.2337/db10-0627.
66. Nigro C, Raciti GA, Leone A, Fleming TH, Longo M, Prevenzano I, Fiory F, Mirra P, D'Esposito V, Ulianich L, Nawroth PP, Formisano P, Beguinot F, Miele C.

Methylglyoxal impairs endothelial insulin sensitivity both in vitro and in vivo. *Diabetologia*. 2014;**57**(7):1485-1494. doi: 10.1007/s00125-014-3243-7.
67. Zemva J, Pfaff D, Groener JB, Fleming T, Herzig S, Teleman A, Nawroth PP, Tyedmers J. Effects of the reactive metabolite methylglyoxal on cellular signalling, insulin action and metabolism - what we know in mammals and what we can learn from yeast. *Exp. Clin. Endocrinol. Diabetes*. 2019;**127**:203-214. doi: 10.1055/s-0043-122382.
68. Giacco F, Du X, D'Agati VD, Milne R, Sui G, Geoffrion M, Brownlee M. Knockdown of glyoxalase 1 mimics diabetic nephropathy in nondiabetic mice. *Diabetes*. 2014;**63**:291-299. doi: 10.2337/db13-0316.
69. Bódis K, Roden M. Energy metabolism of white adipose tissue and insulin resistance in humans. *Eur. J. Clin. Invest*. 2018;**48**(11):13017. doi: 10.1111/eci.13017.
70. Coppack SW. Pro-inflammatory cytokines and adipose tissue. *Proc. Nutr. Soc*. 2001;**60**(3):349-356. doi: 10.1079/pns2001110.
71. Jager J, Grémeaux T, Cormont M, Le Marchand-Brustel Y, Tanti JF. Interleukin-1beta-induced insulin resistance in adipocytes through down-regulation of insulin receptor substrate-1 expression. *Endocrinology*. 2007;**148**(1):241-251. doi: 10.1210/en.2006-0692.
72. Copps KD, White MF. Regulation of insulin sensitivity by serine/threonine phosphorylation of insulin receptor substrate proteins IRS1 and IRS2. *Diabetologia*. 2012;**55**(10):2565-2582. doi: 10.1007/s00125-012-2644-8.
73. Cai W, Ramdas M, Zhu L, Chen X, Striker GE, Vlassara H. Oral advanced glycation endproducts (AGEs) promote insulin resistance and diabetes by depleting the antioxidant defenses AGE receptor-1 and sirtuin 1. *Proc. Natl. Acad. Sci. USA*. 2012;**109**(39):15888-15893. doi: 10.1073/pnas.1205847109.
74. Brouwers O, Niessen PM, Miyata T, Østergaard JA, Flyvbjerg A, Peutz-Kootstra CJ, Sieber J, Mundel PH, Brownlee M, Janssen BJ, De Mey JG, Stehouwer CD, Schalkwijk CG. Glyoxalase-1 overexpression reduces endothelial dysfunction and attenuates early renal impairment in a rat model of diabetes. *Diabetologia*. 2014;**57**(1):224-235. doi: 10.1007/s00125-013-3088-5.
75. Cheng AS, Cheng YH, Chiou CH, Chang TL. Resveratrol upregulates Nrf2 expression to attenuate methylglyoxal-induced insulin resistance in Hep G2 cells. *J. Agric. Food Chem*. 2012;**60**(36):9180-9187. doi: 10.1021/jf302831d.
76. Wang G, Wang Y, Yang Q, Xu C, Zheng Y, Wang L, Wu J, Zeng M, Luo M. Metformin prevents methylglyoxal-induced apoptosis by suppressing oxidative stress in vitro and in vivo. *Cell Death Dis*. 2022;**13**(1):29. doi: 10.1038/s41419-021-04478-x.
77. Wu L, Juurlink BH. Increased methylglyoxal and oxidative stress in hypertensive rat vascular smooth muscle cells. *Hypertension*. 2002;**39**(3):809-814. doi: 10.1161/hy0302.105207.
78. Lai MC, Liu WY, Liou SS, Liu IM. The protective effects of moscatilin against methylglyoxal-induced neurotoxicity via the regulation of p38/JNK MAPK pathways in PC12 neuron-like cells. *Food Chem. Toxicol*. 2020;**140**:111369. doi: 10.1016/j.fct.2020.111369.

79. Lee JH, Parveen A, Do MH, Kang MC, Yumnam S, Kim SY. Molecular mechanisms of methylglyoxal-induced aortic endothelial dysfunction in human vascular endothelial cells. *Cell Death Dis*. 2020;**11**(5):403. doi: 10.1038/s41419-020-2602-1.
80. Kim M, Cho C, Lee C, Ryu B, Kim S, Hur J, Lee SH. *Ishige okamurae* ameliorates methylglyoxal-induced nephrotoxicity via reducing oxidative stress, RAGE protein expression, and modulating MAPK, Nrf2/ARE signaling pathway in mouse glomerular mesangial cells. *Foods*. 2021;**10**(9):2000. doi: 10.3390/foods10092000.
81. Saxton RA, Sabatini DM. mTOR signaling in growth, metabolism, and disease. *Cell*. 2017;**168**(6):960-976. doi: 10.1016/j.cell.2017.02.004.
82. Inoki K, Li Y, Zhu T, Wu J, Guan KL. TSC2 is phosphorylated and inhibited by Akt and suppresses mTOR signalling. *Nat. Cell Biol*. 2002;**4**(9):648-657. doi: 10.1038/ncb839.
83. Nomura W, Inoue Y. Methylglyoxal activates the target of rapamycin complex 2-protein kinase C signaling pathway in *Saccharomyces cerevisiae*. *Mol. Cell Biol*. 2015;**35**:1269-1280. doi: 10.1128/MCB.01118-14.
84. Xu YR, Lei CQ. TAK1-TABs complex: a central signalosome in inflammatory responses. *Front. Immunol*. 2021;**11**:608976. doi: 10.3389/fimmu.2020.608976.
85. Cawthorn WP, Sethi JK. TNF-α and adipocyte biology. *FEBS Lett*. 2008;**582**(1):117-131. doi: 10.1016/j.febslet.2007.11.051.
86. Dimitriadis G, Mitrou P, Lambadiari V, Maratou E, Raptis SA. Insulin effects in muscle and adipose tissue. *Diabetes Res. Clin. Pract*. 2011;**93 Suppl 1**:S52-S59. doi: 10.1016/S0168-8227(11)70014-6.
87. Santoro A, McGraw TE, Kahn BB. Insulin action in adipocytes, adipose remodeling, and systemic effects. *Cell Metab*. 2021;**33**(4):748-757. doi: 10.1016/j.cmet.2021.03.019.
88. White MF. Insulin signaling in health and disease. *Science*. 2003;**302**(5651):1710-1711. doi: 10.1126/science.1092952.
89. Yamauchi T, Tobe K, Tamemoto H, Ueki K, Kaburagi Y, Yamamoto-Honda R, Takahashi Y, Yoshizawa F, Aizawa S, Akanuma Y, Sonenberg N, Yazaki Y, Kadowaki T. Insulin signalling and insulin actions in the muscles and livers of insulin-resistant, insulin receptor substrate 1-deficient mice. *Mol. Cell. Biol*. 1996;**16**(6):3074-3084. doi: 10.1128/MCB.16.6.3074.
90. Huang X, Liu G, Guo J, Su Z. The PI3K/AKT pathway in obesity and type 2 diabetes. *Int. J. Biol. Sci*. 2018;**14**(11):1483-1496. doi: 10.7150/ijbs.27173.
91. Yung HW, Charnock-Jones DS, Burton GJ. Regulation of AKT phosphorylation at Ser473 and Thr308 by endoplasmic reticulum stress modulates substrate specificity in a severity dependent manner. *PLoS One*. 2011;**6**(3):e17894. doi: 10.1371/journal.pone.0017894.
92. Gual P, Le Marchand-Brustel Y, Tanti JF. Positive and negative regulation of insulin signaling through IRS-1 phosphorylation. *Biochimie*. 2005;**87**(1):99-109. doi: 10.1016/j.biochi.2004.10.019.
93. Lee CR, Park YH, Min H, Kim YR, Seok YJ. Determination of protein phosphorylation by polyacrylamide gel electrophoresis. *J. Microbiol*. 2019;**57**(2):93-100. doi: 10.1007/s12275-019-9021-y.

94. Shah OJ, Hunter T. Turnover of the active fraction of IRS1 involves raptor-mTOR-and S6K1-dependent serine phosphorylation in cell culture models of tuberous sclerosis. *Mol. Cell Biol*. 2006;**26**(17):6425-6434. doi: 10.1128/MCB.01254-05.
95. Weigert C, Kron M, Kalbacher H, Pohl AK, Runge H, Häring HU, Schleicher E, Lehmann R. Interplay and effects of temporal changes in the phosphorylation state of serine-302,-307, and-318 of insulin receptor substrate-1 on insulin action in skeletal muscle cells. *Mol. Endocrinol*. 2008;**22**(12):2729-2740. doi: 10.1210/me.2008-0102.
96. Gual P, Grémeaux T, Gonzalez T, Marchand-Brustel L, Tanti JF. MAP kinases and mTOR mediate insulin-induced phosphorylation of insulin receptor substrate-1 on serine residues 307, 612 and 632. *Diabetologia*. 2003;**46**(11):1532-1542. doi: 10.1007/s00125-003-1223-4.
97. Manning BD, Tee AR, Logsdon MN, Blenis J, Cantley LC. Identification of the tuberous sclerosis complex-2 tumor suppressor gene product tuberin as a target of the phosphoinositide 3-kinase/akt pathway. *Mol. Cell*. 2002;**10**(1):151-162. doi: 10.1016/s1097-2765(02)00568-3.
98. Akhand AA, Hossain K, Mitsui H, Kato M, Miyata T, Inagi R, Du J, Takeda K, Kawamoto Y, Suzuki H, Kurokawa K, Nakashima I. Glyoxal and methylglyoxal trigger distinct signals for map family kinases and caspase activation in human endothelial cells. *Free Radic. Biol. Med*. 2001;**31**:20-30. doi: 10.1016/s0891-5849(01)00550-0.
99. Liu BF, Miyata S, Hirota Y, Higo S, Miyazaki H, Fukunaga M, Hamada Y, Ueyama S, Muramoto O, Uriuhara A, Kasuga M. Methylglyoxal induces apoptosis through activation of p38 mitogen-activated protein kinase in rat mesangial cells. *Kidney Int*. 2003;**63**:947-957. doi: 10.1046/j.1523-1755.2003.00829.x.
100. Chan WH, Wu HJ, Shiao NH. Apoptotic signaling in methylglyoxal-treated human osteoblasts involves oxidative stress, c-Jun N-terminal kinase, caspase-3, and p21-activated kinase 2. *J. Cell Biochem*. 2007;**100**:1056-1069. doi: 10.1002/jcb.21114.
101. Fujishita T, Aoki M, Taketo MM. JNK signaling promotes intestinal tumorigenesis through activation of mTOR complex 1 in Apc(Δ716) mice. *Gastroenterology*. 2011;**140**(5):1556-1563. doi: 10.1053/j.gastro.2011.02.007.
102. Kwak D, Choi S, Jeong H, Jang JH, Lee Y, Jeon H, Lee MN, Noh J, Cho K, Yoo JS, Hwang D, Suh PG, Ryu SH. Osmotic stress regulates mammalian target of rapamycin (mTOR) complex 1 via c-Jun N-terminal Kinase (JNK)-mediated Raptor protein phosphorylation. *J. Biol. Chem*. 2012;**287**(22):18398-18407. doi: 10.1074/jbc.M111.326538.
103. Li Y, Inoki K, Vacratsis P, Guan KL. The p38 and MK2 kinase cascade phosphorylates tuberin, the tuberous sclerosis 2 gene product, and enhances its interaction with 14-3-3. *J. Biol. Chem*. 2003;**278**(16):13663-13671. doi: 10.1074/jbc.M300862200.
104. Cully M, Genevet A, Warne P, Treins C, Liu T, Bastien J, Baum B, Tapon N, Leevers SJ, Downward J. A role for p38 stress-activated protein kinase in regulation of cell growth via TORC1. *Mol. Cell Biol*. 2010;**30**(2):481-495. doi: 10.1128/MCB.00688-09.
105. Wu XN, Wang XK, Wu SQ, Lu J, Zheng M, Wang YH, Zhou H, Zhang H, Han J. Phosphorylation of Raptor by p38beta participates in arsenite-induced mammalian target of rapamycin complex 1 (mTORC1) activation. *J. Biol. Chem*. 2011;**286**(36):31501-31511. doi: 10.1074/jbc.M111.233122.

106. Heberle AM, Razquin Navas P, Langelaar-Makkinje M, Kasack K, Sadik A, Faessler E, Hahn U, Marx-Stoelting P, Opitz CA, Sers C, Heiland I, Schäuble S, Thedieck K. The PI3K and MAPK/p38 pathways control stress granule assembly in a hierarchical manner. *Life Sci. Alliance*. 2019;**2**(2):201800257. doi: 10.26508/lsa.201800257.
107. Carriere A, Romeo Y, Acosta-Jaquez HA, Moreau J, Bonneil E, Thibault P, Fingar DC, Roux PP. ERK1/2 phosphorylate Raptor to promote Ras-dependent activation of mTOR complex 1 (mTORC1). *J. Biol. Chem*. 2011;**286**(1):567-577. doi: 10.1074/jbc.M110.159046.
108. Pontrelli P, Ranieri E, Ursi M, Ghosh-Choudhury G, Gesualdo L, Schena FP, Grandaliano G. jun-N-terminal kinase regulates thrombin-induced PAI-1 gene expression in proximal tubular epithelial cells. *Kidney Int*. 2004;**65**(6), 2249-2261. doi: 10.1111/j.1523-1755.2004.00644.x.
109. Vulin AI, Stanley FM. Oxidative stress activates the plasminogen activator inhibitor type 1 (PAI-1) promoter through an AP-1 response element and cooperates with insulin for additive effects on PAI-1 transcription. *J. Biol. Chem*. 2004;**279**(24):25172-25178. doi: 10.1074/jbc.M403184200.
110. Arndt PG, Young SK, Worthen GS. Regulation of lipopolysaccharide-induced lung inflammation by plasminogen activator inhibitor-1 through a JNK-mediated pathway. *J. Immunol*. 2005;**175**(6):4049-4059. doi: 10.4049/jimmunol.175.6.4049.
111. Deak M, Clifton AD, Lucocq JM, Alessi DR. Mitogen-and stress-activated protein kinase-1 (MSK1) is directly activated by MAPK and SAPK2/p38, and may mediate activation of CREB. *EMBO J*. 1998;**17**(15):4426-4441. doi: 10.1093/emboj/17.15.4426.
112. Di Giacomo V, Sancilio S, Caravatta L, Rana RA, Di Pietro R, Cataldi A. Regulation of CREB activation by p38 mitogen activated protein kinase during human primary erythroblast differentiation. *Int. J. Immunopathol. Pharmacol*. 2009;**22**(3):679-688. doi: 10.1177/039463200902200313.
113. Schieber M, Chandel NS. ROS function in redox signaling and oxidative stress. *Curr. Biol*. 2014;**24**(10):453-462. doi: 10.1016/j.cub.2014.03.034.
114. Bo J, Xie S, Guo Y, Zhang C, Guan Y, Li C, Lu J, Meng QH. Methylglyoxal impairs insulin secretion of pancreatic β-cells through increased production of ROS and mitochondrial dysfunction mediated by upregulation of UCP2 and MAPKs. *J. Diabetes Res*. 2016;**2016**:2029854. doi: 10.1155/2016/2029854.
115. Mihaly SR, Ninomiya-Tsuji J, Morioka S. TAK1 control of cell death. *Cell Death Differ*. 2014;**21**(11):1667-1676. doi: 10.1038/cdd.2014.123.
116. Gallot YS, McMillan JD, Xiong G, Bohnert KR, Straughn AR, Hill BG, Kumar A. Distinct roles of TRAF6 and TAK1 in the regulation of adipocyte survival, thermogenesis program, and high-fat diet-induced obesity. *Oncotarget*. 2017;**8**(68):112565-112583. doi: 10.18632/oncotarget.22575.
117. Yamawaki H, Saito K, Okada M, Hara Y. Methylglyoxal mediates vascular inflammation via JNK and p38 in human endothelial cells. *Am. J. Physiol. Cell Physiol*. 2008;**295**(6):1510-1517. doi: 10.1152/ajpcell.00252.2008.
118. Hüttl M, Markova I, Miklankova D, Makovicky P, Pelikanova T, Šeda O, Šedová L, Malinska H. Adverse effects of methylglyoxal on transcriptome and metabolic changes

in visceral adipose tissue in a prediabetic rat model. *Antioxidants*. 2020;**9**(9):803. doi: 10.3390/antiox9090803.
119. Stratmann B, Engelbrecht B, Espelage BC, Klusmeier N, Tiemann J, Gawlowski T, Mattern Y, Eisenacher M, Meyer HE, Rabbani N, Thornalley PJ. Glyoxalase 1-knockdown in human aortic endothelial cells–effect on the proteome and endothelial function estimates. *Sci. Rep*. 2016;**6**:37737. doi: 10.1038/srep37737.
120. Ninomiya-Tsuji J, Kajino T, Ono K, Ohtomo T, Matsumoto M, Shiina M, Mihara M, Tsuchiya M, Matsumoto K. A resorcylic acid lactone, 5Z-7-oxozeaenol, prevents inflammation by inhibiting the catalytic activity of TAK1 MAPK kinase kinase. *J. Biol. Chem*. 2003;**278**(20):18485-18490. doi: 10.1074/jbc.M207453200.
121. Thornalley PJ. Modification of the glyoxalase system in human red blood cells by glucose in vitro. *Biochem. J*. 1988;**254**(3):751-755. doi: 10.1042/bj2540751.
122. Thornalley PJ, Edwards LG, Kang Y, Wyatt C, Davies N, Ladan M J, Double J. Antitumour activity of Sp-bromobenzylglutathione cyclopentyl diester *in vitro* and *in vivo*: inhibition of glyoxalase I and induction of apoptosis. *Biochem. Pharmacol*. 1996;**51**(10):1365-1372. doi: 10.1016/0006-2952(96)00059-7.
123. Needham J, Lehmann H. Intermediary carbohydrate metabolism in embryonic life: Glyceraldehyde and glucolysis. *Biochem. J*. 1937;**31**(11):1913-1925. doi: 10.1042/bj0311913.
124. Nomura W, Aoki M, Inoue Y. Toxicity of dihydroxyacetone is exerted through the formation of methylglyoxal in *Saccharomyces cerevisiae*: effects on actin polarity and nuclear division. *Biochem. J*. 2018;**475**(16):2637-2652. doi: 10.1042/BCJ20180234.
125. Maessen DE, Brouwers O, Gaens KH, Wouters K, Cleutjens JP, Janssen BJ, Miyata T, Stehouwer CD, Schalkwijk CG. Delayed intervention with pyridoxamine improves metabolic function and prevents adipose tissue inflammation and insulin resistance in high-fat diet–induced obese mice. *Diabetes*. 2016;**65**(4):956-966. doi: 10.2337/db15-1390.
126. Oh S, Ahn H, Park H, Lee JI, Park KY, Hwang D, Lee S, Son KH, Byun K. The attenuating effects of pyridoxamine on adipocyte hypertrophy and inflammation differ by adipocyte location. *J. Nutr. Biochem*. 2019;**72**:108173. doi: 10.1016/j.jnutbio.2019.04.001.
127. Rui L, Aguirre V, Kim JK, Shulman GI, Lee A, Corbould A, Dunaif A, White MF. Insulin/IGF-1 and TNF-α stimulate phosphorylation of IRS-1 at inhibitory Ser307 via distinct pathways. *J. Clin. Invest*. 2001;**107**(2):181-189. doi: 10.1172/JCI10934.
128. Gao Z, Zuberi A, Quon MJ, Dong Z, Ye J. Aspirin inhibits serine phosphorylation of insulin receptor substrate 1 in tumor necrosis factor-treated cells through targeting multiple serine kinases. *J. Biol. Chem*. 2003;**278**(27):24944-24950. doi: 10.1074/jbc.M300423200.
129. Shibata T, Takaguri A, Ichihara K, Satoh K. Inhibition of the TNF-α-induced serine phosphorylation of IRS-1 at 636/639 by AICAR. *J. Pharmacol. Sci*. 2013;**122**(2):93-102. doi: 10.1254/jphs.12270fp.
130. de Alvaro C, Teruel T, Hernandez R, Lorenzo M. Tumor necrosis factor alpha produces insulin resistance in skeletal muscle by activation of inhibitor kappaB kinase in a p38

MAPK-dependent manner. *J. Biol. Chem*. 2004;**279**(17):17070-17078. doi: 10.1074/jbc.M312021200.
131. Rabbani N, Thornalley PJ. Dicarbonyl stress in cell and tissue dysfunction contributing to ageing and disease. *Biochem. Biophys. Res. Commun*. 2015;**458**(2):221-226. doi: 10.1016/j.bbrc.2015.01.140.
132. Bollong MJ, Lee G, Coukos JS, Yun H, Zambaldo C, Chang JW, Chin EN, Ahmad I, Chatterjee AK, Lairson LL, Schultz PG. A metabolite-derived protein modification integrates glycolysis with KEAP1–NRF2 signalling. *Nature*. 2018;**562**(7728):600-604. doi: 10.1038/s41586-018-0622-0.
133. Coukos JS, Moellering RE. Methylglyoxal forms diverse mercaptomethylimidazole crosslinks with thiol and guanidine pairs in endogenous metabolites and proteins. *ACS Chem. Biol*. 2021;**16**(11):2453-2461. doi: 10.1021/acschembio.1c00553.
134. Park HH. Structure of TRAF family: current understanding of receptor recognition. *Front. Immunol*. 2018;**9**:1999. doi: 10.3389/fimmu.2018.01999.
135. Das A, Foglizzo M, Padala P, Zhu J, Day CL. TRAF trimers form immune signalling networks via RING domain dimerization. *FEBS Lett.* 2022. doi: 10.1002/1873-3468.14530.
136. Yin Q, Lin SC, Lamothe B, Lu M, Lo YC, Hura G, Zheng L, Rich RL, Campos AD, Myszka DG, Lenardo MJ, Darnay BG, Wu H. E2 interaction and dimerization in the crystal structure of TRAF6. *Nat. Struct. Mol. Biol*. 2009;**16**(6):658-666. doi: 10.1038/nsmb.1605.
137. Afridi SK, Aftab MF, Murtaza M, Ghaffar S, Karim A, Mughal UR, Khan KM, Waraich RS. A new glycotoxins inhibitor attenuates insulin resistance in liver and fat cells. *Biochem. Biophys. Res. Commun*. 2016;**476**(4):188-195. doi: 10.1016/j.bbrc.2016.05.085.
138. Unoki H, Bujo H, Yamagishi SI, Takeuchi M, Imaizumi T, Saito Y. 2007. Advanced glycation end products attenuate cellular insulin sensitivity by increasing the generation of intracellular reactive oxygen species in adipocytes. *Diabetes Res. Clin. Pract*. 2007;**76**(2):236-244. doi: 10.1016/j.diabres.2006.09.016.
139. Aguirre V, Uchida T, Yenush L, Davis R, White MF. The c-Jun NH2-terminal kinase promotes insulin resistance during association with insulin receptor substrate-1 and phosphorylation of Ser307. *J. Biol. Chem*. 2000;**275**(12):9047-9054. doi: 10.1074/jbc.275.12.9047.
140. Nakamori Y, Emoto M, Fukuda N, Taguchi A, Okuya S, Tajiri M, Miyagishi M, Taira K, Wada Y Tanizawa Y. Myosin motor Myo1c and its receptor NEMO/IKK-γ promote TNF-α–induced serine307 phosphorylation of IRS-1. *J. Cell Biol*. 2006;**173**(5):665-671. doi: 10.1083/jcb.200601065.
141. Nawaratne R, Gray A, Jørgensen CH, Downes CP, Siddle K, Sethi JK. Regulation of insulin receptor substrate 1 pleckstrin homology domain by protein kinase C: role of serine 24 phosphorylation. *Mol. Endocrinol*. 2006;**20**(8):1838-1852. doi: 10.1210/me.2005-0536.
142. Weigert C, Hennige AM, Lehmann R, Brodbeck K, Baumgartner F, Schaüble M, Häring HU, Schleicher ED. Direct cross-talk of interleukin-6 and insulin signal

transduction via insulin receptor substrate-1 in skeletal muscle cells. *J. Biol. Chem*. 2006;**281**(11):7060-7067. doi: 10.1074/jbc.M509782200.
143. Moeschel K, Beck A, Weigert C, Lammers R, Kalbacher H, Voelter W, Schleicher ED, Häring HU, Lehmann R. Protein kinase C-ζ-induced phosphorylation of Ser318 in insulin receptor substrate-1 (IRS-1) attenuates the interaction with the insulin receptor and the tyrosine phosphorylation of IRS-1. *J. Biol. Chem*. 2004;**279**(24):25157-25163. doi: 10.1074/jbc.M402477200.
144. Bezy O, Tran TT, Pihlajamäki J, Suzuki R, Emanuelli B, Winnay J, Mori MA, Haas J, Biddinger SB, Leitges M, Goldfine AB. PKCδ regulates hepatic insulin sensitivity and hepatosteatosis in mice and humans. *J. Clin. Invest*. 2011;**121**(6):2504-2517. doi: 10.1172/JCI46045.
145. Sommerfeld MR, Metzger S, Stosik M, Tennagels N, Eckel J. In vitro phosphorylation of insulin receptor substrate 1 by protein kinase C-ζ: functional analysis and identification of novel phosphorylation sites. *Biochemistry*. 2004;**43**(19):5888-5901. doi: 10.1021/bi049640v.
146. Yoshida A, Wei D, Nomura W, Izawa S, Inoue Y. Reduction of glucose uptake through inhibition of hexose transporters and enhancement of their endocytosis by methylglyoxal in *Saccharomyces cerevisiae*. *J. Biol. Chem*. 2012;**287**(1):701-711. doi: 10.1074/jbc.M111.322222
147. Deshmukh AB, Bai S, Aarthy T, Kazi RS, Banarjee R, Rathore R, Vijayakumar MV, Thulasiram HV, Bhat MK, Kulkarni MJ. Methylglyoxal attenuates insulin signaling and downregulates the enzymes involved in cholesterol biosynthesis. *Mol. Biosyst.* 2017;**13**(11):2338-2349. doi: 10.1039/c7mb00305f.
148. Calder PC, Ahluwalia N, Brouns F, Buetler T, Clement K, Cunningham K, Esposito K, Jönsson LS, Kolb H, Lansink M, Marcos A. Dietary factors and low-grade inflammation in relation to overweight and obesity. *Br. J. Nutr*. 2011;**106 Suppl 3**:S5-S78. doi: 10.1017/S0007114511005460.
149. Siklova M, Simonsen L, Polak J, Stich V, Bülow J. Effect of short-term hyperglycemia on adipose tissue fluxes of selected cytokines in vivo during multiple phases of diet-induced weight loss in obese women. *J. Clin. Endocrinol. Metab*. 2015;**100**(5):1949-1956. doi: 10.1210/jc.2014-3846.
150. Reilly SM, Saltiel AR. Adapting to obesity with adipose tissue inflammation. *Nat. Rev. Endocrinol*. 2017;**13**(11):633-643. doi: 10.1038/nrendo.2017.90.
151. Saely CH, Geiger K, Drexel H. Brown versus white adipose tissue: a mini-review. *Gerontology*. 2012;**58**(1):15-23. doi: 10.1159/000321319.
152. Cannon B, Nedergaard JAN. Brown adipose tissue: function and physiological significance. *Physiol. Rev*. 2004;**84**(1):277-359. doi: 10.1152/physrev.00015.2003.
153. Wang G, Meyer JG, Cai W, Softic S, Li ME, Verdin E, Newgard C, Schilling B, Kahn CR. Regulation of UCP1 and mitochondrial metabolism in brown adipose tissue by reversible succinylation. *Mol. Cell*. 2019;**74**(4):844-857.e7. doi: 10.1016/j.molcel.2019.03.021.
154. Sidossis L, Kajimura S. Brown and beige fat in humans: thermogenic adipocytes that control energy and glucose homeostasis. *J. Clin. Invest*. 2015;**125**(2):478-486. doi: 10.1172/JCI78362.

155. Vitali A, Murano I, Zingaretti MC, Frontini A, Ricquier D, Cinti S. The adipose organ of obesity-prone C57BL/6J mice is composed of mixed white and brown adipocytes. *J. Lipid Res*. 2012;**53**(4):619-629. doi: 10.1194/jlr.M018846.
156. Boden G. Obesity and free fatty acids. *Endocrinol. Metab. Clin. North Am*. 2008;**37**(3):635-646. doi: 10.1016/j.ecl.2008.06.007.
157. Ahmed N. Advanced glycation endproducts-role in pathology of diabetic complications. *Diabetes Res. Clin. Pract*. 2005;**67**(1):3-21. doi: 10.1016/j.diabres.2004.09.004.
158. Allaman I, Bélanger M, Magistretti PJ. Methylglyoxal, the dark side of glycolysis. *Front. Neurosci*. 2015;**9**:23. doi: 10.3389/fnins.2015.00023.
159. Beisswenger PJ, Howell SK, Touchette AD, Lal S, Szwergold BS. Metformin reduces systemic methylglyoxal levels in type 2 diabetes. *Diabetes*. 1999;**48**(1):198-202. doi: 10.2337/diabetes.48.1.198.
160. Lapolla A, Flamini R, Vedova AD, Senesi A, Reitano R, Fedele D, Basso E, Seraglia R, Traldi P. Glyoxal and methylglyoxal levels in diabetic patients: quantitative determination by a new GC/MS method. *Clin. Chem. Lab. Med*. 2003;**41**(9):1166-1173. doi: 10.1515/CCLM.2003.180.
161. Sakamoto T, Takahashi N, Sawaragi Y, Naknukool S, Yu R, Goto T, Kawada T. Inflammation induced by RAW macrophages suppresses UCP1 mRNA induction via ERK activation in 10T1/2 adipocytes. *Am. J. Physiol. Cell Physiol*. 2013;**304**(8):C729-C738. doi: 10.1152/ajpcell.00312.2012.
162. Carmen GY, Víctor SM. Signalling mechanisms regulating lipolysis. *Cell Signal*. 2006;**18**(4):401-408. doi: 10.1016/j.cellsig.2005.08.009.
163. Holm C. (2003) Molecular mechanisms regulating hormone-sensitive lipase and lipolysis. *Biochem. Soc. Trans*. 2003;**31(Pt 6)**:1120-1124. doi: 10.1042/bst0311120.
164. Miyoshi H, Souza SC, Zhang HH, Strissel KJ, Christoffolete MA, Kovsan J, Rudich A, Kraemer FB, Bianco AC, Obin MS, Greenberg AS. Perilipin promotes hormone-sensitive lipase-mediated adipocyte lipolysis via phosphorylation-dependent and -independent mechanisms. *J. Biol. Chem*. 2006;**281**(23):15837-15844. doi: 10.1074/jbc.M601097200.
165. Anthonsen MW, Rönnstrand L, Wernstedt C, Degerman E, Holm C. Identification of novel phosphorylation sites in hormone-sensitive lipase that are phosphorylated in response to isoproterenol and govern activation properties in vitro. *J. Biol. Chem*. 1998;**273**(1):215-221. doi: 10.1074/jbc.273.1.215.
166. Ng SP, Nomura W, Mohri S, Takahashi H, Jheng HF, Ara T, Nagai H, Ito T, Kawada T, Goto T. Soy hydrolysate enhances the isoproterenol-stimulated lipolytic pathway through an increase in β-adrenergic receptor expression in adipocytes. *Biosci. Biotechnol. Biochem*. 2019;**83**(9):1782-1789. doi: 10.1080/09168451.2019.1611413.
167. Choi SM, Tucker DF, Gross DN, Easton RM, DiPilato LM, Dean AS, Monks BR, Birnbaum MJ. Insulin regulates adipocyte lipolysis via an Akt-independent signaling pathway. *Mol. Cell Biol*. 2010;**30**(21):5009-5020. doi: 10.1128/MCB.00797-10.
168. Nedergaard J, Golozoubova V, Matthias A, Asadi A, Jacobsson A, Cannon B. UCP1: the only protein able to mediate adaptive non-shivering thermogenesis and metabolic

inefficiency. *Biochim. Biophys. Acta*. 2001;**1504**(1):82-106. doi: 10.1016/s0005-2728(00)00247-4.
169. Collins S, Yehuda-Shnaidman E, Wang H. Positive and negative control of Ucp1 gene transcription and the role of β-adrenergic signaling networks. *Int. J. Obes. (Lond)*. 2010;**34 Suppl 1**:S28-S33. doi: 10.1038/ijo.2010.180.
170. Villarroya F, Peyrou M, Giralt M. Transcriptional regulation of the uncoupling protein-1 gene. *Biochimie*. 2017;**134**:86-92. doi: 10.1016/j.biochi.2016.09.017.
171. Iwase M, Sakai S, Seno S, Yeh YS, Kuo T, Takahashi H, Nomura W, Jheng HF, Horton P, Osato N, Matsuda H, Inoue K, Kawada T, Goto T. Long non-coding RNA 2310069B03Rik functions as a suppressor of Ucp1 expression under prolonged cold exposure in murine beige adipocytes. *Biosci. Biotechnol. Biochem*. 2020;**84**(2):305-313. doi: 10.1080/09168451.2019.1677451.
172. Iwase M, Tokiwa S, Seno S, Mukai T, Yeh YS, Takahashi H, Nomura W. Jheng HF, Matsumura S, Kusudo T, Osato N, Matsuda H, Inoue K, Kawada T, Goto T. Glycerol kinase stimulates uncoupling protein 1 expression by regulating fatty acid metabolism in beige adipocytes. *J. Biol. Chem*. 2020;**295**(20):7033-7045. doi: 10.1074/jbc.RA119.011658.
173. Valladares A, Roncero C, Benito M, Porras A. TNF-α inhibits UCP-1 expression in brown adipocytes via ERKs: opposite effect of p38MAPK. *FEBS Lett*. 2001;**493**(1):6-11. doi: 10.1016/s0014-5793(01)02264-5.
174. Sakamoto T, Takahashi N, Sawaragi Y, Naknukool S, Yu R, Goto T, Kawada T. Inflammation induced by RAW macrophages suppresses UCP1 mRNA induction via ERK activation in 10T1/2 adipocytes. *Am. J. Physiol. Cell Physiol*. 2013;**304**(8):C729-C738. doi: 10.1152/ajpcell.00312.2012.
175. Wells C, Karamitri A, Karamanlidis G, Lomax M. The cJun kinase inhibitor SP600125 stimulates expression of PPARγ co-activator 1α (PGC-1α) and uncoupling protein 1 (UCP1) in the HIB-1B brown fat preadipocyte cell line. *Proc. Nutr. Soc*. 2008;**67**(OCE8):E393. doi: 10.1017/S0029665108000670.
176. Moon H, Choi JW, Song BW, Kim IK, Lim S, Lee S, Hwang KC, Kim SW. Isoliquiritigenin enhances the beige adipocyte potential of adipose-derived stem cells by JNK inhibition. *Molecules*. 2020;**25**(23):5660. doi: 10.3390/molecules25235660
177. Yubero P, Barberá M, Alvarez R, Viñas O, Mampel T, Iglesias R, Villarroya F, Giralt M. Dominant negative regulation by c-Jun of transcription of the uncoupling protein-1 gene through a proximal cAMP-regulatory element: a mechanism for repressing basal and norepinephrine-induced expression of the gene before brown adipocyte differentiation. *Mol. Endocrinol*. 1998;**12**(7):1023-1037. doi: 10.1210/mend.12.7.0137.
178. Cargnello M, Roux PP. Activation and function of the MAPKs and their substrates, the MAPK-activated protein kinases. *Microbiol. Mol. Biol. Rev*. 2011;**75**(1): 50–83. doi: 10.1128/MMBR.00031-10.
179. Newsholme P, Cruzat VF, Keane KN, Carlessi R, de Bittencourt Jr PIH. Molecular mechanisms of ROS production and oxidative stress in diabetes. *Biochem. J.* 2016;**473**(24):4527-4550. doi: 10.1042/BCJ20160503C.

180. Figarola JL, Singhal J, Rahbar S, Awasthi S, Singhal SS. LR-90 prevents methylglyoxal-induced oxidative stress and apoptosis in human endothelial cells. *Apoptosis*. 2014;**19**(5):776-788. doi: 10.1007/s10495-014-0974-3.
181. Liu C, Huang Y, Zhang Y, Chen X, Kong X, Dong Y. Intracellular methylglyoxal induces oxidative damage to pancreatic beta cell line INS-1 cell through Ire1α-JNK and mitochondrial apoptotic pathway. *Free Radic. Res*. 2017;**51**(4):337-350. doi: 10.1080/10715762.2017.1289376.
182. Omran F, Christian M. Inflammatory signaling and brown fat activity. *Front. Endocrinol. (Lausanne)*. 2020;**11**:156. doi: 10.3389/fendo.2020.00156.
183. Nøhr MK, Bobba N, Richelsen B, Lund S, Pedersen SB. Inflammation downregulates UCP1 expression in brown adipocytes potentially via SIRT1 and DBC1 interaction. *Int. J. Mol. Sci*. 2017;**18**(5):1006. doi: 10.3390/ijms18051006.
184. Chiang SH, Bazuine M, Lumeng CN, Geletka LM, Mowers J, White NM, Ma JT, Zhou J, Qi N, Westcott D, Delproposto JB, Blackwell TS, Yull FE, Saltiel AR. The protein kinase IKKε regulates energy balance in obese mice. *Cell*. 2009;**138**(5):961-975. doi: 10.1016/j.cell.2009.06.046.
185. Kumari M, Wang X, Lantier L, Lyubetskaya A, Eguchi J, Kang S, Tenen D, Roh HC, Kong X, Kazak L, Ahmad R, Rosen ED. IRF3 promotes adipose inflammation and insulin resistance and represses browning. *J. Clin. Invest*. 2016;**126**(8):2839-2854. doi: 10.1172/JCI86080.
186. Ouyang C, Nie L, Gu M, Wu A, Han X, Wang X, Shao J, Xia Z. Transforming growth factor (TGF)-β-activated kinase 1 (TAK1) activation requires phosphorylation of serine 412 by protein kinase A catalytic subunit α (PKACα) and X-linked protein kinase (PRKX). *J. Biol. Chem*. 2014;**289**(35):24226-24237. doi: 10.1074/jbc.M114.559963.
187. Kobayashi Y, Mizoguchi T, Take I, Kurihara S, Udagawa N, Takahashi N. Prostaglandin E2 enhances osteoclastic differentiation of precursor cells through protein kinase A-dependent phosphorylation of TAK1. *J. Biol. Chem*. 2005;**280**(12):11395-11403. doi: 10.1074/jbc.M411189200.
188. Hattori K, Naguro I, Okabe K, Funatsu T, Furutani S, Takeda K, Ichijo H. ASK1 signalling regulates brown and beige adipocyte function. *Nat. Commun*. 2016;**7**:11158. doi: 10.1038/ncomms11158.
189. Lu X, Altshuler-Keylin S, Wang Q, Chen Y, Sponton CH, Ikeda K, Maretich P, Yoneshiro T, Kajimura S. Mitophagy controls beige adipocyte maintenance through a Parkin-dependent and UCP1-independent mechanism. *Sci. Signal*. 2018;**11**(527):eaap8526. doi: 10.1126/scisignal.aap8526.
190. Altshuler-Keylin S, Shinoda K, Hasegawa Y, Ikeda K, Hong H, Kang Q, Yang Y, Perera RM, Debnath J, Kajimura, S. Beige adipocyte maintenance is regulated by autophagy-induced mitochondrial clearance. *Cell Metab*. 2016;**24**(3):402-419. doi: 10.1016/j.cmet.2016.08.002.
191. Taylor D, Gottlieb RA. Parkin-mediated mitophagy is downregulated in browning of white adipose tissue. *Obesity (Silver Spring)*. 2017;**25**(4):704-712. doi: 10.1002/oby.21786.
192. Szatmári-Tóth M, Shaw A, Csomós I, Mocsár G, Fischer-Posovszky P, Wabitsch M, Balajthy Z, Lányi C, Győry F, Kristóf E, Fésüs L. Thermogenic activation

downregulates high mitophagy rate in human masked and mature beige adipocytes. *Int. J. Mol. Sci*. 2020;**21**(18):6640. doi: 10.3390/ijms21186640.
193. Kim D, Kim KA, Kim JH, Kim EH, Bae ON. Methylglyoxal-induced dysfunction in brain endothelial cells via the suppression of Akt/HIF-1α pathway and activation of mitophagy associated with increased reactive oxygen species. *Antioxidants (Basel)*. 2020;**9**(9):820. doi: 10.3390/antiox9090820.
194. Kim JH, Kim HY, Lee YK, Yoon YS, Xu WG, Yoon JK, Choi SE, Ko YG, Kim MJ, Lee SJ, Wang HJ, Yoon G. Involvement of mitophagy in oncogenic K-Ras-induced transformation: overcoming a cellular energy deficit from glucose deficiency. *Autophagy*. 2011;**7**(10):1187-1198. doi: 10.4161/auto.7.10.16643.
195. Park JH, Ko J, Park YS, Park J, Hwang J, Koh HC. Clearance of damaged mitochondria through PINK1 stabilization by JNK and ERK MAPK signaling in chlorpyrifos-treated neuroblastoma cells. *Mol. Neurobiol*. 2017;**54**(3):1844-1857. doi: 10.1007/s12035-016-9753-1.
196. Wang YY, Morimoto S, Du CK, Lu QW, Zhan DY, Tsutsumi T, Ide T, Miwa Y, Takahashi-Yanaga F, Sasaguri T. Up-regulation of type 2 iodothyronine deiodinase in dilated cardiomyopathy. *Cardiovasc. Res*. 2010;**87**(4):636-646. doi: 10.1093/cvr/cvq133.
197. Seong KH, Maekawa T, Ishii S. Inheritance and memory of stress-induced epigenome change: roles played by the ATF-2 family of transcription factors. *Genes Cells*. 2012;**17**(4):249-263. doi: 10.1111/j.1365-2443.2012.01587.x.
198. Hondares E, Iglesias R, Giralt A, Gonzalez FJ, Giralt M, Mampel T, Villarroya F. Thermogenic activation induces FGF21 expression and release in brown adipose tissue. *J. Biol. Chem*. 2011;**286**(15):12983-12990. doi: 10.1074/jbc.M110.215889
199. Riboulet-Chavey A, Pierron A, Durand I, Murdaca J, Giudicelli J, Van Obberghen E. Methylglyoxal impairs the insulin signaling pathways independently of the formation of intracellular reactive oxygen species. *Diabetes*. 2006;**55**(5):1289-1299. doi: 10.2337/db05-0857.
200. Che W, Asahi M, Takahashi M, Kaneto H, Okado A, Higashiyama S, Taniguchi N. Selective induction of heparin-binding epidermal growth factor-like growth factor by methylglyoxal and 3-deoxyglucosone in rat aortic smooth muscle cells: the involvement of reactive oxygen species formation and a possible implication for atherogenesis in diabetes. *J. Biol. Chem*. 1997;**272**(29):18453-18459. doi: 10.1074/jbc.272.29.18453.
201. McMahon DK, Anderson PA, Nassar R, Bunting JB, Saba Z, Oakeley AE, Malouf NN. C2C12 cells: biophysical, biochemical, and immunocytochemical properties. *Am. J. Physiol*. 1994;**266**(6 Pt 1):C1795-1802. doi: 10.1152/ajpcell.1994.266.6.C1795.
202. Kinnunen M, Kauppila A, Karmenyan A, Myllylä R. Effect of the size and shape of a red blood cell on elastic light scattering properties at the single-cell level. *Biomed. Opt. Express*. 2011;**2**(7):1803-1814. doi: 10.1364/BOE.2.001803.
203. Stenkula KG, Erlanson-Albertsson C. Adipose cell size: importance in health and disease. *Am. J. Physiol. Regul. Integr. Comp. Physiol*. 2018;**315**(2):R284-R295. doi: 10.1152/ajpregu.00257.2017.

204. Scheijen JL, Schalkwijk CG. Quantification of glyoxal, methylglyoxal and 3-deoxyglucosone in blood and plasma by ultra performance liquid chromatography tandem mass spectrometry: evaluation of blood specimen. *Clin. Chem. Lab. Med*. 2014;**52**(1):85-91. doi: 10.1515/cclm-2012-0878.
205. Han Y, Randell E, Vasdev S, Gill V, Gadag V, Newhook LA, Grant M, Hagerty D. Plasma methylglyoxal and glyoxal are elevated and related to early membrane alteration in young, complication-free patients with Type 1 diabetes. *Mol. Cell. Biochem*. 2007;**305**(1-2):123-31. doi: 10.1007/s11010-007-9535-1.
206. Guillon C, Ferraro S, Clément S, Bouschbacher M, Sigaudo-Roussel D, Bonod C. Glycation by glyoxal leads to profound changes in the behavior of dermal fibroblasts. *BMJ Open Diabetes Res. Care*. 2021;**9**(1):e002091. doi: 10.1136/bmjdrc-2020-002091.
207. Nevin C, McNeil L, Ahmed N, Murgatroyd C, Brison D, Carroll M. Investigating the glycating effects of glucose, glyoxal and methylglyoxal on human sperm. *Sci. Rep*. 2018;**8**(1):9002. doi: 10.1038/s41598-018-27108-7.
208. Song X, Liang G, Shi M, Zhou L, Wang F, Zhang L, Huang F, Jiang G. Acute exposure to 3-deoxyglucosone at high glucose levels impairs insulin secretion from β-cells by downregulating the sweet taste receptor signaling pathway. *Mol. Med. Rep*. 2019;**19**(6):5015-5022. doi: 10.3892/mmr.2019.10163.
209. Carlson CJ, Koterski S, Sciotti RJ, Poccard GB, Rondinone CM. Enhanced basal activation of mitogen-activated protein kinases in adipocytes from type 2 diabetes: potential role of p38 in the downregulation of GLUT4 expression. *Diabetes*. 2003;**52**(3):634-641. doi: 10.2337/diabetes.52.3.634.
210. Chaudhuri J, Bose N, Gong J, Hall D, Rifkind A, Bhaumik D, Peiris TH, Chamoli M, Le CH, Liu J, Lithgow GJ, Ramanathan A, Xu XZS, Kapahi P. A *Caenorhabditis elegans* model elucidates a conserved role for TRPA1-Nrf signaling in reactive α-dicarbonyl detoxification. *Curr. Biol*. 2016;**26**(22):3014-3025. doi: 10.1016/j.cub.2016.09.024.
211. Galligan JJ, Wepy JA, Streeter MD, Kingsley PJ, Mitchener MM, Wauchope OR, Beavers WN, Rose KL, Wang T, Spiegel DA, Marnett LJ. Methylglyoxal-derived posttranslational arginine modifications are abundant histone marks. *Proc. Natl. Acad. Sci. USA*. 2018;**115**(37):9228-9233. doi: 10.1073/pnas.1802901115.
212. Zheng Q, Omans ND, Leicher R, Osunsade A, Agustinus AS, Finkin-Groner E, D'Ambrosio H, Liu B, Chandarlapaty S, Liu S, David Y. Reversible histone glycation is associated with disease-related changes in chromatin architecture. *Nat. Commun*. 2019;**10**(1):1289. doi: 10.1038/s41467-019-09192-z.
213. Seo K, Ki SH, Shin SM. Methylglyoxal induces mitochondrial dysfunction and cell death in liver. *Toxicol. Res*. 2014; **30**(3):193-198. doi: 10.5487/TR.2014.30.3.193.
214. Suh KS, Choi EM, Rhee SY, Kim YS. Methylglyoxal induces oxidative stress and mitochondrial dysfunction in osteoblastic MC3T3-E1 cells. *Free Radic. Res*. 2014;**48**(2):206-17. doi: 10.3109/10715762.2013.859387.
215. Chan CM, Huang DY, Huang YP, Hsu SH, Kang LY, Shen CM, Lin WW. Methylglyoxal induces cell death through endoplasmic reticulum stress-associated ROS production and mitochondrial dysfunction. *J. Cell. Mol. Med*. 2016;**20**(9):1749-1760. doi: 10.1111/jcmm.12893.

216. Chakraborty S, Karmakar K, Chakravortty D. Cells producing their own nemesis: understanding methylglyoxal metabolism. *IUBMB Life*. 2014;**66**(10):667-678. doi: 10.1002/iub.1324.
217. Rachman H, Kim N, Ulrichs T, Baumann S, Pradl L, Eddine AN, Bild M, Rother M, Kuban RJ, Lee JS, Hurwitz R, Brinkmann V, Kosmiadi GA, Kaufmann SHE. Critical role of methylglyoxal and AGE in mycobacteria-induced macrophage apoptosis and activation. *PLoS One*. 2006;**1**(1):e29. doi: 10.1371/journal.pone.0000029.
218. Eskra L, Canavessi A, Carey M, Splitter G. *Brucella abortus* genes identified following constitutive growth and macrophage infection. *Infect. Immun*. 2001;**69**(12):7736-7742. doi: 10.1128/IAI.69.12.7736-7742.2001.
219. Chakraborty S, Chaudhuri D, Balakrishnan A, Chakravortty D. *Salmonella* methylglyoxal detoxification by STM3117-encoded lactoylglutathione lyase affects virulence in coordination with *Salmonella* pathogenicity island 2 and phagosomal acidification. *Microbiology (Reading)*. 2014;**160**(Pt 9):1999-2017. doi: 10.1099/mic.0.078998-0.
220. Shin MG, Lee JW, Han JS, Lee B, Jeong JH, Park SH, Kim JH, Jang S, Park M, Kim SY, Kim, S., Yang YR, Kim JY, Hoe KL, Park C, Lee KP, Kwon KS, Kwon ES. Bacteria-derived metabolite, methylglyoxal, modulates the longevity of *C. elegans* through TORC2/SGK-1/DAF-16 signaling. *Proc. Natl. Acad. Sci. USA*. 2020;**117**(29):17142-17150. doi: 10.1073/pnas.1915719117.
221. Ravichandran M, Priebe S, Grigolon G, Rozanov L, Groth M, Laube B, Guthke R, Platzer M, Zarse K, Ristow M. Impairing L-threonine catabolism promotes healthspan through methylglyoxal-mediated proteohormesis. *Cell Metab*. 2018;**27**(4):914-925. doi: 10.1016/j.cmet.2018.02.004.
222. Nokin MJ, Durieux F, Bellier J, Peulen O, Uchida K, Spiegel DA, Cochrane JR, Hutton CA, Castronovo V, Bellahcène A. Hormetic potential of methylglyoxal, a side-product of glycolysis, in switching tumours from growth to death. *Sci. Rep*. 2017;**7**(1):11722. doi: 10.1038/s41598-017-12119-7.
223. Nokin MJ, Bellier J, Durieux F, Peulen O, Rademaker G, Gabriel M, Monseur C, Charloteaux B, Verbeke L, van Laere S, Roncarati P, Herfs M, Lambert C, Scheijen J, Schalkwijk C, Colige A, Caers J, Delvenne P, Turtoi A, Castronovo V, Bellahcène A. Methylglyoxal, a glycolysis metabolite, triggers metastasis through MEK/ERK/SMAD1 pathway activation in breast cancer. *Breast Cancer Res*. 2019;**21**(1):11. doi: 10.1186/s13058-018-1095-7.

Acknowledgements

This research was supported in part by a Grant-in-aid for Scientific Research for JSPS Fellows from The Ministry of Education, Culture, Sports, Science and Technology, Japan.

First and foremost, I would very much like to express gratitude towards Dr. Kazuo Inoue, my doctoral supervisor and the Professor of the Laboratory of Physiological Function of Food from the Division of Food Science and Biotechnology, Kyoto University, for his continuous support towards the research. His assurance in providing a stable and secure working environment in times of inevitable change was undoubtedly a source of strength in the process of the study.

I would also like to extend my thanks to Sub-chief Examiner of the dissertation committee, Dr. Tsutomu Sasaki, Professor of the Laboratory of Nutrition Chemistry from the same division in Kyoto University. His immense interest and input regarding my dissertation have been very heartening, contributing to a substantial improvement in the final version.

I am also grateful towards the Board of Professors of the Division of Food Science and Biotechnology: Dr. Kazuhiro Irie, Professor of the Laboratory of Organic Chemistry in Life Science; Dr. Fumito Tani, Professor of the Laboratory of Bioengineering; Dr. Kiyoshi Yasukawa, Professor of the Laboratory of Enzyme Chemistry; and Dr. Wataru Hashimoto, Professor of the Laboratory of Basic and Applied Molecular Biotechnology. The completion of this dissertation is, in large part, due to their advices which they have generously provided.

I also thank Dr. Tsuyoshi Goto, Associate Professor of the same laboratory for his guidance in this study. Researching here required his support, and his presence in this journey was an indispensable accelerant towards my academic development.

I feel utmost gratitude Dr. Wataru Nomura, Assistant Professor of the Laboratory of Molecular Microbiology from the Division of Applied Life Sciences, Kyoto University, who has been my mentor from the time of our acquaintance when he was affiliated with my laboratory. It was under his tutelage that I have developed joy and passion for research in spite

of circumstances. His quiet concern and unfailing kindness have provided me loads of much-needed solace, support, and strength, without which I could not have completed my studies.

I am also extremely grateful to Dr. Yoshiharu Inoue, Professor of the Laboratory of Molecular Microbiology from the Division of Applied Life Sciences, Kyoto University. There was absolutely no obligation on his part, but he had willingly given me his time, support, and advice. In times of unease and self-doubt, he had also provided me with relief. Thank you so very much.

I also show my thankfulness to Dr. Kousaku Ohinata and Dr. Takumi Yokokawa, Associate Professor and Assistant Professor, respectively, of my laboratory. Their enthusiasm in my research has led to fruitful discussions that undoubtedly contributed to a deeper understanding towards the research.

I would also like to thank Dr. Haruya Takahashi, Assistant Professor of my laboratory, as well as Ms. Kazue Yano, secretary of the same laboratory, people who I think are never given enough credit. They played a crucial role in making it so that research activities in the laboratory could run smoothly. Without their support, research could never have come this far.

I also want to state my deep appreciation towards Dr. Teruo Kawada, retired Professor of the Laboratory of Molecular Function of Food from the Division of Food Science and Biotechnology, Kyoto University. Although our acquaintance was unfortunately short, he had nothing but goodwill towards me and was the one who supported my dreams and aspirations behind the scenes. Without him, I would never have been connected with the people beyond our immediate circle. He has left an indelible impact on me and I am really thankful to have known him.

I am also grateful for past staff of the lab: Dr. Huei-Fen Jheng from the Research and Development Division, National Laboratory Animal Center, National Applied Research Laboratories, Taipei, Taiwan; Dr. Shinsuke Mohri, Assistant Professor from the Laboratory of Medical Physiology and Metabolism, Department of Biomedical Sciences, Ritsumeikan University; as well as Dr. Takeshi Ara from the Bioinformation and DNA Data Bank of Japan Center, National Institute of Genetics, for their care and support which have nourished me to keep pushing through.

I also want to share feelings of thankfulness to my fellow laboratory-mates, Dr. Satoko Kawarasaki and Jungin Kwon, who have given me friendship and have been my closest confidants. Laboratory life would have been unbearable without their presence. These people were undeniably the ones who covered for me when I was lacking. Words cannot express how grateful I am for their kindness and understanding. A shoutout of thanks also to Assistant Technical Staff, Masaki Asano, and the juniors in the laboratory, Zheng Ni, Haruka Okaze, Yoshimi Watanabe, Saori Sunagawa, Kouta Okudo, Yusuke Yoshiko, Shunta Numano, Mai Takada and Takumi Kishimoto who had been, and will be involved in maintaining lab activities. Each and every one of you were crucial for creating a lively and energetic atmosphere in an otherwise dreary setting. I treasure the days spent with all of you.

Also, a shoutout to Dr. Maria Rohm from HMGU Munich, to Juventia Dimitri Stella from Wageningen University, and to Dr. Shiho Ito from Kyoto University. With a shared understanding from experiences of being in the research field together, being acquainted and talking to all of you have given me hope for a better tomorrow, and made me realise that finishing a doctorate is not the end, but rather, a new beginning.

To Midori, Dong Heng Chu, Kimiharu, Mdm. Leong, Ray Wern Ng and her brother, Ray Min, Grace Xaveria, Siew Vern Ang, Amanda Howard, Kayo Ikeda, Rika Takahashi, Kazuki Matsuo, Dr. Lanxi Zhou, Ana Yuliana, Miho Takase, Motohiro Tokura, Kento Nishitani, Masakazu Shintani, Nozomi Sumida, Maika Hasuike, Megumi, Kaede, and all others that I may have missed out (my apologies). Thank you for rooting for me, for all the help and support given, and for your friendship. Your thoughts and prayers, as well as your compassion towards my endeavours have cheered me to soldier on.

To Dad and Mum, thank you for your unending support, your belief in me, as well as your bottomless encouragement and understanding. To the Angs: Alpert, Mei-Cheen and little Alyssa; and the Occlestons: Hen and Carmen, thank you for everything. You all reminded me that I am not alone, and have pulled me out of my depressing ruminations with all your antics. Your existences in my life undoubtedly propelled me in this journey. I think I may be among the first “Doctor (of Philosophy)” in the family. Although it sounds kinda “cool”, I regret that in cases like an emergency aeroplane setting, that “coolness” would prove completely useless (in such circumstances, I will cling to the Angs, the medical doctors of the family). This

“coolness” would also fade in the face of the financial successes of the Occlestons, the dynamic economic strategist and accountant duo. I am relying on you both to grace me with a pittance of your huge wealth to fund my research in the future. Jokes and humour aside, a heartful thanks to all of you.

Last, but not least, I want to thank my beloved God. It had been a turbulent journey here in Japan for about a decade, and looking back, I feel like I have attempted the impossible. Alone, I would have been devastatingly helpless, but because You were with me, You gave me a miracle by surrounding me with so many wonderful people. Desperately hanging on to 1 Thessalonians 5:18: “*give thanks in all circumstances; for this is God’s will for you in Christ Jesus.*”, I was somewhat able to keep my faith and fight the good fight till the end. I cannot possibly repay every grace given, but let this acknowledgements section be a testament of Your goodness towards me, and a reminder about the people who have been involved in this journey and who have brought me this far. I believe that these debts can only be paid forward while living a Godly and righteous life for as long as I can. You are omniscient and omnipotent, and I will continuously pray that You pay in kind and bless those who have been good to me.

Su-Ping

List of Publications

Original Papers

- **Ng SP**, Nomura W, Takahashi H, Inoue K, Kawada T, Goto T, Inoue Y. Methylglyoxal induces multiple serine phosphorylation in insulin receptor substrate 1 via the TAK1–p38–mTORC1 signaling axis in adipocytes. *Biochemical Journal*, 2022;**479**(21):2279-2296. doi: 10.1042/BCJ20220271.

- **Ng SP**, Nomura W, Takahashi H, Inoue K, Kawada T, Goto T. Methylglyoxal attenuates isoproterenol-induced increase in uncoupling protein 1 expression through activation of JNK signaling pathway in beige adipocytes. *Biochemistry and Biophysics Reports*, 2021;**28**:101127. doi: 10.1016/j.bbrep.2021.101127.

Related Papers

- Jheng HF, Takase M, Kawarasaki S, Ni Z, Mohri S, Hayashi K, Izumi A, Sasaki K, Shinyama Y, Kwon J, **Ng SP**, Takahashi H, Nomura W, Yu R, Ochiai K, Inoue K, Kawada T, Goto T. 8-Prenyl daidzein and 8-prenyl genistein from germinated soybean modulate inflammatory response in activated macrophages. *Bioscience, Biotechnology, and Biochemistry*, in press. doi: 10.1093/bbb/zbad041

- Nomura W, **Ng SP**, Takahara T, Maeda T, Kawada T, Goto T, Inoue Y. Roles of phosphatidylserine and phospholipase C in the activation of TOR complex 2 signaling in *Saccharomyces cerevisiae*. *Journal of Cell Science*, 2022;**135**:jcs259988. doi: 10.1242/jcs.259988.

- Kawarasaki S, Sawazaki H, Iijima H, **Ng SP**, Kwon J, Mohri S, Iwase M, Jheng HF, Takahashi H, Nomura W, Inoue K, Kawada T, Goto T. Comparative Analysis of the Preventive Effects of Canagliflozin, a Sodium-Glucose Co-Transporter-2 Inhibitor, on Body Weight Gain Between Oral Gavage and Dietary Administration by Focusing on Fatty Acid Metabolism. *Diabetes, Metabolic Syndrome and Obesity: Targets and Therapy*, 2020;**13**:4353-4359. doi: 10.2147/DMSO.S269916.

- **Ng SP**, Nomura W, Mohri S, Takahashi H, Jheng HF, Ara T, Nagai H, Ito T, Kawada T, Goto T. Soy hydrolysate enhances the isoproterenol-stimulated lipolytic pathway through an increase in β-adrenergic receptor expression in adipocytes. *Bioscience, Biotechnology, and Biochemistry*, 2019;**83**:1782-1789. doi: 10.1080/09168451.2019.1611413.